Dissertation

Corrosion of Refractory Metals in Aggressive Media

Qamar Abbas

Graz, August 2011

Zur Erlangung des akademischen Grades eines Doktor in der Naturwissenschaften

erreicht an der

Technischen Universitat Graz

AO. Univ.-Prof.-Ing. Dr. rer. nat. Leo Binder

Institute of Inorganic Chemistry, Graz University of Technology, Austria

Deutsche Fassung:
Beschluss der Curricula-Kommission für Bachelor-, Master- und Diplomstudien vom 10.11.2008
Genehmigung des Senates am 1.12.2008

EIDESSTATTLICHE ERKLÄRUNG

Ich erkläre an Eides statt, dass ich die vorliegende Arbeit selbstständig verfasst, andere als die angegebenen Quellen/Hilfsmittel nicht benutzt, und die den benutzten Quellen wörtlich und inhaltlich entnommene Stellen als solche kenntlich gemacht habe.

Graz, am …… ……
(Unterschrift)

Englische Fassung:

STATUTORY DECLARATION

I declare that I have authored this thesis independently, that I have not used other than the declared sources / resources, and that I have explicitly marked all material which has been quoted either literally or by content from the used sources.

…… ……
date (signature)

In the name of Allah, The Most Beneficent, The Most Merciful

To the memories of my Father

Acknowledgment

Many thanks to Allah Almighty for his blessings without which present work could not be completed. Prayers of my mother are always a wonderful source of strength and self-belief. Many thanks to my family for their support, guidance and care they always have for me.

I would like to express my profound gratitude to Prof. Leo Binder for giving me a chance to work with him. He has been a wonderful, cooperative, dynamic and inspirational personality during my PhD studies. His will and availability to help, support and guide me whenever I am in trouble, makes him a man of character. His friendly attitude gave me freedom of thoughts and expressions. I am also thankful for his support and guidance during my conference visits to Hungary, Saudi Arabia, Turkey and Germany.

Special thanks to Prof. Otto Fruhwirth for his experimental help and fruitful discussions on TGA and DSC analysis. I am impressed with his knowledge and command on explaining the thermal behavior of choline chloride based binary mixtures. I am also thankful to Dr. Bernhard Gollas and his team for facilitating me in their lab. They always supported and helped me whenever I needed some equipment or instrument.

I am thankful to Dr. Muhammad Zahid for his selfless support off studies as well as for useful discussions on various aspects of subject matter. Special thanks to Thomas Kern, Amra Suljanovik, Rita Marusch and all the colleagues of Inorganic Chemistry Institute for providing me conducive environment throughout my PhD studies. Very special thanks to Sarfraz Ahmad, Muhammad Tahir Soomro, Muddasar Abbas, Tanveer Bhai, Kashif Nadeem, Saeed Khan, Imam Bakhsh Abdullah and Najam-ur-Rehman for sharing their time in C-15 and delightful discussions on dining table. I am also thankful to my all colleagues and Pakistani scholars in Graz and Vienna for their best wishes and prayers.

I would like to thank NAWI Graz for partial funding to attend conferences in Turkey and Germany.

I am also thankful to Higher Education Commission (HEC) of Pakistan for the financial support of my PhD studies.

Abstract

The weight loss and electrochemical behavior of molybdenum and tungsten using Faraday's law has been investigated in NH_4NO_3/NH_3 and choline chloride based binary mixtures. NH_4NO_3/NH_3 system was prepared at -35 ^oC while choline chloride based binary mixtures were prepared at room temperature under vacuum by mixing choline chloride with a hydrogen bond donor (HBD). TGA and DSC techniques were used to analyze the thermal behavior choline chloride based binary mixtures. IR spectroscopy was used to investigate the molecular interaction among the HBDs and choline chloride.

XRD and XRF techniques were used to check the presence of Mo in NH_4NO_3/NH_3 system after electrochemical dissolution and complex formation of Mo has been discussed. Weight loss analysis show that Mo and W dissolve to great extent into CC/EG and CC/Gly system as compared to other electrolytic systems used for weight loss analysis. It has also been shown that lesser the chloride ion concentration greater is the weight loss of molybdenum and tungsten.

ESR technique was used to estimate the valence of anodically dissolved molybdenum in CC/EG system which shows the presence of molybdenum as Mo^{+5} in the form of $MoCl_5$. Galvanostatic measurements were carried out at room temperature and show the potential oscillation at constant current density of 100 mA/cm^2. The oscillation in potential is due to the periodic formation and removal of thick surface layer at electrode. Anodic dissolution of both Mo and W has been shown to be affected by the molecular interaction among HBDs and the choline chloride.

SEM technique has been used for surface analysis of Mo after anodic dissolution in CC/EG system. The presence of carbon particles at Mo surface show that oxidation of EG has taken place, however a well polished surface of Mo is obtained in this system.

Zusammenfassung

Der Gewichtsverlust und das elektrochemische Verhalten von Molybdän und Wolfram in NH_4NO_3/NH_3 (fl.) und in auf Cholinchlorid (CC) basierenden binären Mischungen ist mit Hilfe des Faraday'schen Gesetzes untersucht worden. Das NH_4NO_3/NH_3 (fl.)-System wurde bei -35 ºC vorbereitet, während die auf Cholinchlorid basierenden binären Mischungen bei Raumtemperatur unter Vakuum durch Mischen von Cholinchlorid mit einem Wasserstoffbrücken-Donor (HBD) hergestellt wurden. TGA- und DSC-Techniken wurden verwendet, um das thermische Verhalten von auf Cholinchlorid basierenden binären Gemischen zu analysieren. Die molekulare Wechselwirkung zwischen den HBDs und CC wurde mittels IR-Spektroskopie untersucht.

XRD- und XRF-Techniken wurden angewendet, um die Anwesenheit von Molybdän im NH_4NO_3/NH_3 (fl.)-System nach der elektrochemischen Auflösung und mögliche Komplexbildung zu überprüfen. Gewichtsverlust-Analysen zeigen, dass sich Mo und W in CC/EG (Ethylenglykol) und CC/Gly (Glycerin) in größerem Umfang lösen als in anderen zur Gewichtsverlust-Analyse verwendeten Elektrolytsystemen. Es wurde auch gezeigt, dass mit Verminderung der Chlorid-Ionen-Konzentration im Elektrolytsystem der Gewichtsverlust von Molybdän und Wolfram größer wird.

ESR-Spektroskopie wurde benutzt, um die Wertigkeit von anodisch gebildeten Mo-Ionen in CC/EG abzuschätzen. Es konnte die Anwesenheit von Mo^{5+} in Form von $MoCl_5$ gezeigt werden. Bei Raumtemperatur durchgeführte glavanostatische Messungen zeigen Potentialschwingungen bei einer konstanten Stromdichte von 100 mA/cm^2. Diese Potentialschwingungen werden durch die periodische Bildung und Entfernung von dicken Oberflächenschichten auf der Elektrode verursacht. Es wurde gezeigt, dass die anodische Auflösung von Mo Und W durch die molekulare Wechselwirkung zwischen HBDs und CC beeinflusst wird.

REM-Aufnahmen wurden zur Oberflächenanalyse von Mo nach anodischer Auflösung im CC/EG-System verwendet. Die Anwesenheit von Kohlenstoff-Teilchen auf der Mo-Oberfläche zeigt, dass eine Oxidation von EG stattgefunden hat. Trotzdem wird in diesem System eine gut polierte Oberfläche des Mo erhalten.

Contents

List of Tables

List of Figures

1 Introduction

Anodic dissolution of a metal is achieved by connecting it with external source of potential, such as battery or rectifier so that it is made anodic with respect to a physically separate counter electrode. An anodic process takes place on corroding metal under these conditions and the electrolyte provides a means of maintaining the anodic and cathodic processes physically separate. By increasing or decreasing the applied potential, the rate of metal dissolution can be controlled. Such a process is called anodic corrosion. As the applied potential reaches a critical anodic value, most of the metals become passive and dissolution process is halted. An idealized potentiostatic polarization curve is sketched in figure 1-1.

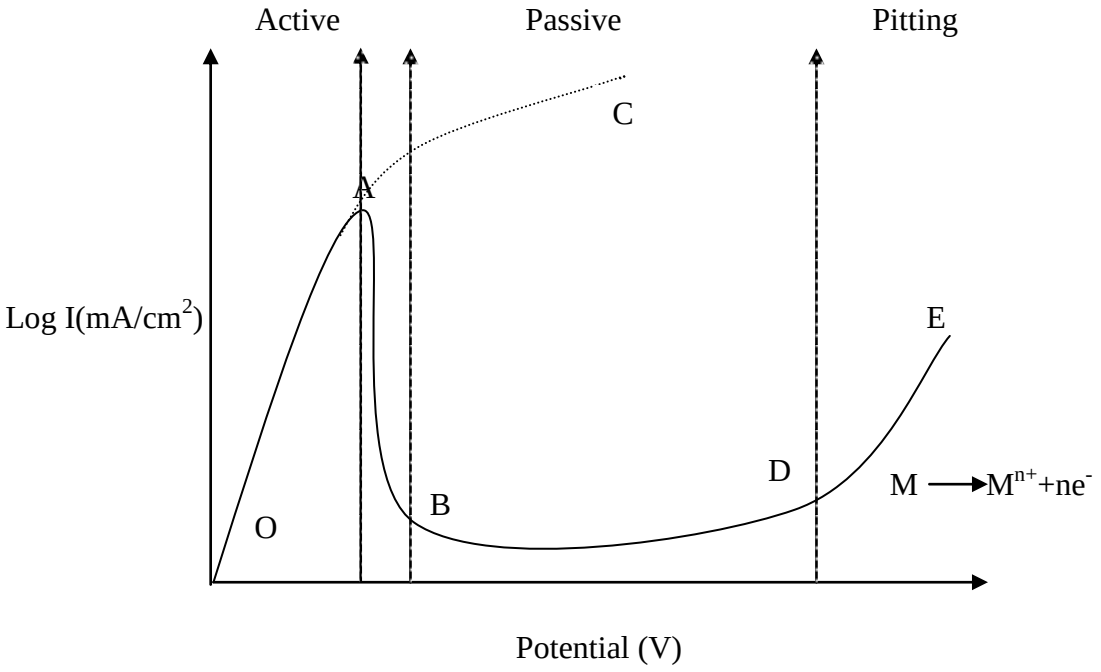

Figure 1-1: Sketch of idealized, steady state, potentiostatic polarization curve obtained on a given anode in a given electrolyte.

In this case, the metal is inert below a threshold potential, O in figure 1-1; and the corrosion rate is zero (region of cathodic protection). At potentials more noble than O, the current increases with increasing potential; and in the absence of passive film formation, the corrosion rate would continuously increase along the curve towards point C. However, the initiation of a passive film usually begins at the critical point, A, after which the current falls off due to the blockage of the active sites by the protective

film. In the passive region, the corrosion rate has fallen to very low values since the surface is covered with protective film. With further increase in potential, a point D, is reached where either the protective film breaks down, exposing the metal surface to attack once more, or a new electrochemical process such as the evolution of oxygen takes place on the filmed surface. In either case the current increases with increasing potential in the transpassive region E. Film breakdown can occur by the interaction of anions adsorbed from solution with the protective film on the anode surface [1-3].

Another important role played by the electrolyte is the strong dependence of the formation and breakdown of anodic films on the electrolyte composition [3]. In 1930, Jacquet [4] reported that certain metals could be polished by anodizing them at high enough current densities in certain acids or mixtures of acids. He referred to this process as electrolytic polishing; but in more recent times, the term, electropolishing is used. A complete history of the development of electropolishing from a laboratory curiosity to an important industrial process has been traced by Jacquet [5]. For more detailed list of electropolishing paths, one may consult the literature [6-10].

In general, the part to be polished is made anodic by connecting it to the positive side of a dc power source (battery or rectifier). The cell is filled with proper electropolishing electrolyte. The cathode may be constructed from an insoluble conductor, such as stainless steel, graphite, lead or platinum. The distance between anode and cathode varies from 2.5 to 15 mm [8, 11]. The applied current density must be high enough to produce and maintain a thick anodic film on the metal surface. To obtain a polished surface, between 0.05 and 0.25 mm of metal must be removed. Consequently, electropolishing may be used to size an oversized part or to deburr a conventionally machined piece [10]. Electropolishing also increases the corrosion resistance of the machined surface [7,12]. Although electropolishing yields a stress free, thermally unchanged, polished surface, it is slow metal removing process compared to electrochemical grinding (ECG) and electrochemical machining (ECM).

Electropolishing solutions may be classified in two general catagories. Those electrolytes having high electrical conductivity comprise the first group which are based on solutions of H_3PO_3, H_2SO_4, and CrO_3 with or without certain organic addition agents, such as glycerol, alcohols, and ethers. To obtain the required polishing current density, low applied potential is required generally between 1 V and 25 V. Water is often added to the mixture of acids to increase the conductivity of the solutions.

In the second classification of electropolishing solutions are those having low conductivity and requiring the application of high applied voltages in the range of 50 to 220 V to obtain the required current densities. These electrolytes are based on mixtures of $HClO_4$ with organic reagents such as acetic acid and acetic anhydride. There is critical current density below which the anodic film is not formed and polishing is not obtained. Above the critical value, the surface becomes more lustrous at the higher current current densities and the polishing time is less.

Anodic dissolution of metals including molybdenum was studied by various researchers in organic electrolytes. Bellucci, at. el. [13] studied the anodic dissolution of nickel and molybdenum in methanol and water-methanol mixtures. The influence of acidity, water contents and chloride concentration was analysed and was found to be negligible, atleast in the intermediate region of anodic potentials which is the most interesting for practical applications. The experimental data show that in MeOH the possible positive action of molybdenum is certainly not linked to the formation of a stable oxide or insoluble chloride containing compounds.

Similarly, anodic dissolution of titanium, aluminium and cadmium was investigated. Rybalka, at. el. [14] investigated the anodic dissolution of aluminium in 1 M $LiAlCl_4$ solution in propylene carbonate. Al electrode showed reasonable values of the available capacity and discharge current in non-aqueous electrolyte. It was finally concluded that aluminium is a promising anode material for developing non-aqueous Al batteries. Biallozor [15] studied the kinetics and mechanism of cadmium anodic dissolution in organic solvents. He concluded that the anodic dissolution of cadmium in the bromide solutions in organic solvents is a complicated process. The accelerating properties of Br- ions can occur only when the concentration of Br- in the vicinity of electrode during the anodic polarization is large enough.

Anodic dissolution of titanium was investigated by Fushimi, at. el. [16] in chloride containing ethylene glycol solution. The role of chloride ions during anodic dissolution of titanium in chloride salt containing ethylene glycol solution was investigated. The chloride ions were necessary to improve the solution conductivity in dilute solutions, while they decreased the dissolution current in concentrated solutions. They determined the dissolution rate under mass transfer conditions by diffusion of titanium species dissolved from the electrode and the formation of highly concentrated titanium chloride salt on the electrode was suggested. They also suggested the probability of formation of $TiCl_4$ as a dissolution product on the titanium substrate

which might be present at the bottom of the diffusion layer and exhibit characteristic impedance behaviors. The rate of the diffusion of titanium chloride in the solution regulates the whole dissolution rate of titanium in the solution.

Zamin and Mayer [17], describe the process of electropolishing of molybdenum in detail. According to them, following points must be considered in evaluating any solution for electropolishing: (i) the solution must produce a mirror finish; (ii) it must be operational under practical conditions of temperature, voltage, current density, and time; (iii) it must be stable over long periods of time; and (iv) it must be safe and pollution free. Orthophosphoric acid, sulphuric acid and molybdic anhydride composition was used having above given qualities. They agreed on the point of view that a viscous layer or salt layer that is formed at the anode exists next to the anode, through which mass transport is diffusion controlled.

As has been pointed out by Hoar [18], the film should be capable of dissolving rapidly at its outer surface as fast as it forms at the metal/film interface. The importance of the thickness of this film is therefore evident. In light of this view, when the potentiostatic polarization observations are combined with the electropolishing results, it is realized that the solution which produces the best surface finish also yields a film which is readily soluble.

The use of fused and molten salts is increasing in industry with the passage of time for electrochemical dissolution and electropolishing purposes. Molten salts along with ionic liquids represent a new class of electrolytic systems which have drawn attention in recent times [19]. Due to their high corrosive ability, molten and fused salts can be important medium for electrodissolution and electropolishing of refractory metals. Since refractory metals represent a class of metals which are hard to machine, dissolve and polish, therefore the electrochemical processes using suitable electrolytic systems like choline chloride based molten salts represent better choice of dissolution and machining [20].

The purpose of present work is to find new electrolytic systems which are corrosive in nature, and can be used for electrodissolution of refractory metals. The corrosion ability and weight loss analysis of these electrolytic systems has been discussed in detail. NH_4NO_3/NH_3 and choline chloride based binary mixtures has been used as electrolytic systems for the weight loss and corrosion analysis of molybdenum and tungsten. High corrosive ability and room temperature stability of choline chloride

based binary mixtures make them a good choice for the electrodissolution of refractory metals like molybdenum (Mo) and tungsten (W).

1.1 Refractory Metals

Refractory metals are a class of metals which are extraordinarily resistant to heat and water. The most common of the refractory metals are niobium (Nb), molybdenum (Mo) from 5th group and tantalum (Ta), tungsten (W) and rhenium (Re) from 6th group. They all share a unique property of having melting point over 2000 °C. They are hard at room temperature, chemically inert and relatively high density. Since refractory metals have high melting point, they can not be fabricated by casting. Powder metallargy processes are used.

Due to thier extraordinary properties, metals like molybdenum are frequently used in steel industry as alloying metal to increase the strength and corrosion resistance of steel. Tungsten alloys are used in incandecent light bulb filaments, X-ray tubes and superalloys. The temperature stability of niobium-containing superalloys is important for its use in jet and rocket engines. Niobium is also used in various superconducting materials. Tantalum is used in tantalum capacitors in electronic equipments such as DVD players and mobiles phones. Table 1-1, shows the melting points and boiling points of above given refractory metals.

Name	Niobium	Molybdenum	Tantalum	Tungsten	Rhenium
Melting Point (C)	2477	2623	3017	3422	3186
Boiling Point (C)	4744	4639	5458	5555	5596
Density (g/cm^3)	8.57	10.28	16.69	19.25	21.02

Table 1-1: Some physical properties of refractory metals

1.1.1 Molybdenum

Molybdenum is a 6^{th} group element which is silvery metal, has sixth-highest melting point of any element. Molybdenum always occurs in various oxidation states in minerals. Molybdenum has 35 known isotopes from atomic mass 83 to 117. Molybdenum-98 is the most abundent isotope, comprising 24.14% of all molybdenum. Most stable oxidation states of molybdenum are +4 and +6 in aqueous systems [21].

The surface of molybdenum is covered with its oxide which is most probably MoO_2 at room temperature. The bulk of oxidation occurs at temperature over 790 °C, resulting in MoO_3 which represents the highest oxidation state in molybdenum [22, 23]. Following table shows the atomic properties of molybdenum.

Oxidation States	Electronegativity	Ionization Energies (KJ/mol)	Atomic Radius	Covalent Radius
6, 5, 4, 3, 2, 1, -1, -2	2.16(Pauling Scale)	1st: 684.3 2nd: 1560 3rd: 2618	139pm	154±5 pm

Table 1-2: Atomic properties of molybdenum with all oxidation states.

Mo(III) compounds are unstable while molybdenum mostly forms oxides and hydroxides in oxidation state +6. Molybdenum (VI) oxides are soluble in alkaline solutions and form molybdates (MoO_4^{2-}) [24]. Due to the broad range of oxidation states of molybdenum, it is found in various molbdenum chlorides [46].

- Molybdenum(II) chloride $MoCl_2$ (yellow solid)
- Molybdenum(III) chloride $MoCl_3$ (dark red solid)
- Molybdenum(IV) chloride $MoCl_4$ (black solid)
- Molybdenum(V) chloride $MoCl_5$ (dark green solid)
- Molybdenum(VI) chloride $MoCl_6$ (brown solid)

Electronic configuration of molybdenum shows the presence of d orbital electrons which gives molybdenum the electronic configuration of [Kr] $5s^1$ $4d^5$ making d block element. Molybdenum (Mo) is a refractory metallic element used principally as an alloying agent in steels, cast irons, and super alloys to enhance hardenability, strength, toughness, wear and corrosion resistance. Moreover, molybdenum finds significant usage as a refractory metal and in numerous chemical applications such catalysts and at high pressure and high temperature as lubricants. Molybdenum scrap (Mo Scrap) and molybdenum alloy scrap (Mo Alloy Scrap) are very unique with their position as a high temperature scrap metal and high temperature alloy scrap [25]. Pure molybdenum scrap has a melting point of 2,612 ^oC, higher than other scrap metals such as steel. High temperature, high stiffness, high thermal conductivity, low coefficient of thermal expansion and chemical compatibility with a variety of environments make this metal attractive candidate for use under aggressive conditions and media. Electrochemical

Machining (ECM) of molybdenum is a significant technique for electrochemical shaping, scrap recycling and preparation of Mo-Compounds by the help of usable electrolytes and conditions [26].

Electrochemical behavior of molybdenum has been studied by [27] which discuss the kinetics of anodic dissolution as well the electrochemical investigation of dissolved metal ions in alkaline solutions. The strong alloying properties and high corrosion resistance makes molybdenum good component of steel industry. The use of organic solvents to study corrosion of molybdenum has been discussed in by Bellucci, et. al. [28]. They used methanol and water methanol mixtures to study the influence of acidity, water contents and chloride ion concentration. It was concluded that these three factors have little influence in the internediate region of anodic potentials which is of great importance from application point of view. They described the corrosion of molybdenum in terms of a specific action of oxide formed by other alloying elements.

Corrosion investigations in agrresive media containing chloride ions were conducted [29] and the effect of chloride ion concentration in acetic acid on steel corrosion was analysed. Potential-time and electrochemical polarization measurements show a step increase in potential indicative of the formation of a protective film and passivation. Polarization scans in 70% acetic acid solution give rise to an active to passive transition. XPS surface analysis show the presence of Mo in the low potential (active) region near electrode surface. Further increase in potential causes a dissolution of molybdenum.

It has been well established that molybdenum resists corrosion in aggressive media due to the formation of oxide film [30-31]. The protective oxide film is maily formed by the oxides of molybdenum either naturally or anodically. In alkaline media MoO_3 and $Mo(OH)_3$ films were identified by Hull [27]. In acidic media Hull identified MoO_3 besides MoO_2 in passive film on molybdenum. However in all the electrolytes including those containing chloride ions, the final soluble anodic product of metal or the oxide film dissolution is molybdenum (VI) in the form of molybdate or molybdic acid according to the pH of the solution [32]. It was also concluded that the most stable oxide film is formed acidic media.

Hull used the linear sweep method to investigate the effect of scan rate and concentration of electrolyte on a stationary wire electrode. He correlated three oxidation waves on the anodic sweep with three visibly distinct films on the electrode

surface. After investigations, he assigned oxidation states of (III), (IV) and (VI) to three oxides. Hull also discussed the possibility of the presence of Mo (V) in different electrolytic systems under different conditions. He also described the similar electrochemical behavior of Mo, Cr and W with same shape of current-voltage curves in alkaline solutions.

Electrochemical behavior of molybdenum in chloride and hydroxyl ions containing systems was discussed by Badawi et.al. [33]. They studied the variation of open circuit potential with time hence investigated the kinetics of the film growth on electrode surface. A gradual increases in potential was observed for the beginning of experiment and then a steady state situation was observed which is an indication of presence of an already existing oxide film which gets thick with the passage of time. Increase in potential towards positive potential values at initial stage is due to the pre-imersion oxide film at electrode surface.

The variation in film thickness on molybdenum with potential and time was also observed by Povey [34]. X-ray photospectroscopy (XPS) technique was used to analyse the ionic species at electrode surface. A dark brown film was observed at electrode surface with grew dark as the thickness of film increased rather than potential. They also agreed on the formation of intermediate oxidation states along with Mo (VI). However it was not possible for them to conclude which specific intermediate oxidation state would be present at certain time and potential range yet they were able to propose a mechanism.

Bojinov et al. discussed the kinetics of formation and properties of barrier oxide film on pure molybdenum in 85% H_3PO_4 [35]. They used photelectrochemical technique to investigate the passivation caused by oxide film and identified the presence of MoO_3. They also measured Mo passivation via the formation of thin continuous barrier like layer which dissolves to maintain quite high values of steady state current density. A number of reaction pathways were discussed involving different intermediates like Mo (III), Mo (IV), Mo (V) and Mo (VI). Presence of Mo (V) was first reported by Bojinov, et. al.

Anodic oxidation of molybdenum in weakly alkaline, nearly neutral and weakly acidic electrolytes was studied by M. Petrova, et. al., using voltammetric and electrochemical impedance spectroscopic measurements [36]. Two parallel pathways of anodic dissolution were suggested by due to the presence of two pseudo-tafel regions. Impedance measurements show the presence of atleast two intermediates.

They discussed in detail the presence of Mo(V) as reaction intermediate in the formation of Mo(VI). However the anodic film formed was supposed to be very thin and conductive. Surface analytical results also show the formation of a mixed valence oxide containing Mo(IV), Mo(V) and Mo(VI).

Bojinov [37] studied the transpassive behavior of Mo in H_2SO_4 using steady state and voltammetric methods. According to them the anodic polarization curve of Mo in H_2SO_4 can be divided into three regions: a Tafel like region, a transition region in which there is pronounced curvature in the log *i*-E and a second Tafel region where current increases more slowly with potential. An anodic peak was observed in the positive sweep, followed by the cathodic peak in negative sweep. The dependence peak current and potential on sweet rate indicates a mass transfer controlled dissolution process.

Corrosion and passivation behavior of molybdenum was aslo studied by Badawi and Al-Kharafi [38]. They used aqueous solutions of different pH and found out the steady state electrode potential of molybdenum as a linear function of the solution pH. The molybdenum surface is always covered with a passive film. Polarization measurements show that passive film is more stable in acidic solutions. However under alkaline conditions the stability of passive film decreasesdue to the formation of soluble species like $HMoO_4^-$ and MoO_4^{2-}. The passive or barrier film was found to be continuous and its behavior was affected by the temperature.

The above given informations show that molybdenum is passivated under both acidic and basic conditions. A continuous passive film acts like a barrier and covers the molybdenum surface. The passive film is formed due to the oxidised metal ions from molybdenum surface. Molybdenum dissolves in different oxidation state but most recent investigation by M. Petrova, et. al., show that Mo(V) oxidation state is the start in dissolution process. A change in the oxidation state and surface reactions go on has been observed and Mo(VI) and Mo(IV) can be other species at electrode surface.

1.1.2 Tungsten

Tungsten is a group 6^{th} element found naturally on earth only in chemical compounds. In general, due to the presence of impurities, tungsten is very brittle making it difficult to work. However pure tugnsten is ductile and be cut with hacksaw [39].

Tungsten is found in five isotopic forms whose half lives are so long that they can be considered stable. The most common oxidation state of tungsten is +6, but it has all oxidation states from -2 to +6. Tungsten typical forms tungsten oxide WO_3 with oxygen, which dissolves in aqueous alkaline solutions to form tungstate ions, WO_4^{2-} . Following table shows the atomic properties of tungsten.

Oxidation State	Electronegativity (Pauling Scale)	Ionization Energies (kJ/mol)	Atomic Radius	Covalent Radius
6, 5, 4, 3, 2, 1, 0, −1, -2	2.36 (Pauling scale)	1st: 770 2nd: 1700	139 pm	162±7 pm

Table 1-3: Atomic properties of tungsten with all oxidation states.

Tungsten reacts with oxygen to form tungsten oxide, WO_3. Tungsten resists the attacks of oxygen, acids and alkalis [40]. Heating of powdered tungsten with carbon produces tungsten carbides (W_2C). W_2C is resistant to chemical attack, although it reacts strongly with chlorine to form tungsten hexachloride (WCl_6). In aqueous solution, tungstate gives the heteropoly acids and polyoxometalate anions under neutral and acidic conditions. As tungstate is progressively treated with acid, it first yields the soluble, metastable "paratungstate A" anion, $W_7O_{24}^{6-}$, which over time converts to the less soluble "paratungstate B" anion, $H_2W_{12}O_{42}^{10-}$. Further acidification produces the very soluble metatungstate anion, $H_2W_{12}O_{40}^{6-}$, after which equilibrium is reached [41].

Tungsten and other refractory metals are distinguished from rest of the metals by their ability to form highly protective oxide films which dissolved anodically in aqeuous media. Open circuit potential was found to be pH and nature of electrolyte dependent by Koerner [42]. This dependence was thought to be due to the presence of appreciable amount of oxides and hydroxides mainly $W(OH)_6$. This compound was believed to be breakdown to tungstic cations in acidic electrolytes and anions in basic electrolytes. Anodic polarization however forces a surface film color change with a definite sequence. Earlier passivation of tungsten was attributed to the low solubility of oxide film in acidic media while active solubility in basic media. Besson and Drautzburg reported a study of anodic dissolution of tungsten in various electrolytes and believed that tungsten dissolves in +6 oxidation state [43].

Anodic dissolution of tungsten was studied by Johnson and Wu in H_2SO_4-K_2SO_4 and K_2SO_4-K_2CO_3-KOH solutions [44]. They determined the faradaic efficiency in these basic solutions and suggested that tungsten dissolved in +6 oxidation state and tungsten forms protective film of WO_3. According to them when tungsten is placed in solution, it quickly forms a film of W_2O_5 that completely covers the electrode surface and further reaction is not possible until a change in pH. When tungsten is polarized, appreciable conductivity of W_2O_5 allows further electrochemical oxidation to WO_3 which is then solvated by H_2O to form H_2WO_4 which slightly soluble in acidic media and is soluble in basic media.

Lillard, et. al., used surface enhanced raman spectroscopy (SERS) to investigate the nature of oxide film on tungsten in acidic and alkaline media. They investigated that at anodic potentials $WO_3(H_2O)x$ content in oxide film is greater than the WO_3 content, while at cathodic potentials the WO_3 content was larger. A dissolution mechanism was proposed in which tungsten metal dissolution is limited by the presence of loosely bound $WO_3(H_2O)x$ layer from the surface. In other words, passive dissolution is limited by mass transport of a loosley bound $WO_3(H_2O)x$ layer. Further experiments demonstrated that the rate determining step for the dissolution of tungsten in acidic media is always the discharge of the adsorbed species [45].

From practical and fundamental point of view, anodic film growth is an important field of investigation in electrochemistry. Bojinove [46] described the barrier film growth on tungsten in acidic solutions. He proposed a model which represent a further development of the surface charge approach which is consistent with experimental data of passive tungsten in H_2SO_4 and H_3PO_4 solutions in a wide range of potentials and acid concentrations.

Kinetics of growth of the passive film on tungsten was also discussed by Macdonald, et. al., in acidic phosphate solutions [47]. They described the growth of passive film in terms of Point Defect Model (PDM). PDM predicted a linear relationship between the steady state film thickness and applied potenial. The predictions of this model were also consistent with the experimental observations for passive tungsten.

The electronic structure of passive film formed on tungsten was discussed by Sikora, et. al., [48]. They considered the existance of outer insulating layer on a defective WO_3 barrier layer. They found that primary defect in the barrier layer is due to the oxygen vacancy, which is concentrated in the region of barrier layer adjacent to

the metal. Outer layer is formed either restructuring of the outer surface of barrier layer or by hydrolysis of the incepient cations or both. The calculated and experimental data were in agreement and authors were convinced that tungsten surface film is nonhomogeneously doped bilayer structure.

Potentiodynamic investigations by Seo, et. al., were done using some different mixtures of oxidizers ($Fe(NO_3)_3$, KIO_3 and H_2O_2) in order to examine the electrochemical corrosion behavior of tungsten [49]. Electrochemical polishing mechanism of tungsten is greatly influenced by the already mechanically and chemically polished surface. The nature of tungsten oxide layer formed at electrode surface was characteristic to the electrolytic system used and hence showing different corrosion effects.

pH has a great influence on the anodic behavior of tungsten in an electrolytic system. Anik, et. al., used potentiodynamic and potentiostatic polarization to study the anodic behavior of tungsten in different pH systems from 0.5 to 13.5 [50]. The oxide layer on tungsten showed a typical amphoteric behavior in acidic pH region and there was no observed diffusion effect in acidic region. However dissolution was H^+ assisted in the region below pH 1. The dissolution process in pH between 4.5 and 6.5 was mixed control of reaction kinetics and WO_4^{2-} dffusion. Anodic dissolution kinetics and hence the current was controlled by slow diffusion of OH^- ions.

Further investigation on the anodic oxide growth were carried out in H_2SO_4 and Na_2SO_4 mixture on stationary and rotating electrodes by Verge, et. al., [51]. With the use of different electroanalytical techniques like impedence spectroscopy and electrochemical quartz crystal microbalance, they were able to show that convective condition have affect on the film growth and film thickness. However on stationary electrode, film growth continued for prolonged time, because the mass transport of dissolution products away from anode. They also confirmed the dissolution of tungsten in hexavalent state at 100% efficiency. They explained the behavior with bilayer model of anodic film where only outer layer thickness depended on the convextion.

One of the important factor affecting the dissolution process of tungsten is concentration of the active species in electrolyte. Anik [52] investigated the effects of concentration gradiant on the anodic behavior of tungsten. Several electrochemical techniques including potentiostatic polarization surface pH measurements were used to investigate the effects of tungstate ions on the anodic behavior of the tungsten. He added tungstate ions in the electrolyte which is also the dissolved anodic specie in the

solution from tungsten, this addition decreased the anodic current around the point of zero charge. This addition of WO_4^{2-} also increased the the current from neutral to weekly basic range and have no effect on the anodic current in strongly basic conditions. This difference and variable effect is due to the competition between the stabilization of tungsten oxide due to higher concentration of the dissolved species at the metal metal surface and the stabilization of the local pH as result of enhanced polymerization reactions of tungstate species.

Anik recently used DC polarization techniques to investigate the pH dependence of anodic behavior of tungsten in basic solutions [53]. He concluded that anodic current of W was independent between pH 8 to 11. In more basic media however, anodic current increased with the increase in pH. Hydrate layer formation of tungsten oxide appears in all pH ranges but this hydrate layer is loosly bonded at higher pH and results in polished surface of W. At higher pH, the slow OH^- diffusion from bulk solution to the electrode surface took place in the diffusion control and the anodic process was controlled by diffusion at higher pH values.

1.2 Deep Eutectic Solvents

Deep Eutectic Solvents (DESs) are liquids at room temperature that have physico-chemical properties very similar to ionic liquids (ILs). These liquids are more environmentally friendly than volatile organic solvents because of their near-zero volatility, suggesting that these are attractive substitutes for conventional solvents for use in electrochemistry [54]. One of the well known liquids of this kind was first prepared by Abbott, et. al. [55] by mixing choline chloride with urea; this solution is liquid at 12 $^{\circ}$C. Due to their growing importance in the field of chemistry and beyond, these solutions are being used as room temperature solvents for many organic and inorganic chemical processes [56].

Hence, it is important to measure the thermal stabilities as well as their electrochemical potential windows for further applications in this field. Different cations and anions have been shown to influence the properties exhibited by these liquids, including viscosity, density, conductivity, melting and decomposition temperatures [57]. It has also been reported that oxidation and reduction of anionic and cationic components, respectively, determine the cathodic and anodic limits [58].

Developing new kind of liquids and investigating their properties has been the topic of much interest in recent years [59, 60, and 61].

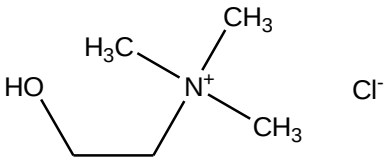

choline chloride

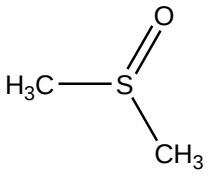

dimethyl sulphoxide

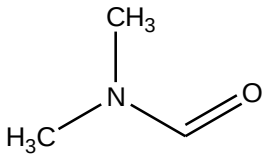

dimethyl formamide

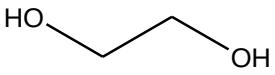

ethylene glycol

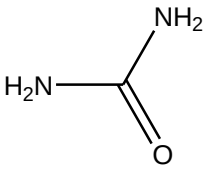

urea

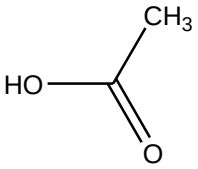

acetic acid

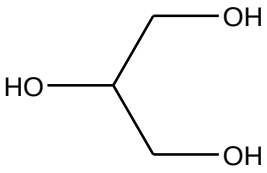

glycerol

Figure 1-2: Choline chloride and various hydrogen bond donors.

Present work focuses on the TGA and DSC analysis of binary mixtures based on choline chloride and any one of the hydrogen bond donors (HBD), which are AA (acetic acid) EG (ethylene glycol), PG (propylene glycol), DMSO (dimethyl sulphoxide), DMF (dimethyl formamide) and Urea. Part of the present work is also investigating the electrochemical studies of these solutions [62]. Zhang and Bond studied the electrochemical window of numerous ionic liquids and more conventional solvents on gold, glassy carbon and platinum working electrodes [63]. Herein we report the electrochemical windows at platinum and tungsten as working electrodes.

Choline chloride is a quaternary ammonium salt that has the ability to form bondings with hydrogen bond donors (HBD) shown in figure 1-2. The eutectic mixtures formed have potential windows that tend to be controlled by the stability of the carboxylic acid, amid or alcohol. In general the potential windows depend upon the pKa of the HBD. The potential windows observed in these mixtures are smaller than some imidazolium based ionic liquids but still wide enough for metals like zinc and nickel to be electrodeposited with high current efficiencies. These eutectics of type III have the advantage that they are relatively benign and inexpensive and can thus be applied to large scale processes [64-66].

1.3 Electrolytic systems for dissolution and polishing

Choline chloride based binary mixtures are prepared by mixing choline chloride in certain molar ratio with a hydrogen bond donor (HDB) e.g. urea and ethylene glycol to make so called deep eutectic solvents (DES) [67,68]. The term deep eutectic solvents (DES) has been used to differentiate these liquids from traditional molten salts. They are environment friendly solvents and have been of major interest in the field of electrochemistry in recent years [69]. Their physicochemical properties are comparable to those of room temperature ionic liquids (RTILs). Due to low lattice energies which results in low melting points, these DESs are liquid at room temperature and compared to conventional organic solvents, these have low vapor pressure and high thermal and chemical stability [70].

DESs have an advantage over ionic liquids (ILs) in terms of being cheap and can be easily prepared from non-toxic chemicals. They have fairly large electrochemical window and this makes them a good choice for electrochemical investigations of reaction mechanisms and mechanistic pathways. Their electrolytic properties make them a good future candidate for application in electropolishing, electrodeposition and photoelectrochemistry [71]. Looking at their stability over a wide potential range, DES can be of major interest in near future as green reaction medium for several chemical and electrochemical reactions in chemistry and biology.

Cyclic voltammetry is a versatile electrochemical technique that helps in understanding the reactions mechanism going on at the electrode-electrolyte interface. This method gives valuable information regarding the stability of oxidation state and

rate of electron transfer between electrode and analyte [72]. Applications of cyclic voltammetry have been extended to almost every aspect of chemistry: for example, the investigation of biosynthetic reaction pathways and the investigation of ligand effect on the metal complex potential as well as enzymatic catalysis [73-76]. Cyclic voltammetry is the basic electrochemical technique for the measurement of current as a function of applied potential over a certain range. Ferrocene, namely bis-cyclopentadienyl iron (II), is a molecule with a sandwich type structure in which iron atom is sandwiched between two five member carbon rings [77,78]. It has been proposed that the oxidation of Ferrocene $Fe(C_5H_5)_2$ to the ferrocenium cation $Fe(C_5H_5)_2^+$ is a standard one electron transfer reversible process because the rate of electron transfer is very fast [79,80]. Consequently, the redox system $Fe(C_5H_5)_2^+/Fe(C_5H_5)_2$ has received considerable attention in electrochemistry and this system was used for instrumental and reference potential calibration in organic media [81].

CC/PEG200 (choline chloride/polyethylene glycol 200) and CC/PEG600 (choline chloride/polyethylene glycol 600) systems are proposed for the first time and have been used to investigate the electrochemistry of ferrocene. A comparison of electrochemical behavior of ferrocene has been made among previously reported electrolytic systems [82-88] and newly reported CC/EG, CC/PEG200 and CC/PEG600. Investigations of $Fe(C_5H_5)_2^+/Fe(C_5H_5)_2$ couple in three deep eutectic solvents of choline chloride with ethylene glycol (EG), polyethylene glycol (PEG200) and polyethylene glycol (PEG600). The purpose of investigation was to broaden the applicability of DES in various fields of chemistry and biology by studying the electrochemical reaction of ferrocene in these solvents.

During the last few years, non-aqueous media have been widely investigated for a variety of applications: the use as solvents for chemical synthesis [89,90], media for electrodeposition of metals [91–93], electrolyte for electrochemical devices such as battery [94], supercapacitors [95-96]. Previous investigations show that it is impossible to deposit molybdenum electrochemically from aqueous system, reason being molybdenum metal ions form complexes immediately with OH^- [97-98]. The part of present work is conducted to study the possibility of NH_4NO_3/NH_3 system as electrolyte for the electrochemical dissolution of molybdenum under non-aqueous conditions. 1.0 M solution of ammonium nitrate in liquid ammonia from -35 ^oC to -60 ^oC was investigated. The following reaction mechanisms are responsible for the

conduction with simple dissociation of NH_4NO_3 into ammonium cation and nitrate anion and self dissociation of ammonia into NH_4^+ and NH_2^-.

$$NH_4NO_3 \xrightleftharpoons{NH_3} NH_4^+ + NO_3^- \quad (1\text{-}1)$$

$$2NH_3 \rightleftharpoons NH_4^+ + NH_2^- \quad (1\text{-}2)$$

Complex formation of nickel, cobalt and chromium is known from literature [99-100] which combines with NH_3 and NO_3^- to form various complexes. Similar complex formation can be suggested for Mo and the immediate color change of electrolyte from white to dark brown and then to light yellow may be due to the formation of $[Mo(NH_3)_5(NO_3)]^{4+}$.The electrolyte showed conductivity up to 50mS/cm, which makes electrolyte highly conductive. Anodic dissolution of metal in this medium was significant at +4.0 V and the cell potential difference increased at constant current with the passage of time. Later the electrolyte was analyzed for possible molybdenum complex and XRF showed the presence of molybdenum. The major achievement of the present investigation was the electrodeposition of anodically dissolved molybdenum at molybdenum cathode with a redeposition ratio up to 76%.

1.4 Electrodissolution of Molybdenum and Tungsten

The dissolution of a metal can be increased by connecting the metal with a dc, external source of potential, such as a battery or rectifier, to the metal so that it is made anodic with respecto to a physically separate counter electrode. Only the anodic process takes place on the corroding metal under these conditions, and electrolyte provides a means of maintaining the anodic and cathodic process physically separate. The rate of metal dissolution can be lowered or increased by decreasing or increasing the applied potential. Such a process is called electrodissolution or anodic corrosion.

Surface treatment is often required for the practical application of refractory metals like molybdenum (Mo) and tungsten (W). Previously sulfuric and nitric acids have been used for electrochemical polishing of molybdenum [101]. However these solutions are hazardous and very toxic. Deguchi et al. reported electropolishing method using ethylene glycol solution containing NaCl that has a weak toxicity

compared with conventional solutions [102-103]. Some of the authors have also investigated the electrochemical reaction in a NaCl-ethylene glycol solution where tetravalent species were formed by the anodic polarization of titanium [104].

A part of present work focuses on the study of choline chloride based deep eutectic solvents (DESs) as electrolytes for the electrochemical dissolution of molybdenum and tungsten. Deep eutectic solvents possess physicochemical properties that are comparable to the room temperature ionic liquids (RTILs).

Unlike the chloroaluminate and chlorozincate melts former of which are water sensitive and later are more viscous, choline chloride and urea produce eutectics that are liquid at ambient temperature and have unusual solvent properties. The eutectics are formed at a urea to choline chloride ratio of 2:1, EG to choline chloride ratio of 2:1 and glycerin to choline chloride ratio 1:1. The freezing point of the mixture is generally considerably lower than the melting point of either of the constituents, e.g. freezing point of urea and choline chloride mixture is 12^{o}C, which is lower than melting point of choline chloride 302^{o}C and urea 133^{o}C, hence allowing the mixture to be used as an ambient temperature solvent [105, 106].

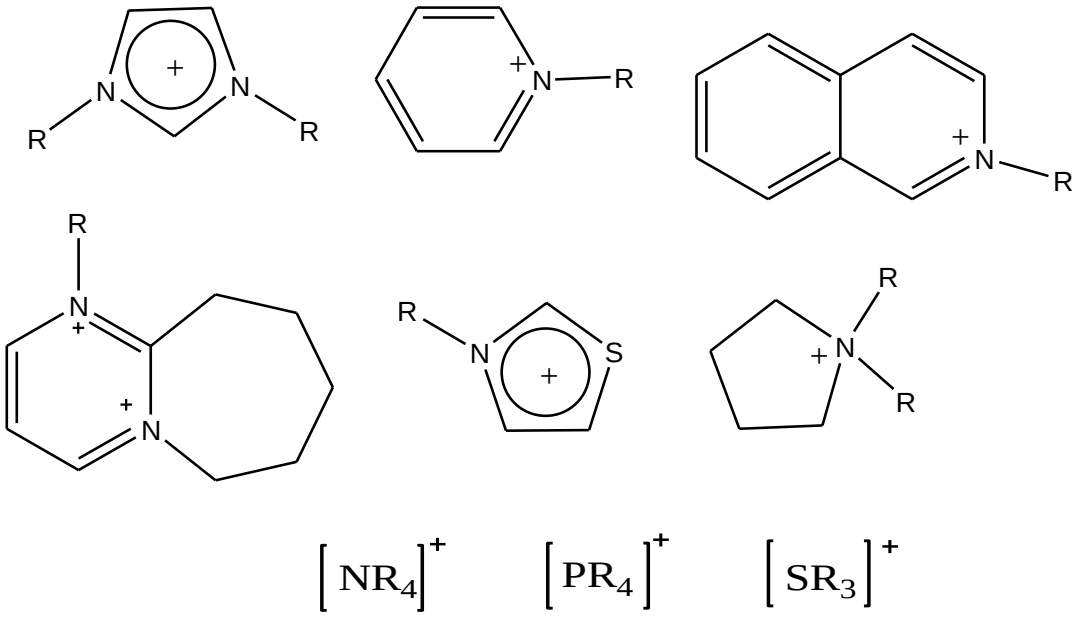

Figure 1-3: Examples of cations commonly used in ionic liquids ("Ionic Liquids in Synthesis" by Peter Wasserscheid)

a.

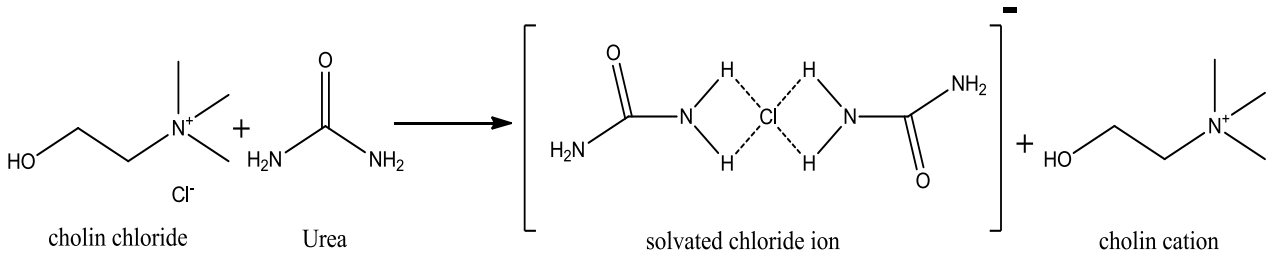

b.

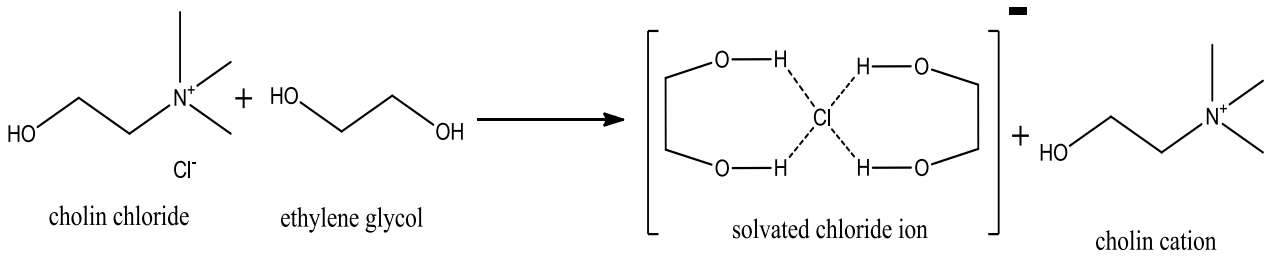

c.

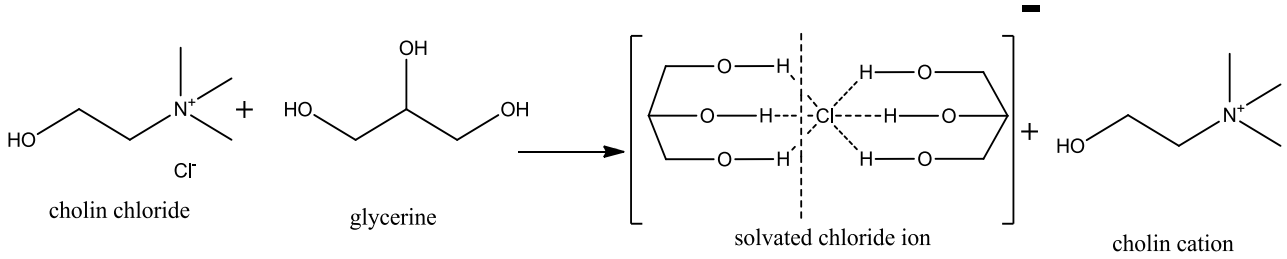

Figure 1-4 (a, b, c): Structure of choline chloride and different hydrogen bond donors (HBDs) indicating the hydrogen bonding of chloride ions with a. urea (CC/Urea), b. ethylene glycol (CC/EG) and c. glycerin (CC/Gly), forming quaternary ammonium cations and large anions.

Eutectic solvents are highly conducting (ca. 1 mS cm^{-1} at 30^{o}C), confirming that the ionic species are dissolved in the liquid and can move independently [107]. Ionic species in this type of eutectics are quaternary ammonium cation and chloride anion. Cations move independently in the solution while anions are surrounded by the hydrogen bond donors (HBDs) which in this case are urea, ethylene glycol (EG) and

glycerin (Gly). Molybdenum (Mo) and tungsten (W) belong to the group of refractory metals which are hard to machine, tool and polish as they have high melting points, hardness and mechanical strength. Electrochemical Machining (ECM) of refractory metals is a significant technique for electrochemical shaping, scrap recycling and preparation of Mo-Compounds by the help of usable electrolytes and conditions [108].

Anionic and cationic species formed within these binary mixtures are given above. Figure 1-3 shows the cationic species usually used to make ionic liquids [109]. Figure 1-4 (a, b, c) shows the formation of anionic and cationic species in choline chloride and three HBDs namely urea, ethylene glycol and glycerin. It can be seen that the chloride ions are surrounded by the HBD species via strong hydrogen bond. This bonding mechanism also assists in the movement of ions within the solution [110].

1.5 Weight Loss Calculations by Faraday's Law

Corrosion of a metal can be calculated using Faraday's law, which shows that one singly charged ion carries q = 1.6×10^{-19} coulumb (A-sec) of charge. The transfer of one mole corresponds to a charge of F = q. N_A = 96500 A.sec, (N_A is avogadro's number). F = 96500 coulumb is Faraday's constant. The dissolution of a mole of metal at the anode of a metal with valence *n* requires a total charge of *n*F. The weight loss w (in grams), at the anode, is

$$w = ItM/nF \qquad (1\text{-}3)$$

where M is the atomic or molecular weight. The quantity *w/t* can be viewed as corrosion rate. Calculation of weight loss using this methode is an application of Faraday's Law [111]. The percentage weight loss during anodic dissolution is calculated by dividing the original weight loss by calculated weight loss using Faraday's law and multiplying by 100.

2 Experimental Work

Experimental work is divided into two parts, first part comprises of the intrumental setup and chemicals and preparation of samples, second part consists of experimental techniques used during all the work.

2.1 Ammonia-Ammonium Nitrate System with Molybdenum

A conventional double jacket corrosion cell was used for checking the electrochemical dissolution and electrochemical deposition of molybdenum. Anode made of pure Mo (99.9 %) with an exposed surface area of 1.0 cm^2 was used while three types of cathodes (Mo, Cu and Fe) each with surface area 1.0 cm^2 were used. The surface of electrodes was treated by mechanical polishing with finer grade emery paper (600), rinsing with distilled water and drying. A cryostat was used to cool and condense ammonia gas to liquid ammonia in the cell and the experiment was carried out at -35 ^oC.

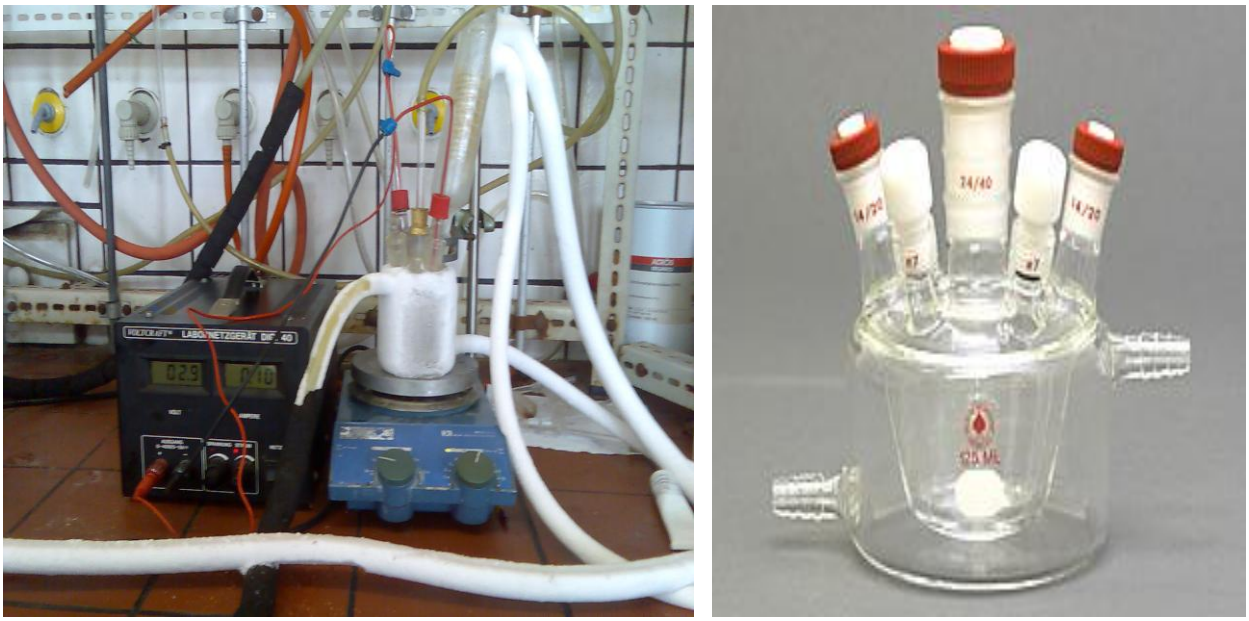

Figure 2-1: (Left) Instrumental setup used for anodic dissolution of molybdenum in NH_4NO_3/NH_3 system at -60 ^oC. (Right) A typical double jacket cell used for anodic dissolution.

Ammonium nitrate used as electrolyte was dried for 24h at temperature 150^{o}C and transferred immediately into the cell after cooling the desired amount. 1.0 molar solution of NH_4NO_3 in liquid ammonia was prepared by the help of magnetic stirring inside the cell. A DC power supply was used for applying constant current of 100 mA at varied potential (+2.1 to +5.1 V).

For the cyclic voltammetry experiments to check the electrochemical potential window and the electrochemical behavior of molybdenum in NH_4NO_3/NH_3, three electrodes system was used with platinum as a counter electrode and silver gauze as reference electrode. Cyclic voltammograms were measured by an Autolab apparatus PGSTAT128N from Eco Chemie, Netherlands. The experiments were carried out under continuous supply of nitrogen in the cell to avoid water and moisture contents. After the electrochemical treatment the electrolyte was washed with methanol. Since ammonium nitrate dissolves up to 40% in methanol at 60^{o}C, the un-dissolved material was separated as residue.

The residue left behind was dried and then analysed for possible molybdenum compound. XRF and XRD techniques were used for checking the molybdenum deposited on cathode and molybdenum dissolved in the electrolyte. XRF measurements were made on Fischerscope X-Ray XAN-FD 603-153 instrument while XRD measurements were carried out at Bruker AXS Kappa APE II diffractometer using Mo Ka radiation. Cyclic voltammetry of molybdenum was also performed with imidazolium/1-Butyl-3-methyl-imidazolium-trifluoromethansulfonat at room temperature and the results were compared with NH_4NO_3/NH_3 system

2.2 Anodic dissolution of molybdenum in choline chloride based binary mixture

A conventional double jacket corrosion cell was used for checking the electrochemical dissolution of molybdenum and tungsten. Both metals of purity Mo (99.9 %), W (99.9%) with an exposed surface area of 1.0 cm^2 for each were used while tungsten as cathode with surface area 1.0 cm^2 was used in galvano-static experiments. For anodic polarization experiments along with working electrodes W and Mo, platinum (Pt) was used as counter electrode and silver wire as reference electrode. For galvano-static experiments two electrode system was used. The surface of each electrode was treated

by mechanical polishing with finer grade emery paper, rinsing with distilled water and drying.

Choline chloride was dried up to 110^{o}C under vacuum to remove water contents. Ethylene glycol (Aldrich 99.8%) contains 0.1% of water, glycerin (Aldrich 99.8%) contains 0.1% of water and urea (99%) contains 0.05% of water, were used as such obtained. Each eutectic was formed at different temperature. Choline chloride and urea mixture was heated up to 90^{0}C, the melt was then transferred into the cell and it stayed liquid at room temperature. Choline chloride with ethylene glycol and glycerin forms eutectic mixtures that are liquid at room temperature. The experiments were performed at 25^{o}C.

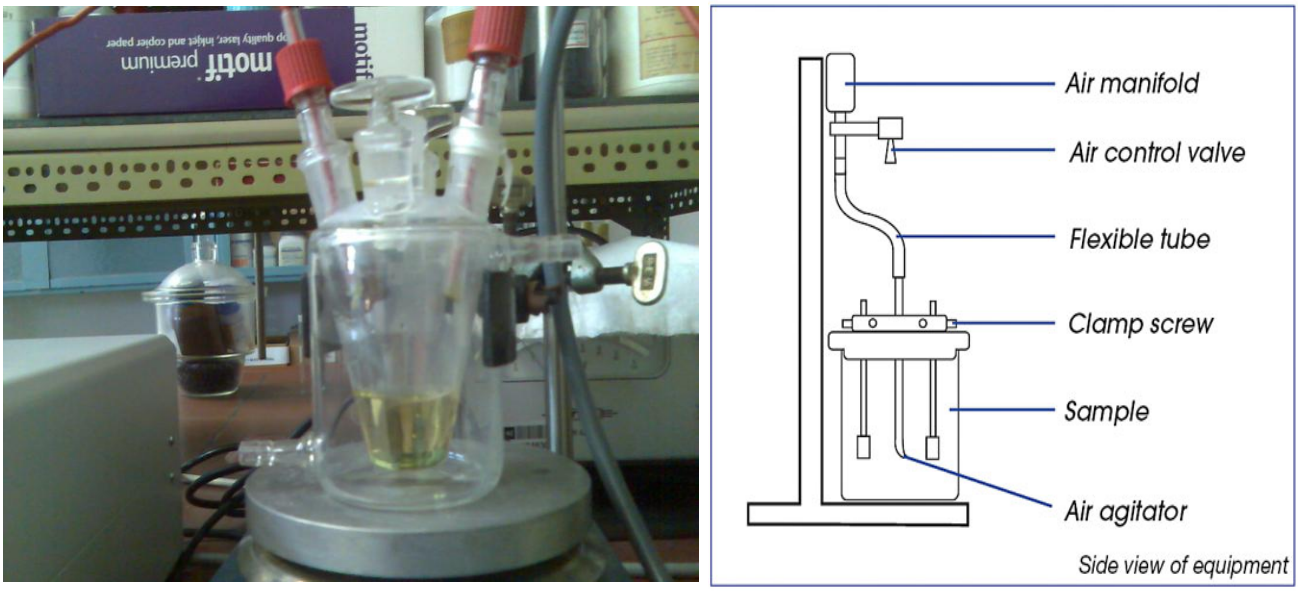

Figure 2-2: (Left) Instrumental setup for checking the anodic dissolution of molybdenum and tungsten in choline chloride based binary mixtures. (Right) The side view of the corrosion cell.

A continuous supply of helium was passed through the cell to avoid moisture. Galvano-static experiments were conducted between 10mA and 150mA and the potential varied between 2 to 6 V at 25^{o}C. Ministat (Sycopel) apparatus was used for galvanostatic experiments and weight loss of molybdenum and tungsten was calculated after one hour time. Radiometer (voltalab PGZ 301) was used for anodic polarization experiments and cyclic voltammograms were obtained.

It is important to mention that galvanostatic experiments were conducted at different current densities. However a typical current density of 100 mA/cm^2 was used to calculate the weight loss of molybdenum and tungsten. Cell voltage was measured with two electrode systems for weight loss experiments at constant current. Three electrode system was only used in cyclic voltammetry experiments.

2.3 Sysnthesis of Choline chloride based binary mextures

2.3.1 Chemicals

Choline chloride (CC), ethylene glycol (EG), polyethylene glycol (PEG200), polyethylene glycol (PEG600) and ferrocene were all reagent grade. Choline chloride was dried under vacuum at 110^{o}C for 48 hours to get rid of moisture contents while all other chemicals were used as received. DES was formed by mixing choline chloride with EG, PEG200 and PEG600 in molar ratio 1:2, 1:5 and 1:10 respectively at room temperature. Ferrocene was dissolved in all three solutions at an initial concentration of 0.0025 $mmol/dm^3$.

2.3.2 Preparation of solutions

Binary mixtures of choline chloride with EG, PEG200 and PEG600 were prepared at room temperature by carefully mixing the desired ratio of both the components. CC:EG mixture was in 1:2 ratio, CC:PEG200 mixture was in 1:5 ratio and CC:PEG600 mixture was in 1:10 ratio. The solubility of choline chloride in these three liquids decreases in the order EG > PEG200 > PEG600. Binary mixture produced thereafter was a stable liquid at room temperature and was kept under argon to avoid the moisture. 10ml of 0.0025 mM ferrocene solutions were taken in double jacket cell for each cyclic voltammetry experiment. Samples for IR experiments were prepared carefully avoiding moisture contents. CsBr (cesium bromide) pellets were used as windows in IR cell.

2.3.3 Instrumental Setup

Computer controlled electrochemical measurement system equipped with potentiostate PGZ 301 of Voltalab-Radiometer Analytical for cyclic voltammetry experiment was used. Infrared spectroscopy was done by Perkin-Elmer 300 spectrometer with computer controlled setup. Karl Fischer titration instrument from Metrohm was used for water content determination in three solutions and it was possible to bring the water content level down between 200 ppm to 250ppm.

The cyclic voltammograms were recorded at different scan rates (from 0.001 to 0.15 V/sec) depending on the solution. Typical corrosion cell with double wall was used for these experiments and cell was thermostated using a bath of water at 25^0C to keep temperature of the cell constant. Platinum (Pt) and glassy carbon (GC) electrodes with surface 0.07 cm^2 each from Metrohm were used as working electrodes for these investigations. Silver (Ag/Ag^+) wire was used as reference electrode and platinum (Pt) was used as counter electrode for these experiments. It was checked and verified that there is no other electroactive specie present in the potential region of interest from 0.0 V to 1.0 V versus Ag. Before each experiment the working electrodes were cleaned using emery paper and distilled water and were properly dried for use.

2.4 Experimental Techniques

Following experimental techniques were used which are given below with brief introduction.

2.4.1. Cyclic voltammetry (CV)
2.4.2. Galvano-static Method
2.4.3. Infrared Spectroscopy (IR)
2.4.4. Thermogravimetric Analysis and Differential Scanning Calorimetry (TGA, DSC)
2.4.5. X-ray Diffraction (XRD)
2.4.6. X-ray Fluorescence (XRF)
2.4.7. Electron Scanning Microscopy (SEM)
2.4.8. Electron Spin Resonanace (ESR) spectroscopy

2.4.1 Cyclic Voltammetry (CV)

Cyclic voltammetry is the most renowned potentiodynamic electrochemical technique. In this experimental technique the potential of the working electrode is ramped linearly versus time. While the current at working electrode is plotted versus the applied voltage to give the cyclic voltammogram. Cyclic voltammetry is generally used to study the electrochemical properties of an analyte in solution.

A cyclic voltammetry technique has a forward and backward varying scan of potential versus current. Forward scan is used to investigate the oxidation processes at the electrode surface, while backward process indicates the reduction process going on at the same electrode surface. Figure 2-3 shows the typical cyclic voltammogram with both forward and backward scans. Both of these processes are characterized by the peak current and peak potential of each scan.

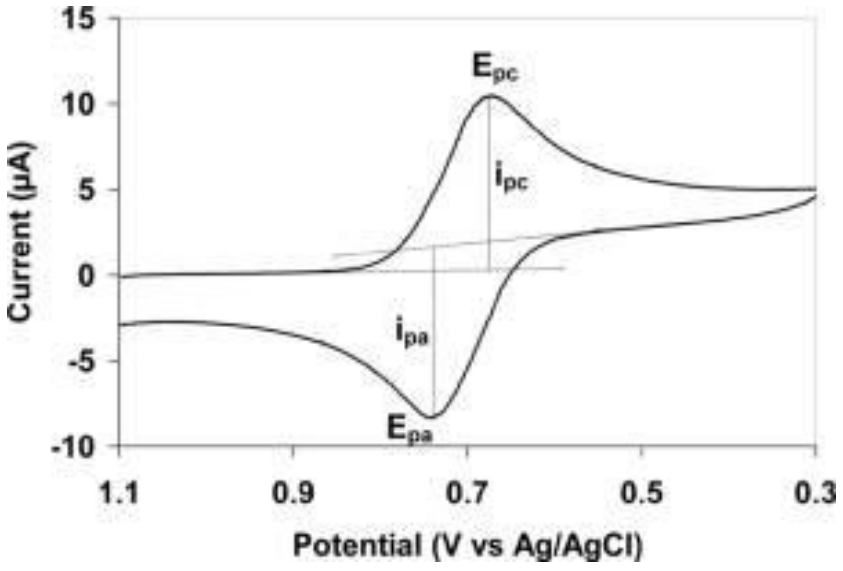

Figure 2-3: A typical cyclic voltammogram for a reversible electrochemical reaction.

In an ideal reversible electrochemical process, the forward and backward scans are of similar shape. This gives the information about the reaction mechanism and electrochemical reaction rate. In an irreversible reaction, where oxidised species are either chemically or electrochemically consumed in another reaction, these oxidised species are not completely available for the reduction process. Most of the electrochemical reactions for example electrochemical synthesis and battery processes

are not fully reversible electrochemically. In our experiments cyclic voltammograms were measured by an Autolab apparatus PGSTAT128N from Eco Chemie, Netherlands.

2.4.1.1 Characterization of choline chloride based binary mixtures by cyclic voltammetry

Cyclic voltammetry experiments were carried out using platinum (Pt) and glassy carbon (GC) as the working electrodes to assess the reversibility of Fc^{+}/Fc couple. Three binary mixtures used in the present work behave as electrochemical solvents. Potential window of three binary mixtures was found stable from 0.2 V to 1.0 V and this potential region was used for checking the electrochemistry of ferrocene.

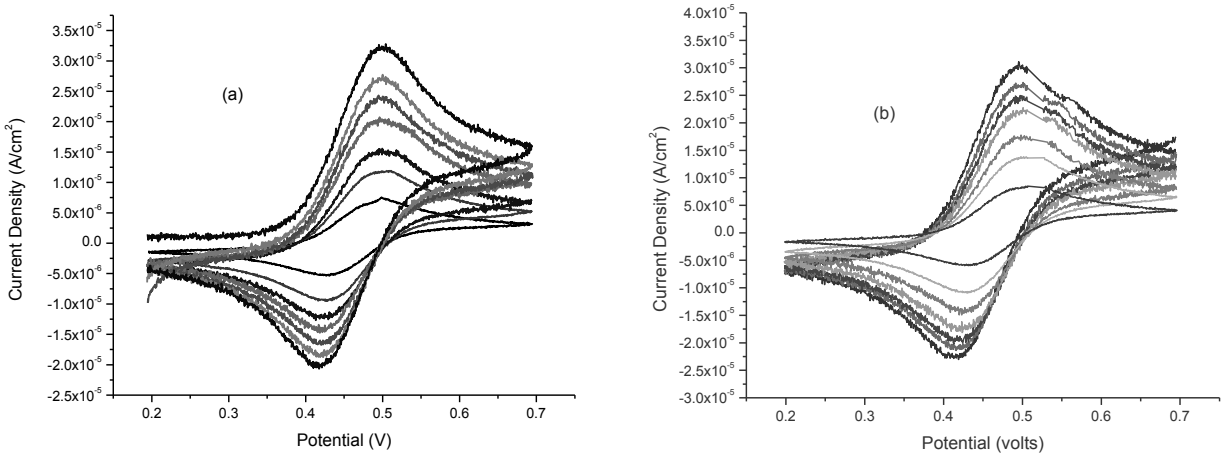

Figure 2-4: Cyclic voltammograms of 0.0025 mol/dm^3 ferrocene in CC/EG at two working electrodes (GC, Pt) (a) CC/EGGC (b) CC/EGPt at scan rate 10 mV/s, 30 mV/s, 50 mV/s, 80 mV/s, 100 mV/s, 120 mV/s and 150 mV/s. *CC=choline chloride, EG=ethylene glycol, GC=glassy carbon, Pt=platinum.

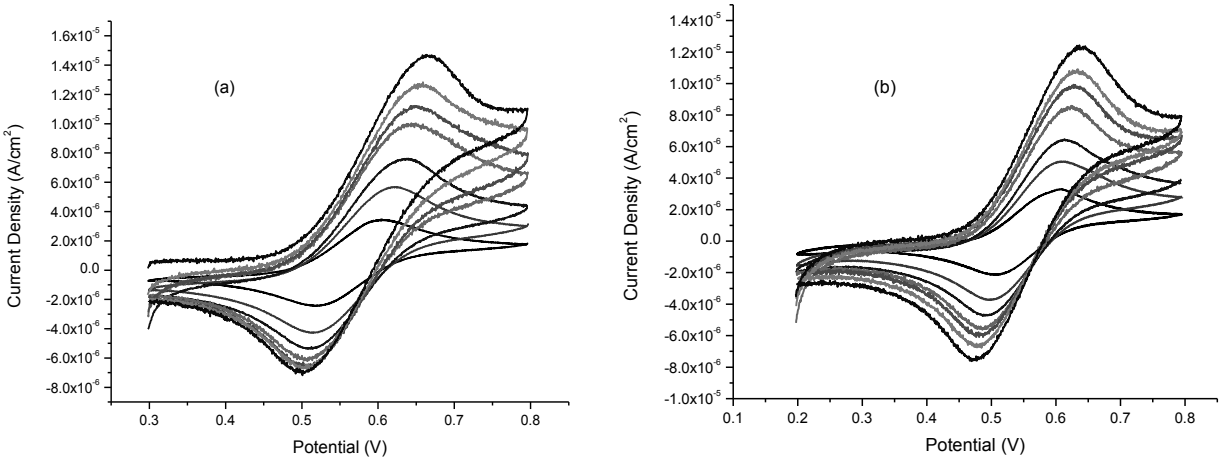

Figure 2-5: Cyclic voltammograms of 0.0025 mol/dm^3 ferrocene in CC/PEG200 at two working electrodes (GC, Pt) (a) CC/PEG200GC (b) CC/PEG200Pt at scan rate 10 mV/s, 30 mV/s, 50 mV/s, 80 mV/s, 100 mV/s, 120 mV/s and 150 mV/s. *CC=choline chloride, PEG200=polyethylene glycol 200, GC=glassy carbon, Pt=platinum.

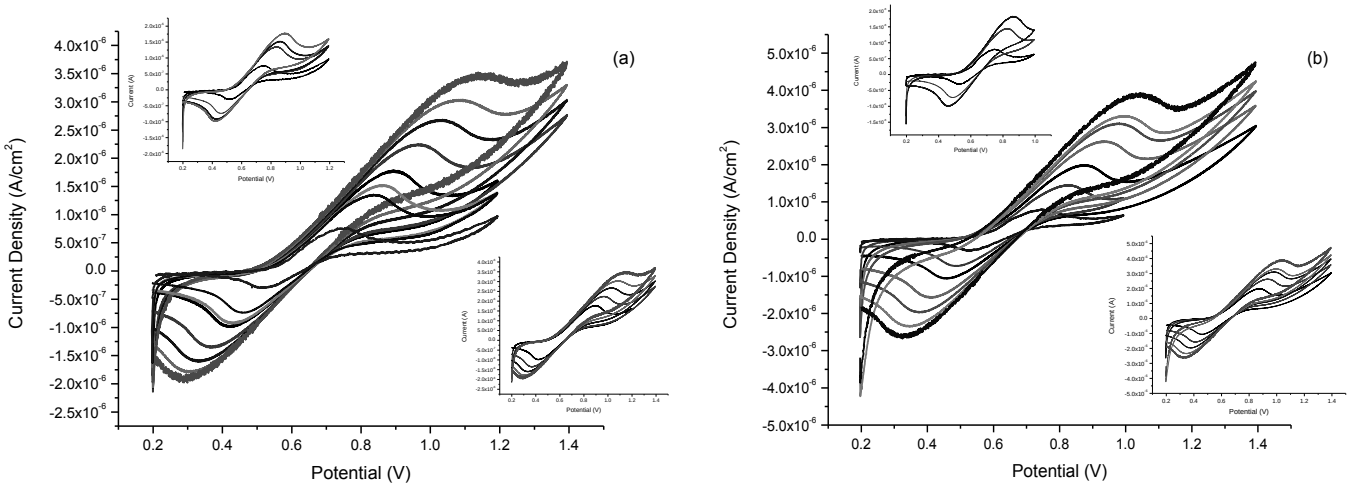

Figure 2-6: Cyclic voltammograms of 0.0025 mol/dm^3 ferrocene in CC/PEG600 at two working electrodes (GC, Pt), (a) CCPEG600GC (b) CC/PEG600Pt at scan rates 1 mV/s, 5 mV/s, 10 mV/s, 20 mV/s, 30 mV/s, 40 mV/s, 50 mV/s, 80 mV/s, 100 mV/s, 120 mV/s and 150 mV/s for CC/PEG600 increasing from inside to upward. Smaller voltammograms for CC/PEG600 system show a difference at smaller scan rate (upper) and lower scan rates (lower). *CC=choline chloride, PEG600=polyethylene glycol, GC=glassy carbon, Pt=platinum.

Figures.2-4, 2-5, 2-6 show cyclic voltammograms of 0.0025 mol/dm^3 ferrocene in CC/EG, CC/PEG200 and CC/PEG600 respectively at platinum (Pt) and glassy carbon (GC) as working electrode with 0.07 cm^2 surface areas for both at various scan rates versus silver Ag/Ag$^+$ as reference electrode. The peak current for ferrocene in three binary mixtures increases with increase in scan rate.

The observed shift (ΔEp) of the peak potential in CC/EG system is low as compared to CC/PEG200 and very low as compared to CC/PEG600. The difference in the electrochemical behavior (ip, ΔEp) of CC/EG and CC/PEG200 systems is smaller than that to the CC/PEG600. However electrochemical behavior of ferrocene moves from reversibility to quasi-reversibility in the order CC/EG > CC/PEG200 > CC/PEG600.

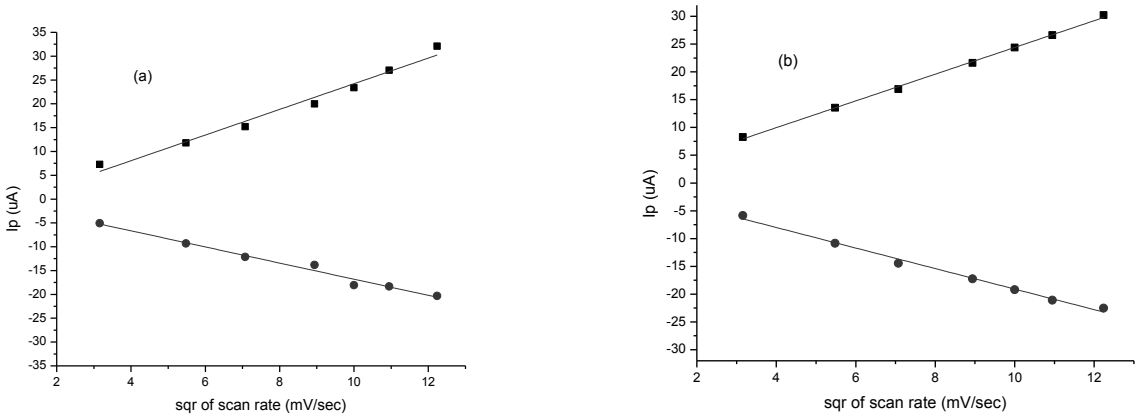

Figure 2-7: Anodic and cathodic peak heights as a function of square root of the scanning rate for (a) CC/EG at GC (b) CC/EG at Pt. *CC=choline chloride, EG=ethylene glycol, GC=glassy carbon, Pt=platinum

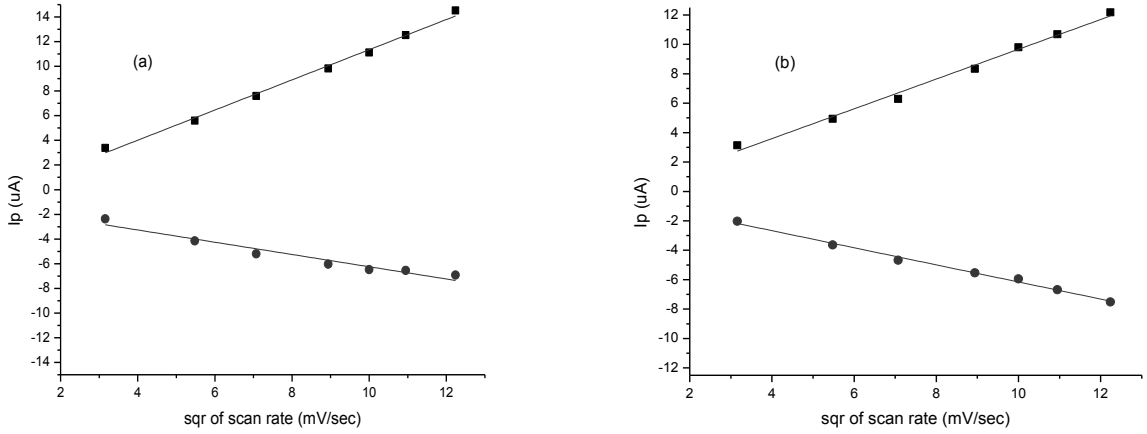

Figure 2-8: Anodic and cathodic peak heights as a function of square root of the scanning rate for (a) CC/PEG200 at GC (b) CC/PEG200 at Pt. *CC=choline chloride, PEG200=polyethylene200, GC=glassy carbon, Pt=platinum

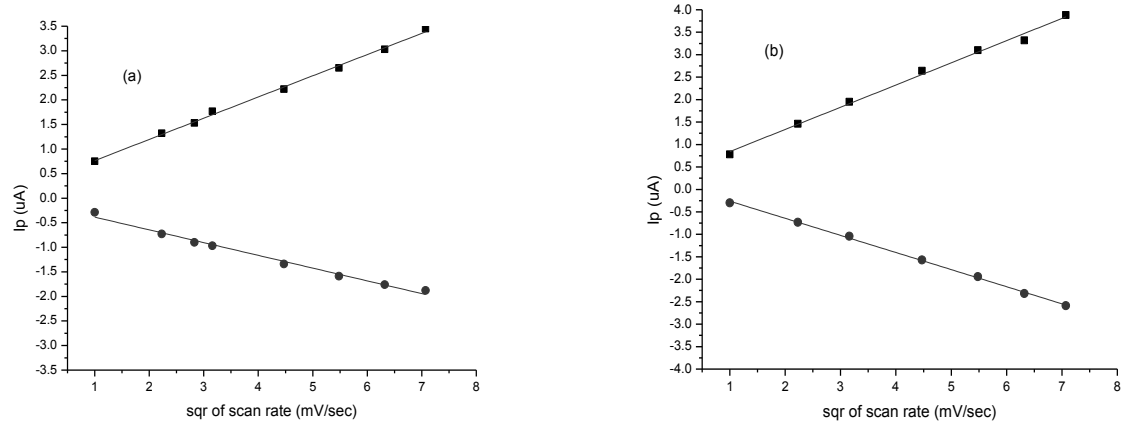

Figure 2-9: Anodic and cathodic peak heights as a function of square root of the scanning rate for (a) CC/PEG600 at GC (b) CC/PEG600 at Pt. *CC=choline chloride, PEG600=polyethylene600, GC=glassy carbon, Pt=platinum

Following the theory of cyclic voltammetry for electron transfer coupled to diffusion, Figures. 2-7, 2-8, 2-9 show the graphs with linear behavior between peak currents and square root of scan rate which clearly indicate the diffusion controlled mechanism of ferrocene redox process at electrode surface. Larger peak current (i_p) values for CC/EG system indicate the ease with which electron transfer process occurs in this system. CC/PEG200 system has relatively smaller i_p values as compared to CC/EG but still high enough when compared with that of CC/PEG600 system. Amount of current generated by the Fc/Fc^+ couple in three binary mixtures varies in the order CC/EG > CC/PEG200 > CC/PEG600.

Both CCEG and CC/PEG200 systems can be used as electrolytic solutions for various electrochemical processes. Peak potential shift (ΔE) for ferrocene in CC/EG system is small and does not change with the change in scan rate, which shows the ability of CC/EG to be used as non-aqueous system. The anodic and cathodic peak separation (ΔE_p) in CC/EG cyclic voltammograms was found to be in the range between 60 mV and 90 mV. On the other hand, there is a slight increase in peak shift for CC/PEG200 system at both GC and Pt working electrodes which shows a trend from reversibility to quasi-reversibility but still the difference between CC/EG and CC/PEG200 system is low.

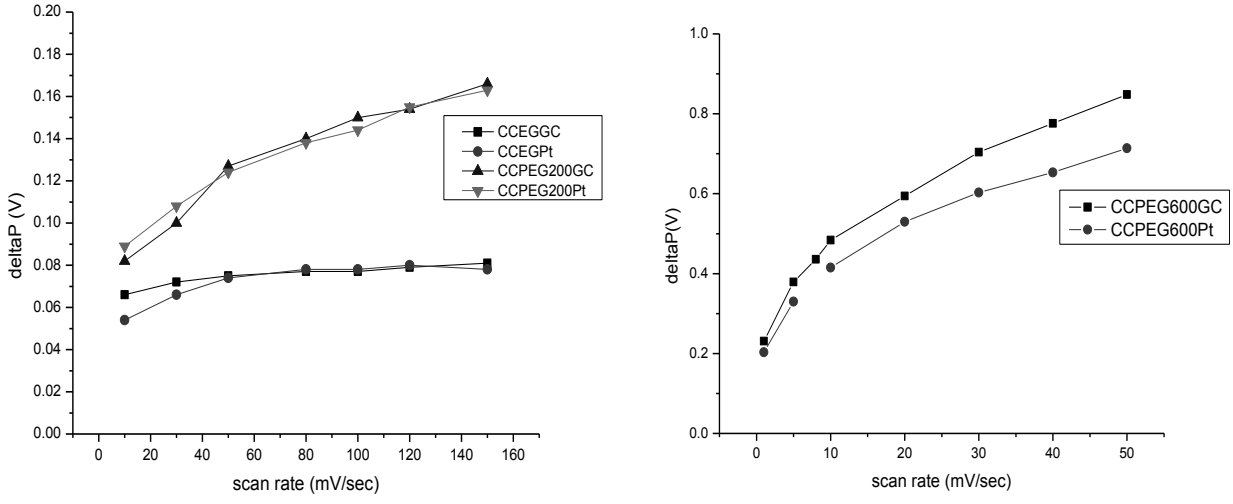

Figure 2-10: The peak shift ($\Delta E = E_{pa} - E_{pc}$) as a function of scan rate for CC/EG, CC/PEG200 and CC/PEG600 at GC and Pt as working electrodes.

CC/PEG600 shows a lot of difference from other two media and ΔE_p and ΔP values are larger than those in the CC/EG and CC/PEG200 systems as in figur 2-10. An increase

in ΔP value from CC/EG to CC/PEG200 and then to CC/PEG600 shows the consequence of slow electron transfer and the peak current ratio of forward and reverse scan equal to 1 (i_{pa}/i_{pc}=1.0) shows a reversible electron transfer process. Such results indicate the absence of any chemical reaction coupled with electron transfer, indicating that the Fc^+ specie is stable and overall charge transfer process is reversible. i_{pa}/i_{pc}>1.0 shows that the electron transfer process is no more reversible rather it is quasi-reversible. The peak current for a reversible process is described by the Randles-Sevcik equation [112], which assumes that charge transfer is very fast and therefore the mass transport is controlled only by diffusion:

$$i_p = 0.4463(n^3F^3/RT)^{1/2} A.D^{1/2}C.v^{1/2} \qquad (2\text{-}1)$$

for A in cm^2 D in cm^2/sec, C in mol/cm^3 and v in V/sec, i_p in amperes, where I_p is the peak current (A), n is the electron equivalents exchanged during the redox process, A is the active surface area of working electrode, D is the diffusion coefficient, C is the bulk concentration of the diffusing species, v is the scan rate, F is the Faraday's constant, and R the universal gas constant. i_p is proportional to $v^{1/2}$ in equation (1) which is a condition for the reversibility of a system. Using equation (1) we have calculated the diffusion coefficient values for ferrocene and ferrocenium cation at both Pt and GC working electrodes and the results are given in table.2-1 and table 2-2. Table 2-3 shows the calculated heterogeneous reaction rate constants (k) of Fc/Fc^+ couple in CC/EG, CC/PEG200 and CC/PEG600 systems.

		CC/EG	CC/PEG200	CC/PEG600
D (cm^2/sec)	Pt	2.62E-06	4.625E-07	1.1E-07
	GC	3.274E-06	4.625E-07	8.47E-08

Table 2-1: Diffusion coefficient of ferrocene (Fc)

		CC/EG	CC/PEG200	CC/PEG600
D (cm^2/sec)	Pt	1.54E-06	1.53E-07	6.54E-08
	GC	1.29E-06	1.53E-07	3.05E-08

Table 2-2: Diffusion coefficient of ferrocenium ion (Fc^+)

	CC/EGGC	CC/EGPt	CC/PEG200GC	CC/PEG200Pt	CC/PEG600GC	CC/PEG60Pt
k_Fc (cm/sec)	6.72E-03	4.70E-03	4.20E-04	4.20E-04	2.10E-05	2.50E-05
k_Fc^+(cm/sec)	6.72E-03	4.70E-03	4.20E-04	4.20E-04	2.10E-05	2.50E-05

Table 2-3: Heterogenous reaction rate constant values for three solutions at GC and Pt working electrodes.

2.4.1.2 Electrochemical Electron Transfer Kinetics

Heterogeneous electron transfer rate constants (k^o) for both oxidation and reduction process at Pt and GC was calculated from observed differences between the cathodic and the anodic peak potentials (ΔE_p) as a function of scan rate (v) according to the relationship derived by Nicholson [113].

$$\kappa^o = \psi / \gamma^{\alpha} \left(\pi n F v D / RT\right)^{1/2} \qquad (2\text{-}2)$$

Where ψ is calculated by the equation (3), taking x equal to ΔE_p.

$$\psi = (0.6288 - 0.0021\,x)/(1 + 0.017\,x) \qquad (2\text{-}3)$$

$$\gamma = \sqrt{D_{ox} / D_{red}} \qquad (2\text{-}4)$$

$$\alpha = nFv / RT \qquad (2\text{-}5)$$

α is the transfer coefficient and its value is taken 0.5 while ψ is the kinetic parameter also called charge transfer parameter related to ΔE_p and calculated by Lavagnini [114], and n=1 for one electron transfer reaction of ferrocene. Table 2-4 shows a comparison of the values of diffusion coefficients of Fc/Fc^+ calculated in CC/EG, CC/PEG200 and

CC/PEG600 with those reported in literature. While Table 2-5 shows a comparison of k values calculated in this study with those reported in literature.

D (cm^2/sec)	System	Ref
1.7E-07 (Fc)	BMIM(NfT2)	a
2.5E-12 (Fc)	DMPIBF4	b
7.63E-09 (Fc)	BMIMPF6	c
4.2E-07 (Fc^+)	EMITFSI	d
2.6E-07 (Fc)	CC/EG	This study
4.6E-07 (Fc)	CC/PEG200	This study
1.1E-07 (Fc)	CC/PEG600	This study

Table 2-4: Comparison of diffusion coefficients (cm^2/s) of Fc/Fc^+ couple in various ionic liquids with those in choline chloride systems.

k (cm/sec)	System	Ref
1.94E03 (Fc)	PEG.LiClO4	e
1.08E03 (Fc)	PEG200	f
5.5E02 (Fc)	PEG600	f
1.5E-02 (Fc)	EMITFSI	d
4.7E-03 (Fc)	CC/EG	This study
4.2E-04 (Fc)	CC/PEG200	This study
2.5E-05(Fc)	CC/PEG600	This study

Table 2-5: Comparison of heterogeneous rate constant (cm/s) of Fc/Fc+ couple in various ionic liquids with those in choline chloride systems.

[a] Reference [115] [d] Reference [118]
[b] Reference [116] [e] Reference [119]
[c] Reference [117] [f] Reference [120]

The solvent dependence of electron transfer processes has experienced substantial research attention, for both homogenous and heterogeneous reactions [121-123]. Solvent properties affect both the activation barrier to electron transfer and the barrier crossing frequency [124,125]. Heterogeneous rate constant is related to activation energy ΔG^* by the Marcus equation [126].

$$k_{het} = \kappa Z_{het} \exp(-\Delta G^*/RT) \qquad (2\text{-}6)$$

where κ is the transmission coefficient (=1 for adiabatic reaction), Z is the collision frequency, R is the gas constant, ΔG* is the sum of outer and inner-sphere reorganizational energy barriers. A detailed review on this account is given by Weaver and Fawcett [127,128].

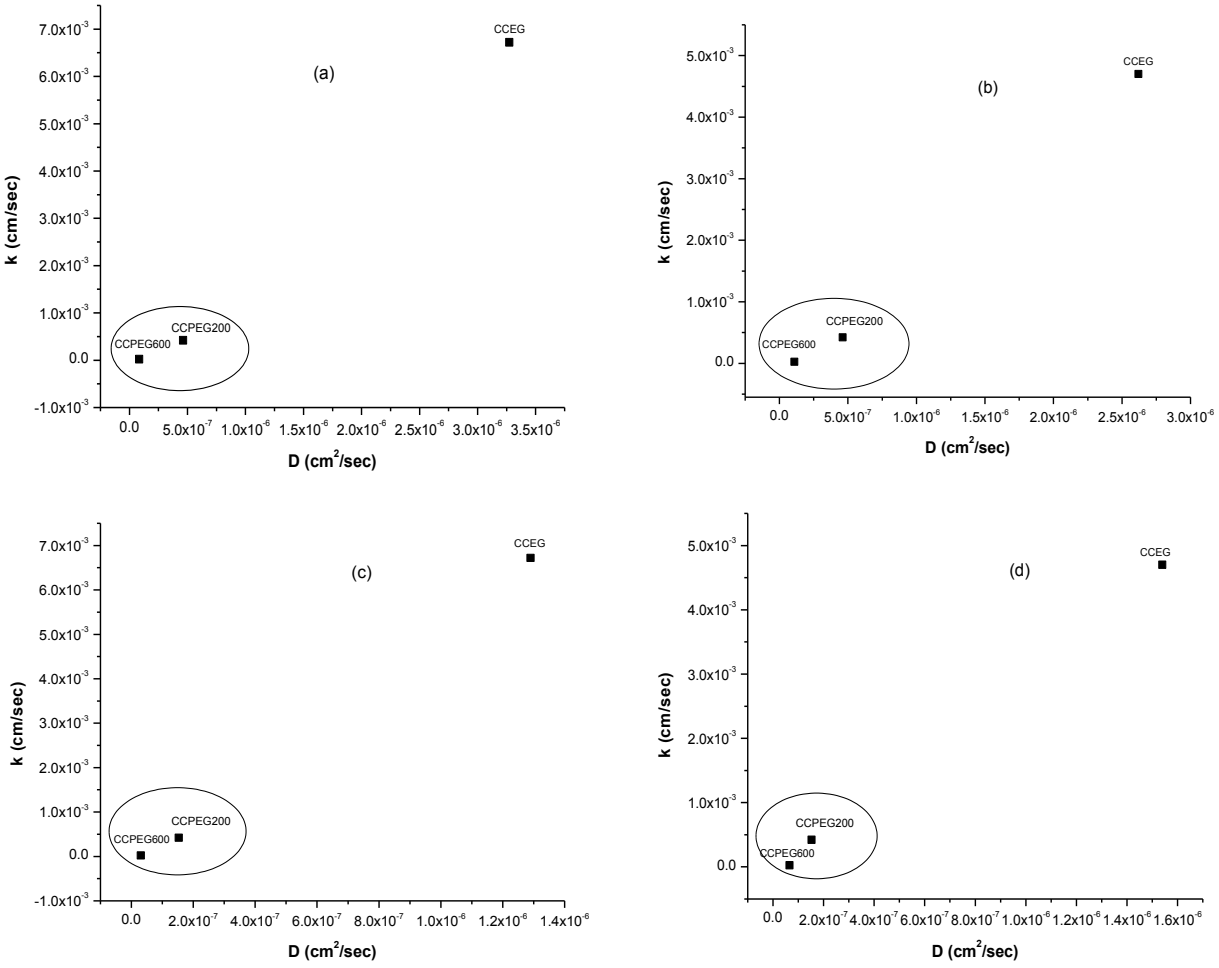

Figure 2-11: Plots of heterogeneous rate constant k^0 vs. the diffusion coefficient *D* of 2.5 mM ferrocene in CC/EG, CC/PEG200 and CC/PEG600 (a) ferrocene (Fc) at glassy carbon (b) ferrocene (Fc) at platinum (c) ferrocinium (Fc^+) at glassy carbon (d) ferrocinium ion (Fc^+) at platinum.

Figure 2-11 shows that the rate constant k^0 varies proportionately to the diffusion coefficient D for both Fc/Fc^+ redox species. This also explains the correlation between reaction kinetics and diffusion properties of the solvent showing that the solvent properties affect the energy barrier and hence the diffusive motion of ion-solvent incipient species. Three data points for three electrolyte systems tend to lie on

the same line and shows a trend in the behavior of electrolyte as we move from monomer to polymer. As explained by Pyati and Murray [129], this is not the only explanation as CC/PEG200 point does not clearly lie on the same line which indicates a need of better manipulation of data to lessen the secondary influences on k and D. Similar trend of rate constant can be obtained versus viscosity of the solutions (as increase in molecular weight causes an increase in viscosity) which is in comparison of rate constant k vesus diffusion coefficient D.

This trend can also be related to the solution behavior from reversibility to quasi-reversibility which follows the order CC/EG >> CC/PEG200 > CC/PEG600. These results are also in agreement with the theories where reaction rate and reactant distances are inter-related showing that electron transfers always favor short distances when the reactants are physically very mobile [130-132]. It becomes clear from above data that the solution dynamics potentially affect the electron exchange processes as we head towards polymeric medium. The electron exchange rate is depressed 50 fold from CC/EG to CC/PEG200 system and 10 fold from CC/PEG200 to CC/PEG600 system. As described by Wooster such an effect most likely occurs at larger D values and k values since reaction there would be most nearly adiabatic [133,134].

2.4.1.3 Electrochemical Potential Windows

A key criterion for selection of a solvent for electrochemical studies is the electrochemical stability of the solvent [135]. This is most clearly shown by the range of voltages over which the solvent is electrochemically inert. The potential window depends on the oxidative and reductive ability of the solvent. In other words, in case of such liquids comprising of the cations and anions, potential window depends primarily on the resistance of the cations to reduction and the resistance of the anions to oxidation. The choline chloride when mixed with HBDs dissociates to release Cl^- ions, these chloride ions then bond with the HBSs and make the choline cations free to move. Hydrogen bond is established between the HBD and chloride ion hence giving whole specie a negative charge.

Following are the electrochemical potential windows of the solutions developed, determined largely with platinum as working electrode. Deep Eutectic

Solvents (DES) that we have made have reasonably large potential window comparable to the ionic liquids.

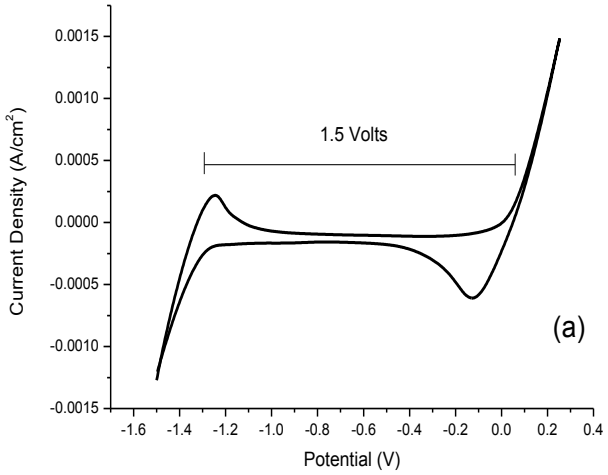

Figure 2-12: Cyclic voltammogram of CC/AA System at the scan rate of 50mV/sec. Working electrode (Pt), Reference electrode (W), Counter Electrode (Pt).

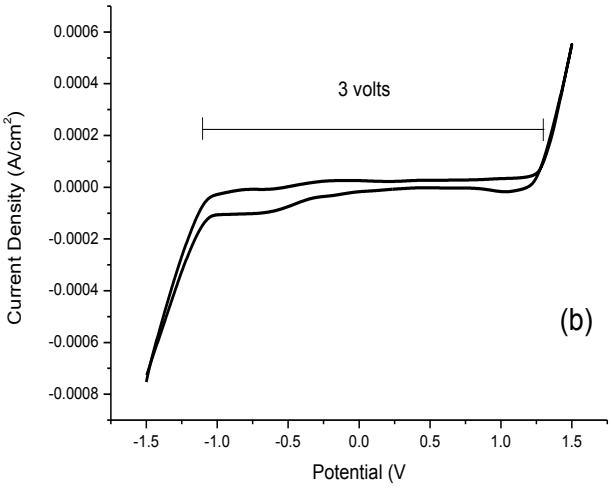

Figure 2-13: Cyclic voltammogram of CC/DMF System at the scan rate of 50mV/sec. Working electrode (Pt), Reference electrode (W), Counter Electrode (Pt).

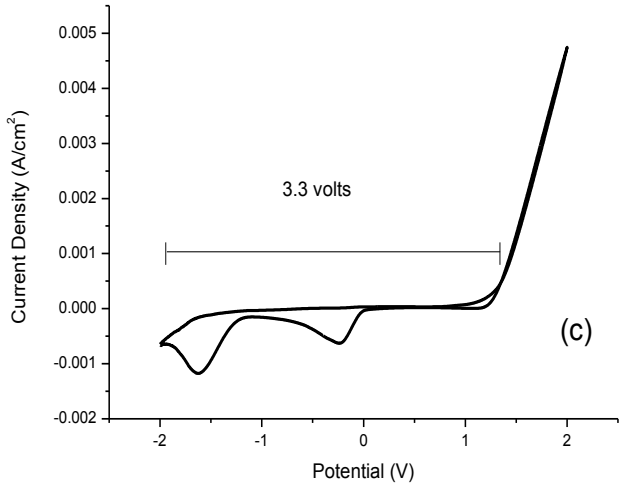

Figure 2-14: Cyclic voltammogram of CC/DMSO System at the scan rate of 50mV/sec. Working electrode (Pt), Reference electrode (W), Counter Electrode (Pt).

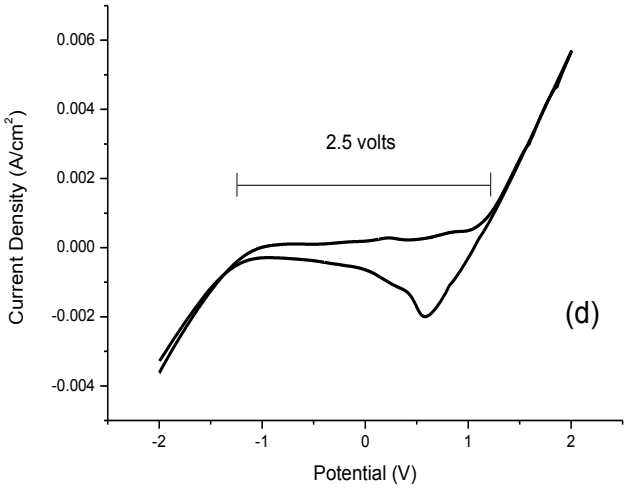

Figure 2-15: Cyclic voltammogram of CC/EG System at the scan rate of 50mV/sec. Working electrode (Pt), Reference electrode (W), Counter Electrode (Pt).

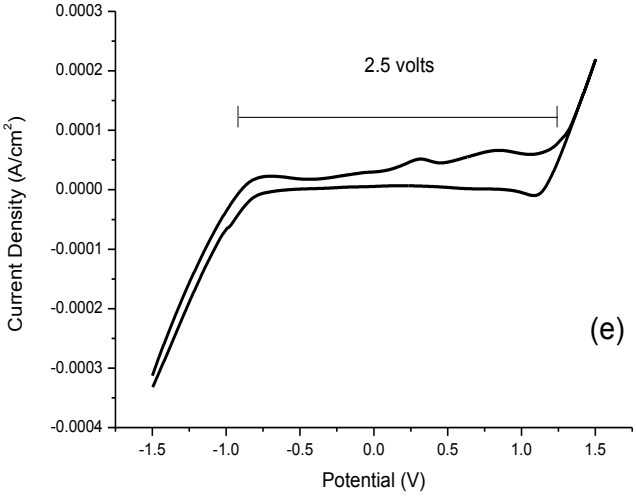

Figure 2-16: Cyclic voltammogram of CC/PG System at the scan rate of 50mV/sec. Working electrode (Pt), Reference electrode (W), Counter Electrode (Pt).

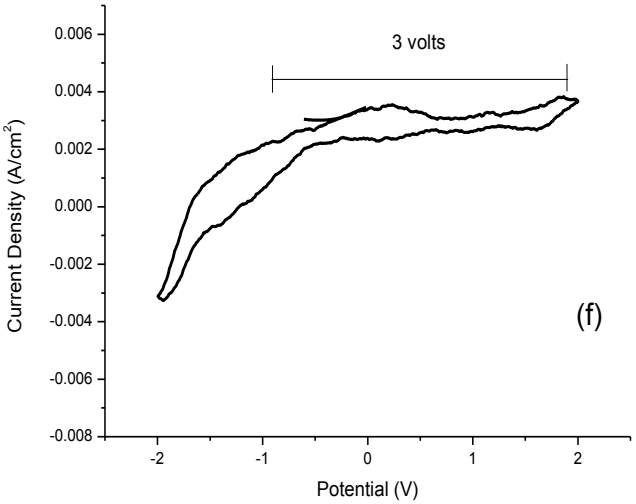

Figure 2-17: Cyclic voltammogram of CC/Urea System at the scan rate of 50mV/sec. Working electrode (Pt), Reference electrode (W), Counter Electrode (Pt).

Electrochemical windows for the binary mixtures of choline chloride with different hydrogen bond donors (HBDs) are shown in figures 2-12 to 2-17. Platinum (Pt) was used as working electrode in all the cyclic voltammetric measurements. Silver wire

(Ag/Ag+) reference electrode and platinum as counter electrode. Table 2-6 shows a comparison of the electrochemical potential windows of choline chloride based binary mixtures with ionic liquids reported in literature.

Ionic Liquid	Electrochemical Window (V)	Reference
[C2mim][NTf2]	4.3	136
[C4mim][NTf2]	4.8	136
[C8mim][NTf2]	5.0	136
[C4mim][NO3]	3.7	137
CC/DMF	3.0	138
CC/DMSO	3.3	138
CC/EG	2.5	138
CC/Gly	2.5	138
CC/Urea	3.0	138

Table 2-6: A comparison of potential windows of ILs and DES.

2.4.2 Galvano-static Method

In galvanostatic method the redox behavior of organic and inorganic species is observed at the surface of electrode. A constant current is applied and variation in potential is observed as a function of time. A galvanostate is a control and measuring device used to keep constant current flowing through an electrolytic cell. A voltage source of varying capability is used to produce a constant voltage V, with resistor R_x connected in series: in order to force a flow of constant current through the load. This resistor is higher than the load resistor R_{load}. The current I flowing through the load is given by:

$$I = U/R_x + R_{load} \quad (2\text{-}7)$$

$$I = U/R_x \quad \text{if} \quad R_x >> R_{load} \quad (2\text{-}8)$$

Galvano-static setup was used for two purposes, first to anodically dissolve molybdenum and tungsten in all the electrolytic systems described further in results and discussion section and second to check the electrochemical behavior of different species e.g. oxide and chlorides of molybdenum and tungsten. Two electrodes were used to complete the electric circuit and anode was made of molybdenum and tungsten metals. When anode was supposed to dissolve in the electrolyte, a current of 10mA to 150 mA was set and potential was observed over a number of seconds and minutes. The ministate XL from sycopel company was used for all galvanostatic experiments.

2.4.2.1 Weight Loss Calculations

Weight loss measurements were done using a double jacket corrosion cell as shown above in figure 2-2. The cell was filled with selected electrolyte up to 20 ml. The electrolyte were either choline chloride based binary mixtures or ammonium chloride/ammonia system. For former experiments were conducted at room temperature while for the later, experiments were carried out at -60 ^{o}C.

Two metals system was used for corrosion measurements in all weight loss experiments. The metal whose weight loss was to determine, was made anode. When molybdenum was anode in all the experiments, tungsten was made cathode, hence measuring the cell voltage against tungsten. But when tungsten was anode in weight loss experiments, platinum was used as cathode. The cell voltage was measured at constant current of 100 mA/cm^2 with exposed surface area of each molybdenum and tungsten 1 cm^2. As described earlier in the last section of chapter 1, weight loss was calculated using the following formula in all calculations.

$$w = ItM/nF$$

The exposed surface area of anode and cathode was 1 cm^2 each. The surface of electrodes was treated by mechanical polishing with finer grade emery paper (600), rinsing with distilled water and drying before each experiment. Anode was weighed before and after each dissolution experiment for 1 hour at 100 mA/cm^2 and weight loss was calculated. Different electrolytic systems gave different dissolution efficiency of

molybdenum and tungsten depending on their ability to accomodate metal ionic species.

2.4.2.2 Conductivity of electrolyte solutions.

The conductivity of choline chloride based binary mixtures depends on the concentration of the ionic species as for general electrolytic systems [139]. The electrolytic data can be used to calculate conductivity parameters of choline chloride based binary mixtures. Like metallic conducting materials, electrolyte solutions follow Ohm's Law:

$$V = IR \qquad (2\text{-}9)$$

Where R is the resistance (Ω, "ohms"), V is the potential difference (V, "volts"), and I is the current (A, "amperes"). Conductance G (S, siemens or Ω^{-1}) is then defined as reciprocal of the resistance.

$$G = 1/R \qquad (2\text{-}10)$$

Conductance of a given liquid sample decreases when the distance between the electrodes increases and increases when the effective area of electrodes increases. This is shown in the following relation:

$$G = \kappa \times A/l \qquad (2\text{-}11)$$

Where κ is the conductivity (Sm^{-1}), A is the cross sectional area of electrodes and l is the distance between the electrodes (m). Galvano-static measurements based on two electrode setup show potential values at constant current density and by keeping electrode surface area 1 cm^2 and distance between anode and cathode 1 cm, we calculated following parameters given in table 2-7. These calculations show that choline chloride based binary mixtures have high conductivity values keeping in view that the polarization effects were not eliminated in these calculations. All parameters based on constant current of 100mA/cm^2 using W as working electrode.

	Potential (v)	Resistance (Ω)	Conductance(Ω^{-1})	Conductivity(Sm^{-1})
CC_Urea	3.0 (W)	30	0.033	3.33
CC_EG	2.71 (W)	27.1	0.036	3.69
CC_Glycerin	5.32 (W)	53.2	0.018	1.88

Table 2-7: Conductivity parameters of choline chloride based binary mixtures.

Conductivity of CC_Urea system and CC_EG system is good and high at room temperature while for CC_Gly system viscosity is the issue that's why it has little less conductivity but in the range of other two electrolytic systems. Conductivity of choline chloride based binary mixtures is comparable to that of the ionic liquids [140]. Low vapor pressure, stability at room temperature and high conductivity values make these systems an attractive alternative electrolytic system in modern day chemistry.

2.4.3 Infra Red Spectroscopy

Infrared spectroscopy is the spectroscopic technique which deals with the infrared region of electromagnetic spectrum. Infrared spectroscopy exploits the fact that molecules absorb specific frequencies that are characteristic of their structure. Infrared is the light with longer wavelength and lower frequency than visible light. It is mostly based on absorption spectroscopy. Now the absorptions are resonate frequencies (the frequency of the absorbed radiation matches the frequency of the bond or group that vibrates). Sample preparation for infrared spectroscopy was done by using the two CsBr pellets. Liquid choline chloride based mixture was taken in amount of a drop on the pellet and pressed with other pellets before it was put into the sample holder of IR instrument.

Choline chloride based binary mixtures are room temperature molten salts derived from the combination of choline chloride and hydrogen bond donors. They have been used as non-aqeuous electrochemical solutions in present work and are potential candidate for future use in various fields of electrochemistry. Infrared spectroscopy has been used by many researchers to show hydrogen bond in ionic liquids as has been used to show O-H…Cl^- and C-H...Cl^- hydrogen bonds in present work [141-144]. The presence of C-H…Cl^- hydrogen bonds in liquid state can be determined by examining the C-H stretching in chloroaluminate molten salts and

generally stretching vibrations for this type of hydrogen bonding is observed at > 2500 cm^{-1} [145-147].

Figures 2-18 (a, b, c) show the transmittance of all three solutions (a) CC/EG, (b) CC/PEG200, (c) CC/PEG600, respectively. The data indicates C-H and O-H bonds are stretched due to the presence of chloride ions in surrounding. A hydrogen atom attached to a relatively electronegative atom is a hydrogen bond donor which in this case is oxygen [148]. Hydrogen atom attached to carbon can also participate in hydrogen bonding when the carbon atom is bound to electronegative atoms, as is the case in chloroform, $CHCl_3$. The electronegative atom attracts the electron cloud from around the hydrogen nucleus and, by decentralizing the cloud, leaves the atom with a positive partial charge. Because of the small size of hydrogen relative to other atoms and molecules, the resulting charge, though only partial, represents a large charge density.

A hydrogen bond results when this strong positive charge density attracts a lone pair of electrons on another heteroatom, which becomes the hydrogen-bond acceptor [149]. In the case of CC/EG, carbon atom attached to oxygen of hydroxyl group is attached with hydrogen atoms as well. These hydrogen atoms may offer hydrogen bond since electron cloud around these nuclei is attracted towards oxygen. Based on these facts, it can be assumed that the region between 3350 cm^{-1} to 3365 cm^{-1} shows the O-H bond stretching and a slight split curve at 3339 cm^{-1} suggests the interaction of chloride ions present in the solution. .

In the absence of chloride ions the curve generally shows a smooth concavity without small split in the band rather this is an interaction band for O-H…Cl^-. Bands at 2940 cm^{-1} and 2874 cm^{-1} are C-H stretching vibrations which can be assymetric and symmetric C-H stretching vibrations respectively. The interaction band is more prominent in CC/EG solution than in other two solutions which indicates its dependence on the chloride ions concentration; increase in chloride ions concentration results in more splitting and hence the interaction between C-H…Cl^-.

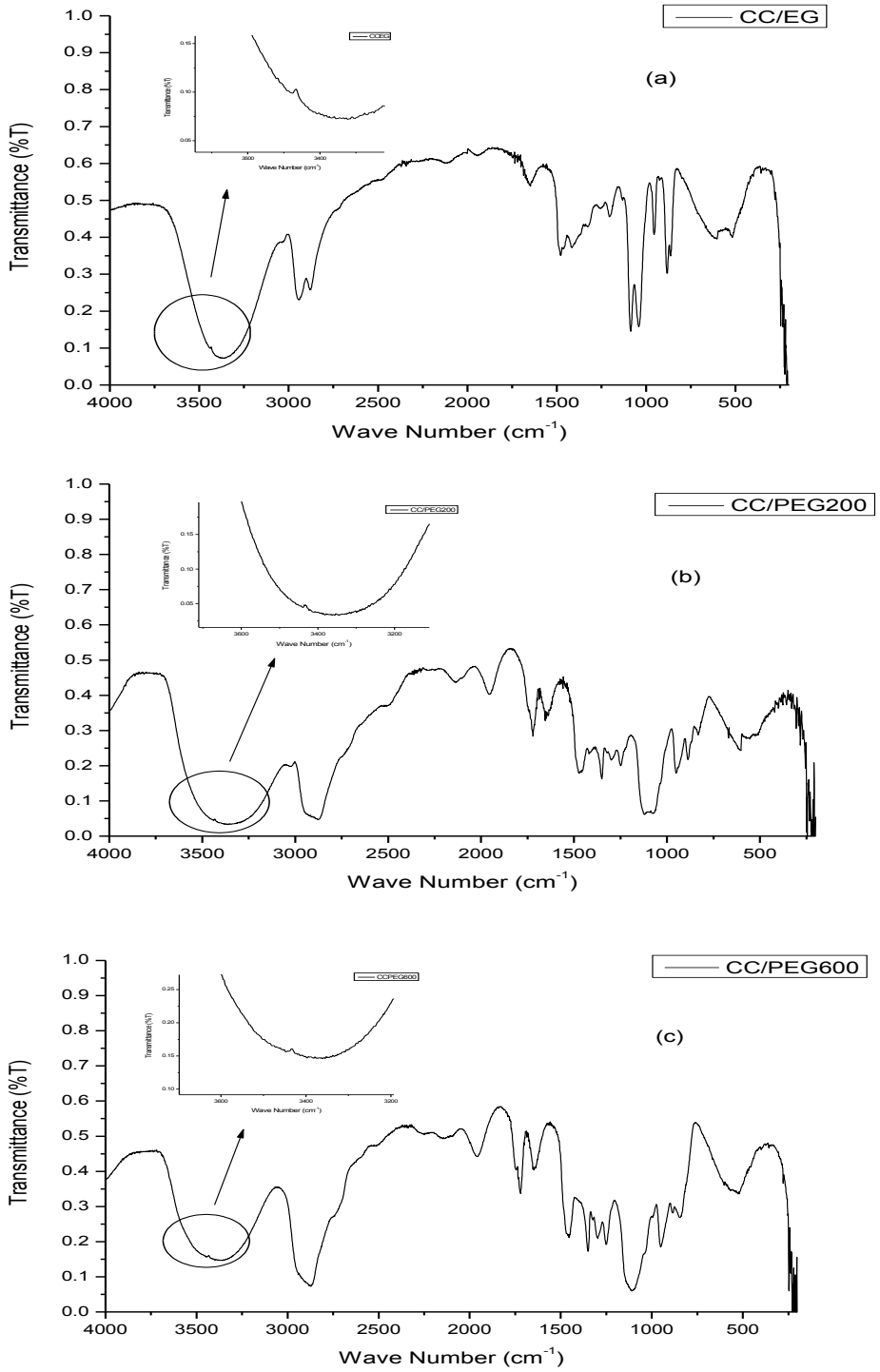

Figure 2-18: The IR spectra of three solutions namely (a). CC/EG, (b). CC/PEG200 and (c). CC/PEG600. Peaks in the region between 3500 cm^{-1} to 2800 cm^{-1} are due to C-H…Cl^- and O-H…Cl^- interactions. Instes show the region of O-H…Cl^- interactions in a, b, c.

It is clear though that an increase in chloride ions concentration does not shift the transmittance band values to larger extent. Due to the big structures of hydrogen bond donors in present case, the possibility of forming tetrahedral structure around chloride ion is very small. It can be confirmed from this work that CC/EG system shows strong hydrogen bonding as compared to CC/PEG200 and CC/PEG600 systems, which is logical to the structural constraints of bigger polymer than smaller polymers and monomers.

2.4.4 Thermogravimetric (TGA) and Differential Scanning Calorimetry (DSC) Analysis

TGA is a tachnique in which the mass of a substance is measured as a function of temperature or time while the substance is subjected to a controlled temperature program. On the other hand DSC is a technique in which the difference in energy inputs into a substance and a reference material is measured as a function of temperature while the substance and reference material are subjected to a controlled temperature program. The upper limit of the liquidus range is usually bounded by the thermal decomposition temperature of the ionic liquid, since most ionic liquids are non-volatile. Thermo-gravimetric analysis (TGA) and differential scanning calorimetry (DSC) have been used to investigate the decomposition limits and decomposition products.

2.4.4.1 Preparation of choline chloride based mixtures for TGA and DSC analysis

Choline chloride and urea were dried separately at 110°C over night. All the binary mixtures were prepared under vacuum. These liquids were prepared by mixing of choline chloride and HBD in the ratio of 1:2 and 1:1. Later each mixture was heated up to 60°C and investigated further. A conventional double jacket corrosion cell was used for checking the electrochemical behavior of deep eutectic solvents. Platinum (Pt) electrode was used as working electrode for the electrochemical studies of mixtures except one of the mixtures of choline chloride and urea system where working electrode was tungsten (W). The surface of electrode was treated by mechanical polishing with finer grade emery paper, rinsing with distilled water and drying.

Choline chloride and urea were dried up to 110 ^{o}C to make them water free. Remaining hydrogen bond donors were kept under vacuum. After making a eutectic melts at 90 $^{\circ}$C, for choline chloride and urea, the melts were transferred into the cell.

Eutectic mixtures of choline chloride with urea, EG, PG, DMF, DMSO and Acetic acid were prepared by continuous stirring at 40 $^{\circ}$C and then these mixtures were shifted to electrochemical cell. All these solutions are stable liquids at room temperature. All the experiments were performed at 25 $^{\circ}$C. A continuous supply of helium was passed through the cell to avoid moisture. Thermo-gravimetric analyses (TGA), differential scanning calorimetry (DSC) along with mass spectral lines were done on computer controlled instrument described below.

2.4.4.2 Instrumental Setup for TGA and DSC analysis

In our experiments, to check the thermal properties of choline chloride based binary mixtures, we used the NETZSCH-thermogravimetric analyzer TG 409 which is based on an asymmetrical, electromagnetically compensated substitution type balance. In the TG 409 the sample carrier with the crucible for the sample substance is plugged onto the balance beam and positiones the sample in the center of the furnace. NETZSCH-furnaces provide temperature ranges from -150 ^{o}C to 2400 ^{o}C. The electronic control unit TASC 414/2 comprises the temperature controller for the furnace system, the amplifier for the temperature signal and the balance signal and analog-to-digital converter.

Differential Scanning Calorimeter (NETZSCH DSC 404) was used in DSC analysis. The measuring head has a special, unique design which is optimized for time constant and homogenous heat flow. This results in high sensitivity, excellent reproducibility and extremely low noise espacially at temperature above 800^{o}C up to 1500 ^{o}C (type S-sample carrier), and a very stable baseline with low drift. This design is the essential prerequisite to calibrate the instrument for heat flow measurements and for the determination of the specific heat c_p. Following are choline chloride based binary mixture with thier TGA and DSC analysis.

The temperature ranges extend from -150 ^{o}C to 1600 ^{o}C. The measurement setup and control as well as the data acquisition of the temperature difference are

performed by MS-DOS computer via the TASC 414/2 TA-system controller using the NETZCH software.

2.4.4.3 Choline Chloride and Urea System.

TGA in figure 2-19 shows the first decomposition at 210 °C and second at 271.4 °C. DSC scan shows total three peaks, first belongs to urea and second and third belong to choline chloride as shown on the graph, the first peak shows the presence of NH_3^+ and OH^+ at 263.9 °C while first DSC peak is observed at 253.4 °C which clearly indicates that these two species belong to the urea. About second peak which belongs to choline chloride, below these peaks the mass spectra show increased concentration of N^+ and CH_2^+, confirming that this second peak is for choline chloride. Water gives a peak at 309.4 °C indicating absorption by choline chloride which is hygroscopic in nature.

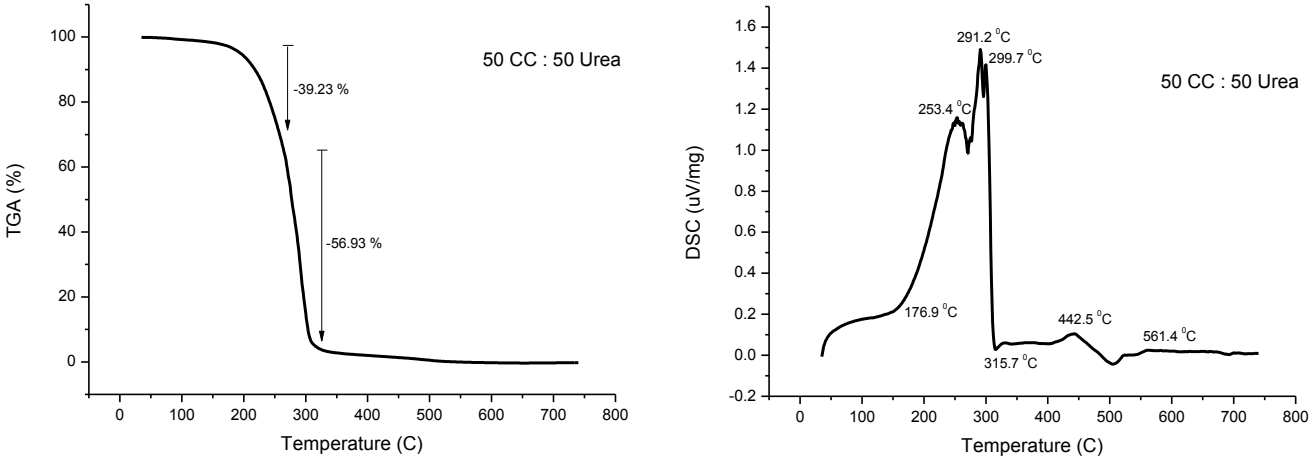

Figure 2-19: TGA (left) and DSC (right) analysis of choline chloride and urea based mixture (50:50).

In 30:70 (choline chloride and urea) sample, TGA shows the first decomposition at 204 °C and second at 278 °C DSC scan shows first peak belonging to urea at 240.7 °C. There is clear difference between TGA of two scans where in 30:70 sample the second decomposition is minor while in 50:50 sample the second decomposition step is obvious and shows the dependence on choline chloride contents. In both the scans there is a peak at 245 °C which might be the presence of some bigger species, may be the HBD (urea) surrounded the chloride ions. CO_2 at 240 °C and O at 244.7 °C indicate the oxidation of carbon in both urea and choline chloride.

2.4.4.4 Choline Chloride and Acetic Acid System.

In figure 2-20, Weight loss immediately at the start in CC/AA system at 35°C and a peak at 64.3 °C shows the first obvious weight loss. This belongs to acetic acid because in 30:70 sample, weight loss is -30.17% while in 50:50 sample it is -27.98%.

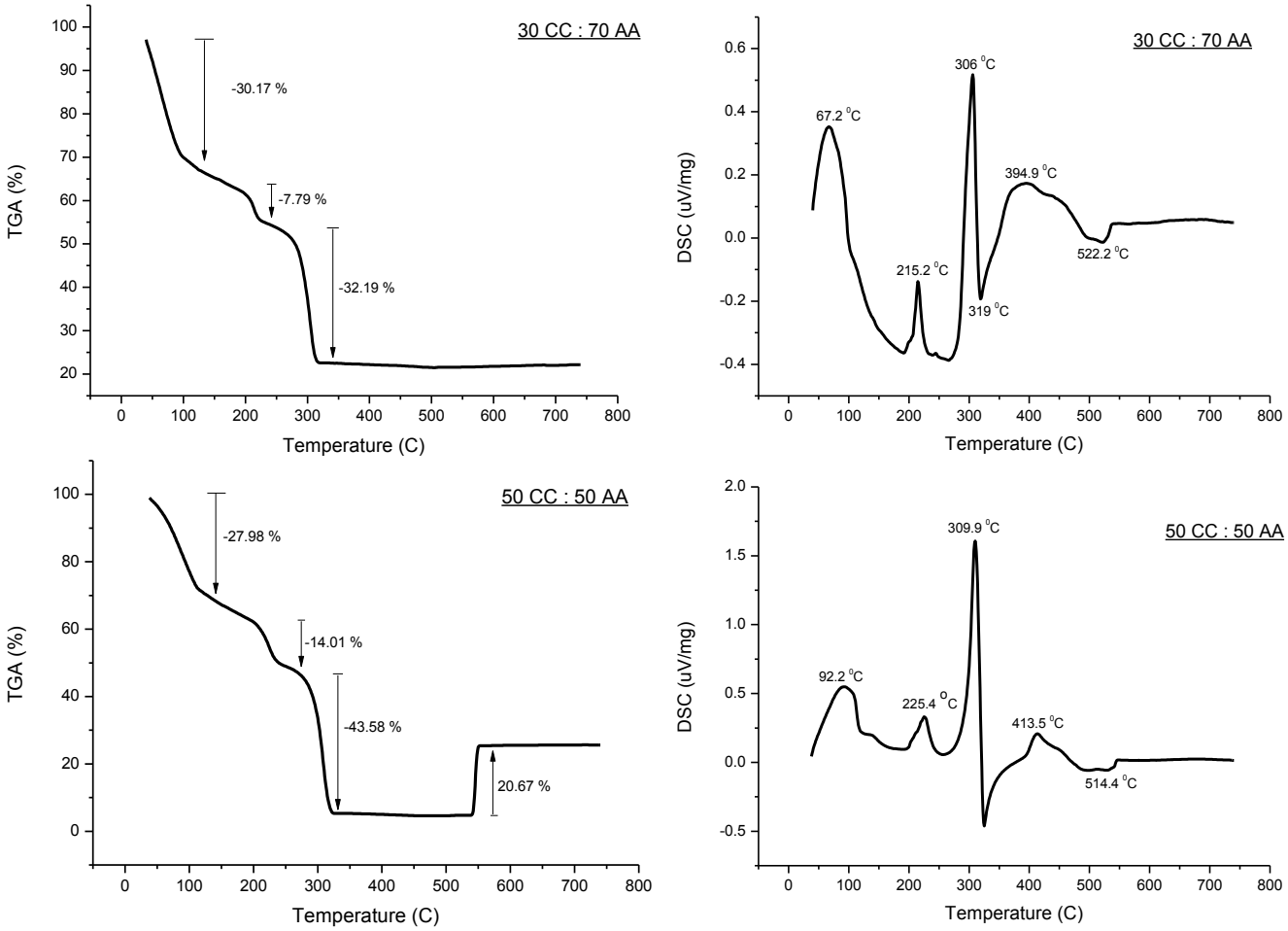

Figure 2-20: TGA (left) and DSC (right) analysis of choline chloride and acetic acid based binary mixtures (50:50 and 30:70).

Second peak in TGA belongs to choline chloride where weight loss is -14% in 50:50 sample and -7.79% in 30:70 sample. The decrease in the amount of choline chloride had lessened the weight loss percentage. The increase in the amount of choline chloride increases the decomposition limit of the mixture. The mixture contained water in it and mass spectral line shows peak at 116 °C while at 331.8 °C the peak of water came from the oxidation of organic matter generating water as there is immediate decrease in oxygen amount at same point of temperature.

In TGA, the third weight loss came at about 300 °C where the whole organic matter is burned and weight loss is -32.19%, at the same point DSC signal shows peak at 306 °C. Peaks showing either $(NH_2)_2CO$, $C_2H_6O^+$, $C_2H_3O^+$ or $(CH_3)N^+$ belong to the decomposed choline chloride. There is also HCl peak coming from choline chloride, showing increase at the point of maximum weight loss. It becomes clear from 30:70 sample where these peaks get more flat. Another important line is of N^+ as there is increase in concentration of choline chloride for 50:50 sample while in 30:70 sample it is more flat.

2.4.4.5 Choline Chloride and DMSO System.

50:50 sample in figure 2-21 shows choline chloride is responsible for the second peaks of H2O, CH3+, NH+, N2O+ and C+ while DMSO is responsible for the SO^+, S_2^+ and SO_2^+. First TGA peak at 136 °C belongs to choline chloride as the $(CH_3)_3N^+$ concentration is increased at this point. This is also supported by the fact from 30:70 sample where the TGA inclination at that point is decreased. In 50:50 sample weight loss is -88.96% while in 30:70 sample weight loss is -85.65% which shows that increased amount of choline chloride is responsible for more weight loss.

In sample 50:50 further peak inclination of weight loss of -4.13% and -5.21% at 309 °C indicates that the remaining choline chloride decomposes in steps as there is no stirring present in the sample. In 30:70 sample there is flat line with weight loss of -0.86% showing evaporation of some part of sample.

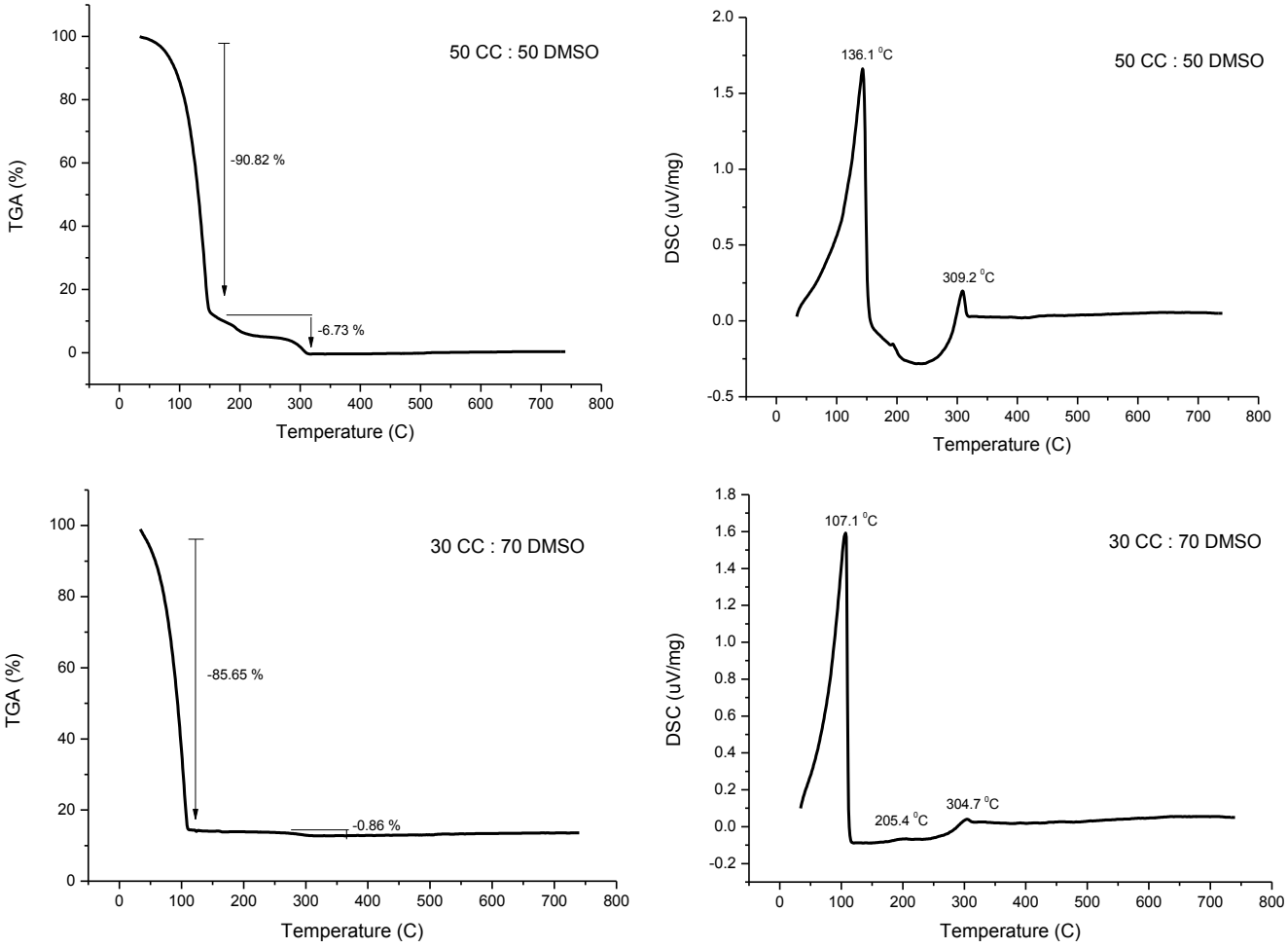

Figure 2-21: TGA (left) and DSC (right) analysis of choline chloride and DMSO based binary mixtures (50:50 and 30:70).

2.4.4.6 Choline Chloride and Ethylene Glycol System.

In figure 2-22, TGA analysis shows the first peak at 129 °C, second at 243 °C and third at 295 °C, in 50:50 sample there are four steps of weight loss with -38%, -3.51%, -14.44% and -36.05% which clearly shows that these eutectic mixtures are stable under 100 °C. The DSC peaks show that first peak at 168 °C belongs to ethylene glycol (EG) as its size is increased with the increase in EG amount in sample 30:70. Second peak at 303 °C belongs to choline chloride as its size is decreased for 30:70 sample as compared to 50:50 sample.

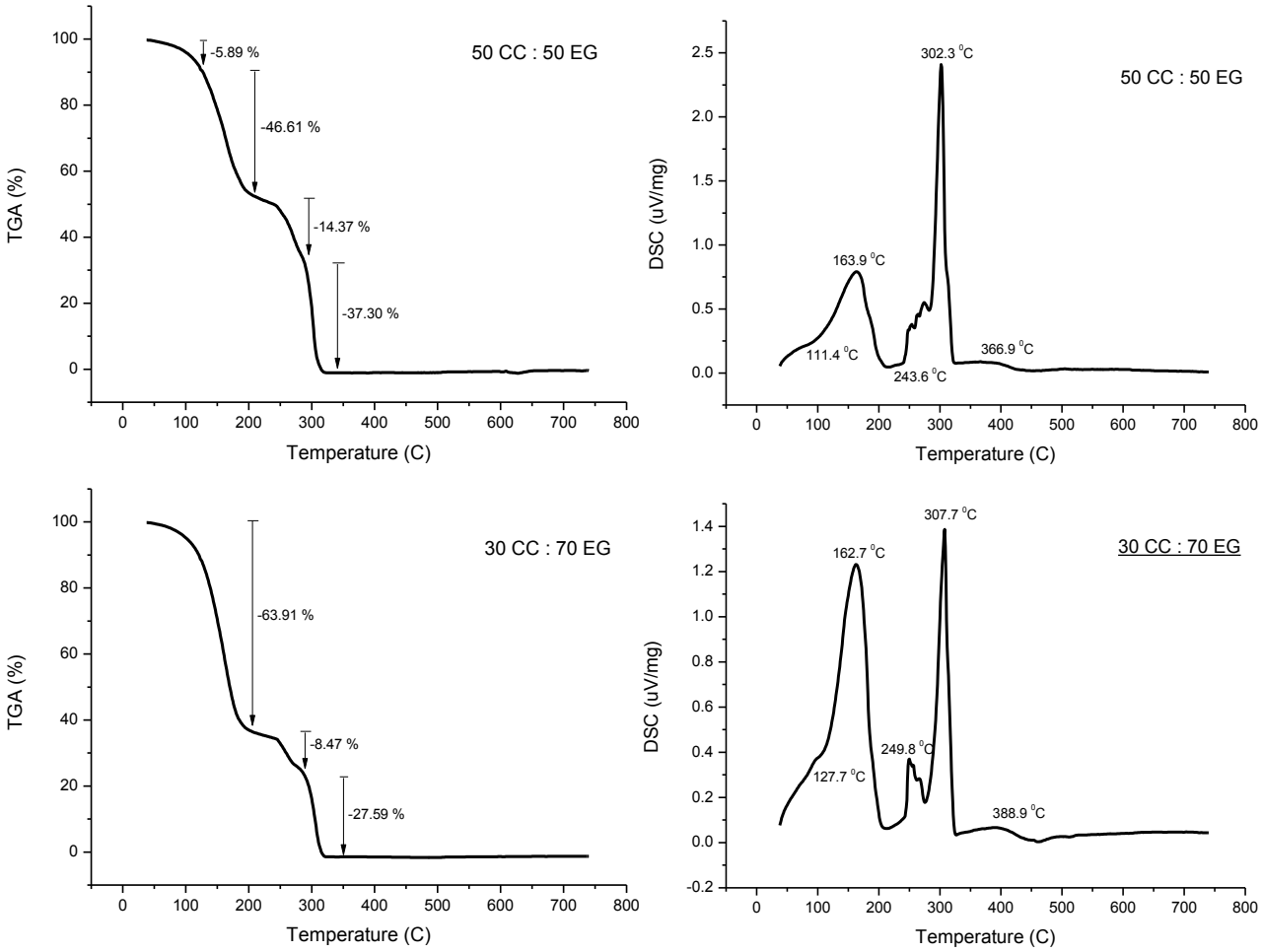

Figure 2-22: TGA (left) and DSC (right) analysis of choline chloride and ethylene glycol based binary mixtures (50:50 and 30:70).

DSC signals indicate that water present in choline chloride reacts to form some oxidized product because there is depression in the DSC signal with increased water contents. N^+, CH_2^+ and C^+ lines belong to choline chloride. DSC scan indicates the formation of some complex molecule at 227 °C which is then decomposed along with choline chloride. At temperature range 320 °C, there is again depression in DSC and at the same point water peak is increasing. Figure 2-17 (left) shows three steps of weight loss in 30:70 sample. Amount of CO_2 that is produced by the decomposition of organic matter also increased with choline chloride peak. CH_3^+ and NH^+ lines are produced due to the decomposition of choline chloride as well.

2.4.4.7 Choline Chloride and Glycerol System.

Figure 2-23 shows 50:50 sample weight loss in four steps with -4%, -28.82%, -41.31% and -36.97% while in 30:70 sample it is -3.14%, 49.64%, -40.64% and -5.33%. At this point there are two distinct peaks at DSC scan in 30:70 while one peak in 50:50 sample.

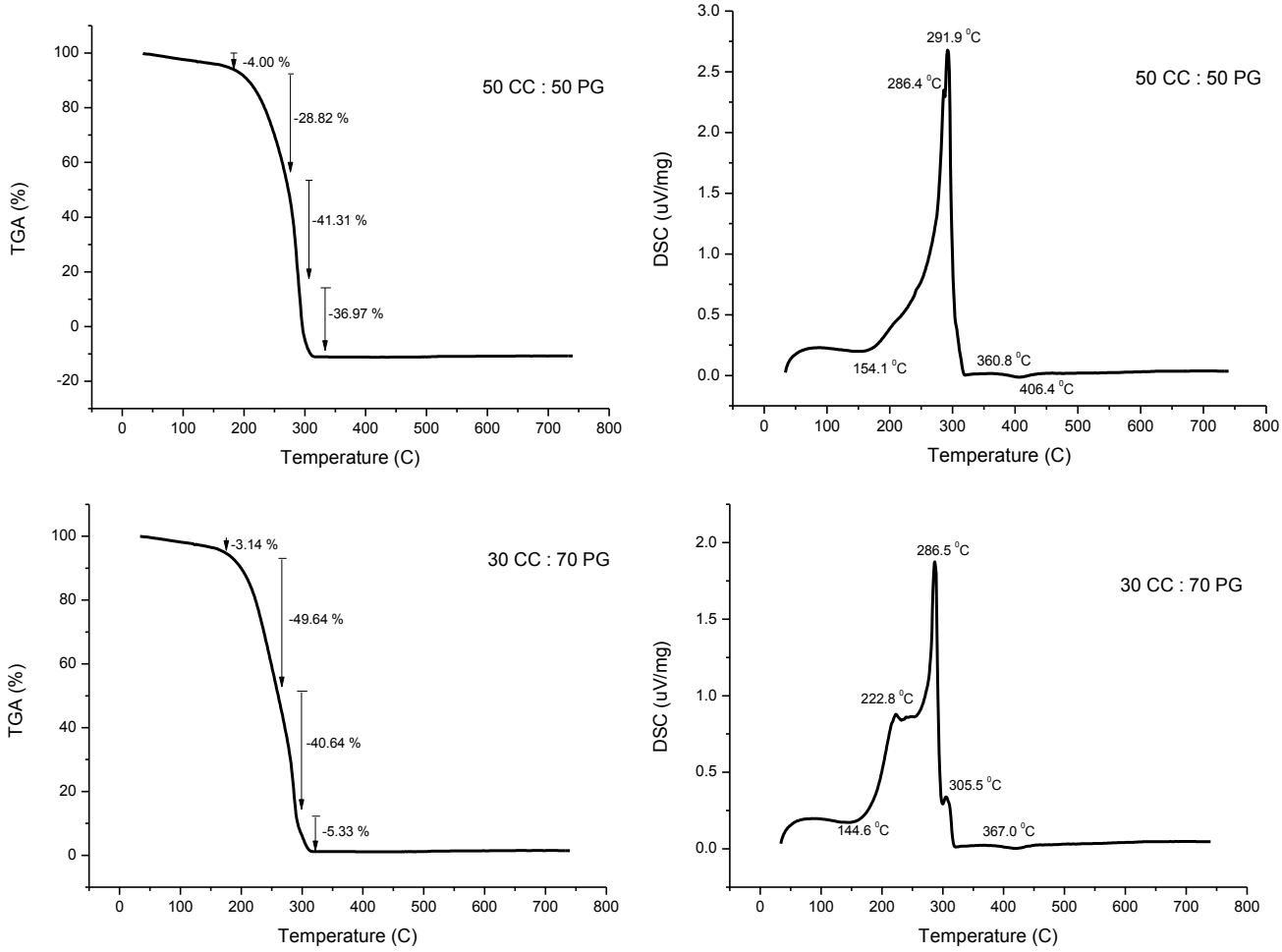

Figure 2-23: TGA (left) and DSC (right) analysis of choline chloride and glycerol based binary mixtures (50:50 and 30:70).

It shows that in DSC first peak belongs to EG as it becomes more obvious in 30:70 sample at 222.8 °C, second peak belongs to choline chloride at 286.5 °C which is around usual choline chloride peak region. Further the O^+, CH_4^+ and NH_2^+ lines showed increased shift in 50:50 as compared to 30:70 sample. There is the gain in water contents due to the decomposition of organic matter. Further CH_3^+ and NH^+ lines also got upward shift along with choline chloride at same position. DSC peak at

305 $^{\circ}$C is possibly due to formation of EG complex with chloride ions present due to the dissociation of choline chloride.

2.4.5 X-ray Diffraction

X-ray diffraction technique is a powerful tool to analyse and identify the crystal structure. Waves of x-ray are diffracted by the sample. Two types of XRD analysis were done, one with the electrolytic solutions at low temperature where they get hard, second were done at molybdenum metal surface to investigate the crystal structure of oxides of molybdenum if any of them is present. XRD technique was used to analyse $NH4NO_3/NH_3$ system after dissolving molybdenum in it anodically. The electrolyte was washed with methanol and after drying it was analysed in XRD. XRD measurements were carried out at Bruker AXS Kappa APE II diffractometer using Mo Ka radiation.

2.4.6 X-ray Fluorescence

X-ray fluorescence is characterised by the emission of secondary X-ray from a maretial which is excited by bombarding with high energy X-rays or gamma rays. This technique is widely used for the elemental analysis particularly in the investigation of metals. In this technique metal sample is exposed to the short wavelength X-rays or gamma rays, which causes ionisation of their atoms. The electrons from inner orbits are removed which causes a fall of electrons from outer orbits to inner orbits, which results in the emission of energy in the form of photon, the energy of which is equal to the energy difference of the two orbitals involved. In this way material emits the photon which has energy characteristic of the atoms present. XRF measurements were made on Fischerscope X-Ray XAN-FD 603-153 instrument.

2.4.7 Scanning Electron Microscopy (SEM)

Scanning electron microscopy (SEM) is a technique in which an image of a sample is obtained by scanning it with high-energy beam of electrons in a raster scan pattern.

The electrons interact with the atoms making sample to produce signals that contain informations about the sample surface topography, composition and properties like electrical conductivity. Signals produced by SEM are of different kinds including, secondary electrons, back scattered electrons, characteristic X-rays, specimen current and transmitted electrons. Secondary electron detectors are common in all SEMs, but it is rare that a single machine would have detectors for all possible signals.

The signals are produced by the interaction of the electron beam with atoms at or near the surface od sample. Characteristic X-rays are emitted when the electron beam removes an inner shell electron from the sample, causing a higher energy electron to fill the shell and release energy. These characteristic X-rays are used to identify the composition and measure the abundance of elements in the sample. In our experiments, SEM was used to analyse the surface of molybdenum after its anodic dissolution in choline chloride based binary mixture with ethylene glycol.

2.4.8 ESR Experiments

Electron spin resonance (ESR) experiments were conducted to investigate the dissolved molybdenum cation in the CC/EG system. The main purpose of these experiments was to monitor any paramagnetic species formed during the anodic dissolution of molybdenum in the CC/EG system. Figure 2-24 shows two scans, one in which the sample (CC/EG) was deoxygenated and one in which it was not, were conducted at 25°C. Both experiments show identical spectra, having a g value of 1.957 and a line width of 2.9 G, which indicates no sign of interactions with oxygen. Additionally, weak signals from ^{95}Mo and ^{97}Mo isotopes, which both have a nuclear spin of 5/2, were detected at the same g value as the principal signal, but with slightly wider lines and a hyperfine coupling constant of about 20 G.

The narrow and symmetric ESR signal with g value of 1.95 suggests the symmetry approximating octahedral one [150].Similar ESR signals with g values in the range of 1.945 to 1.95, but of differing line shapes, were obtained earlier for isolated Mo^{5+} ions stabilized by matrices of different zeolites [151]. Computer simulations of the experiments suggest the presence of only one paramagnet specie in the ESR spectrum. Furthermore, ESR results in our experiments closely resemble the ones reported earlier by Usmanov et.al. on the paramagnetic behavior of Mo^{5+} species

under similar conditions and in an ethylene glycol system [152]. ESR spectra of our system do not indicate any notable interaction of the Mo^{5+} specie with other species in the system, however it can be safely concluded that molybdenum in this oxidation state is present in the solution.

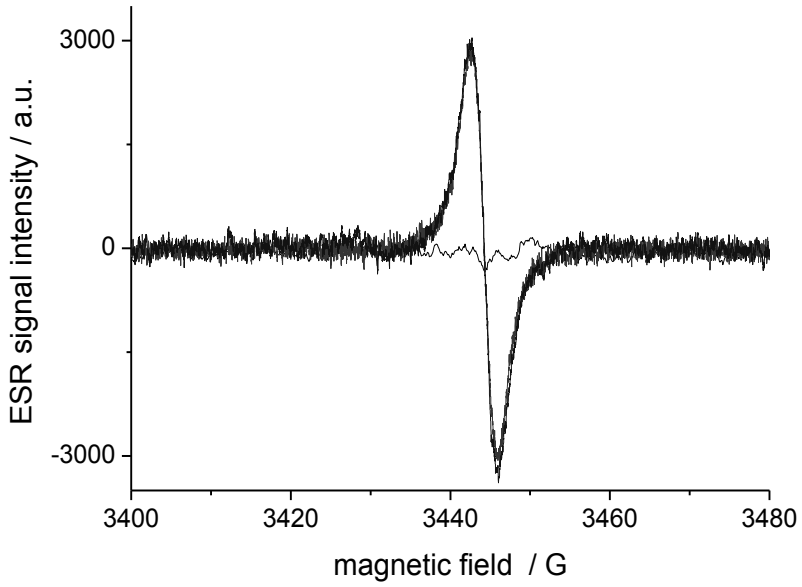

Figure 2-24: ESR spectra of anodically dissolved molybdenum in choline chloride/ethylene glycol (CC/EG) system at 25 ^{o}C.

3 Results and Discussion

The results and discussion include the electrochemical dissolution behavior of Mo and W in NH_4NO_3/NH_3 and choline chloride based binary mixtures which are listed in separate sections. Electrochemical dissolution of both the metals has been discussed with respect to weight loss analysis and anodic polarization both galvanostatically and potentiodynamically. All the galvanostatic studies were made between 50 mA/cm^2 to 150 mA/cm^2 , while potentiodynamic studies were made at a scan rate of 50 mV/sec. Weight loss measurements and hence the Faradaic weight loss efficiency was calculated by taking Mo and W valence of +5. Following table 3-1 shows the Theoretical weight loss of Mo and W considering both the metals have a valence of +5 at various current densities.

Current Density (mA/cm^2)	Mo (+5) weight loss	W (+5) weight loss
10	0.00715 g	0.0137 g
30	0.0214 g	0.0411 g
50	0.0358 g	0.0685 g
80	0.0572 g	0.1097 g
100	0.0716 g	0.1371 g
120	0.0859 g	0.1646 g
150	0.1073 g	0.2057 g

Table 3-1: Theoretical weight loss as calculated by using Faraday's law for metal dissolution.

Theoretical weight loss is the maximum amount of a metal that can be achieved by dissolving metal anodically at given current density as given in Table 3-1. Mo and W dissolved to great extent in all the electrolytic systems espacially in choline chloride based binary mixtures. The dissolution of metal in these electrolytes shows, how corrosive these electrolytic media are. Molybdenum theoretical weight loss is less that that of tungsten for respective current density value. This is because of the higher atomic mass of tungsten than that of molybdenum. Corrosion rate has also been calculated for Mo in NH_4NO_3/NH_3 system by using analytical tool in PEG200

software, which shows the corrosion rate in mm/year. Mo and W metal density was required for this purpose.

3.1 Anodic Dissolution of Mo in Ammoium Nitrate/Ammonia system.

Faradaic weight loss efficiency was calculated by using Faraday's Law of Electrolysis and putting the valency of molybdenum as +5. First theoretical weight loss was calculated and then divided by the actual weight loss to calculate percentage weight loss of electrode from its surface into the solution [153]. Faradaic weight loss efficiency indicated the strong corrosive property of NH_4NO_3/NH_3 (non aqueous) system with molybdenum as anode that is shown in the graph in figure 3-1. Dissolution efficiency went up to 79% while 76% of the dissolved molybdenum was redeposited on parent electrode.

Table 3-2 shows the amount of dissolved molybdenum and weight loss efficiency as calculated by using Faraday's law. The deposition efficiency was calculated by dividing the weight gain at molybdenum cathode with amount of dissolved molybdenum in the sample.

Current Density (mA/cm^2)	Cathode	Anode	Mass of Mo anode before A.D	Mass of Mo anode after A.D	Mass of Mo Dissolved	Weight Loss Efficiency (%age)
50	W	Mo	3.495 g	3.48 g	0.015 g	42
80	W	Mo	3.452 g	3.426 g	0.0257 g	45
100	W	Mo	3.322 g	3.287 g	0.035 g	49
120	W	Mo	3.251 g	3.183 g	0.0678 g	79
150	W	Mo	3.119 g	3.078 g	0.0407 g	38

Table 3-2: Weight loss efficiency of Mo in NH_4NO_3/NH_3 at 100 mA/cm^2 calculated by using Faraday's law. *A.D stands for anodic dissolution.

The weight loss of molybdenum (Mo) as anode was measured against tungsten (W) as cathode. Each measurement was taken three times and five experiment were conducted at different current densities from 50 mA/cm^2 to 150 mA/cm^2. Only

intermediate values of current density (between 100 to 120 mA/cm^2) gave good dissolution efficiency as shown in figure 3-1.

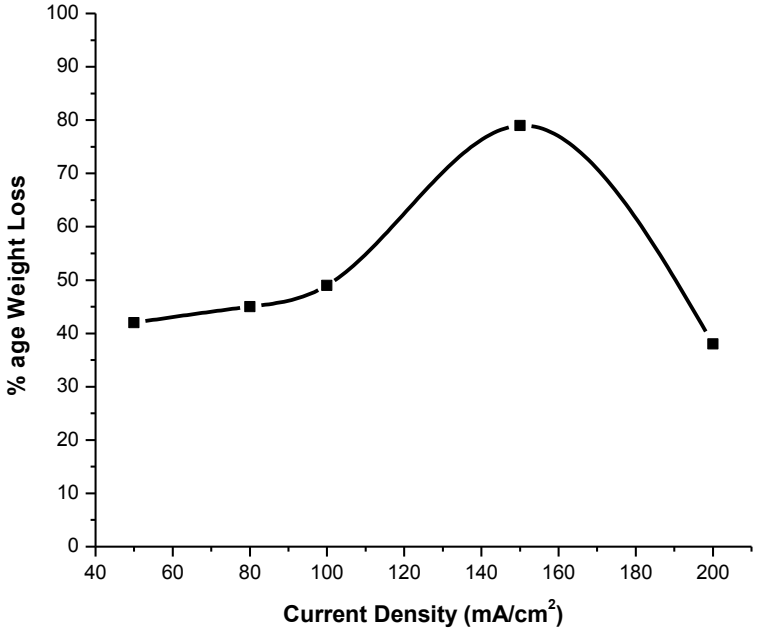

Figure 3-1: Graph showing the faradaic weight loss efficiency of Mo versus current density in NH_4NO_3/NH_3 system.

The faradaic dissolution efficiency was observed to be high in the range of 100 to 150 mA/cm^2 and it decreased with decrease in current density. Initially weight loss increased with the passage of time but it decreased after some time. The galvanostatic measurements show the initial increase in potential profile indicating the formation of passive layer at the surface of electrode. With the passage of time, the electrolyte was used up and decrease in weight loss efficiency indicates the saturation of solution with soluble complex close to the electrode surface.

The passive layer formation was analysed by the galvanostatic polarization of molybdenum in NH_4NO_3/NH_3 system at 100 mA/cm^2 for an hour. Initially a rise in cell potential is due to the formation and growth of surface layer. The start potential is 4.3 V and it increaes to a value with oscillation between a maximum and a minimum value. The potential becomes constant after sometime and oscillation in potential value continues. The oscillation in potential between minimum and maximum value might be due to the repeated formation and breakage of surface layer. Surface layer may be

formed due to the adsorbed species and it then breakes off or peals off from the electrode surface due to the diffusion of metals ions into the solution. When metal ion depart from the surface, they come accros a barrier of adsorbed layer, which hinder their diffusion for some time, which is obvious from the gradual increase in potential.

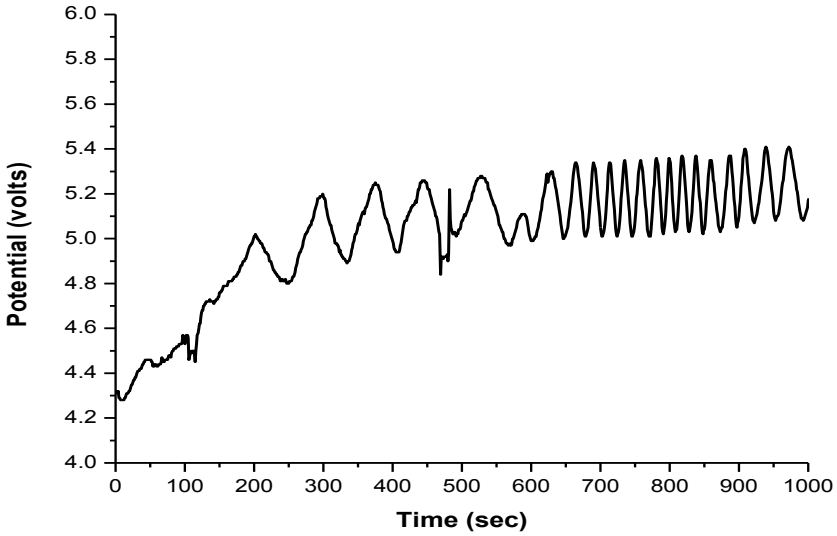

Figure 3-2: Galvanostatic diagram of molybdenum in NH_3/NH_4NO_3 system vs Ag/Ag^+ at 100 mA/cm^2.

Formation of molybdenum-ammonia complex at the surface of electrode seems to passivate the surface from further dissolution shown in figure 3-2. Under hydrodynamic conditions (stirred solution) the weight loss continued until the electrolyte became saturated with complex.

At low current density and initial stage of measurements, development of surface layer describes the passivation phenomena in figure 3-2 resulting in an increase in the potential with time. Weight loss and weight gain measurements performed on molybdenum show that molybdenum is deposited from NH_4NO_3/NH_3 system. Electrochemical deposition of molybdenum on parent substrate indicates the dissolution in stable +5 oxidation state in non-aqueous systems. Deposition on copper and iron was not successful. Cyclic voltammetry experiment showed a flat scan with NH_4NO_3/NH_3 system due to narrow electrochemical window of ammonia, which oxidizes to nitrogen (N_2) at +0.04 V vs Ag/Ag^+ [154].

Cyclic voltammetry performed with 1-Butyl-3-methyl-imidazolium-trifluoromethanesulfonate ($Bmim^+/CF_3SO_3^-$) at room temperature showed initial passivation at the surface of electrode and then dissolution takes place.

Electrochemical dissolution of Mo in aqueous system occurs in +6 oxidation state and it forms complexes with OH^- immediately after dissolution [155]. While in non-aqueous systems Mo dissolves in +5 oxidation state which forms complexes with ligands like NH_3 and is assumed to be stable and can be redeposited on cathode.

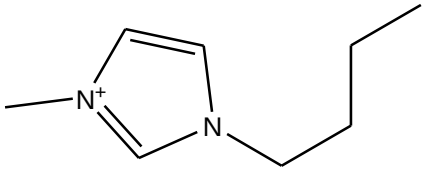

1-butyl-3-methyl-imidazolium

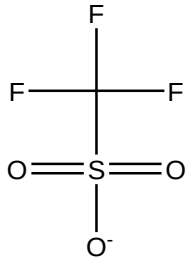

trifluoromethanesulfonate

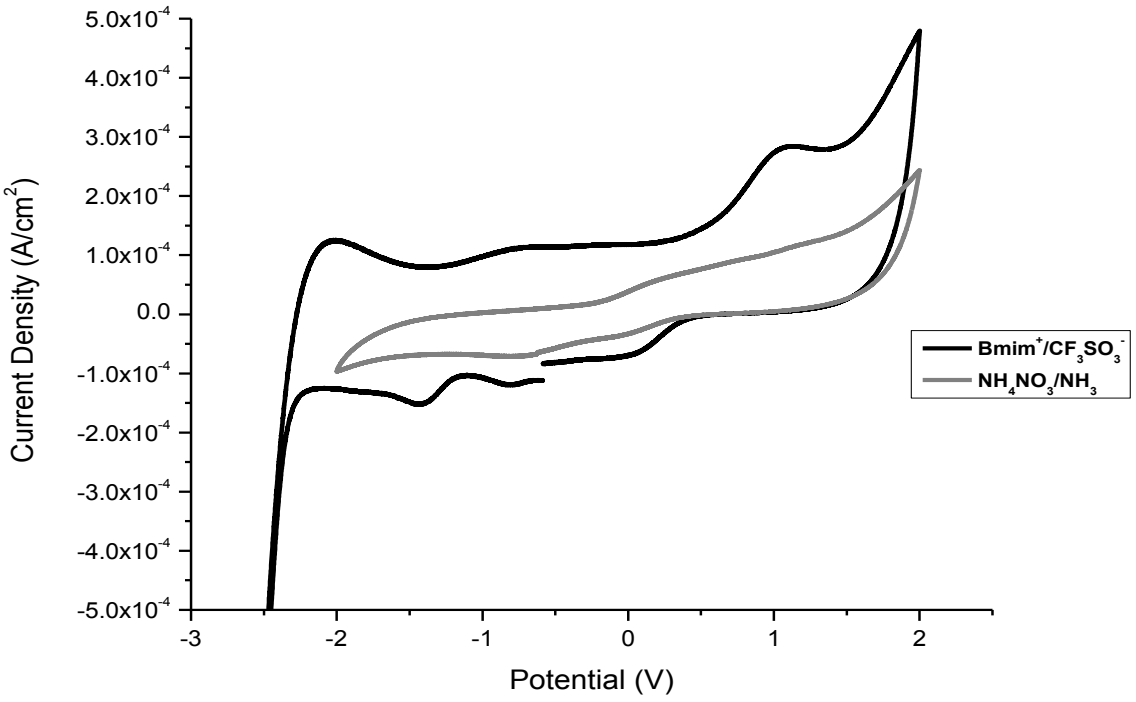

Figure 3-3: Cyclic voltammograms taken at scan rate of 50mV/sec at 25 ^oC for $[Bmim]^+/CF_3SO_3^-$ while at -35 ^oC for NH_4NO_3/NH_3 system vs Ag/Ag^+ reference electrode.

Cyclic voltammetry in figure 3-3, shows the dissolution of Mo in NH_4NO_3/NH_3 system and Mo dissolves and deposits from the electrolyte with obvious passivation. In other cyclic voltammogram behavior of Mo in $[Bmim]^+/CF_3SO_3^-$ is

shown where after initial passivation further dissolution of molybdenum takes place. Cyclic voltammetry in $[Bmim]^+/CF_3SO_3^-$ shows that Mo can be deposited from non-aqueous system at room temperature. Both diagrams are comparable and corrosion potential and corrosion current data gives nice picture about the
behavior of Mo in non-aqueous environment. When comparing the voltammograms of both the electrolytes, it can be realized that NH_4NO_3/NH_3 system has the ability and a potential window broad enough to be used as an alternate for ionic liquids.

	NH_4NO_3/NH_3				$Bmim/CF_3SO_3$			
	1^{st} Ox	1^{st} Red	2^{nd} Ox	2^{nd} Red	1^{st} Ox	1^{st} Red	2^{nd} Ox	2^{nd} Red
Potential (V)	-1.24	1.27	0.375	-0.743	-0.82	.079	1.08	-1.39
Current Density (A/c m^2)	-2.47×10^{-6}	1.01×10^{-5}	6.91×10^{-5}	-7.14×10^{-5}	8.74×10^{-5}	-6.41×10^{-5}	2.83×10^{-4}	-1.51×10^{-5}

Table 3-3: Oxidation/reduction data for $[Bmim]^+/CF_3SO_3^-$ and NH_3/NH_4NO_3 system.

Above given oxidation/reduction quantities in table 3-3, are obtained from the electrochemical behavior of Mo in both the electrolytic systems. From the potential and current density values, a comparison can be made between two electrolytic systems. Oxidation and reduction potential values for NH_3/NH_4NO_3 system shown in figure 3-4 are close to that of ionic liquid used.

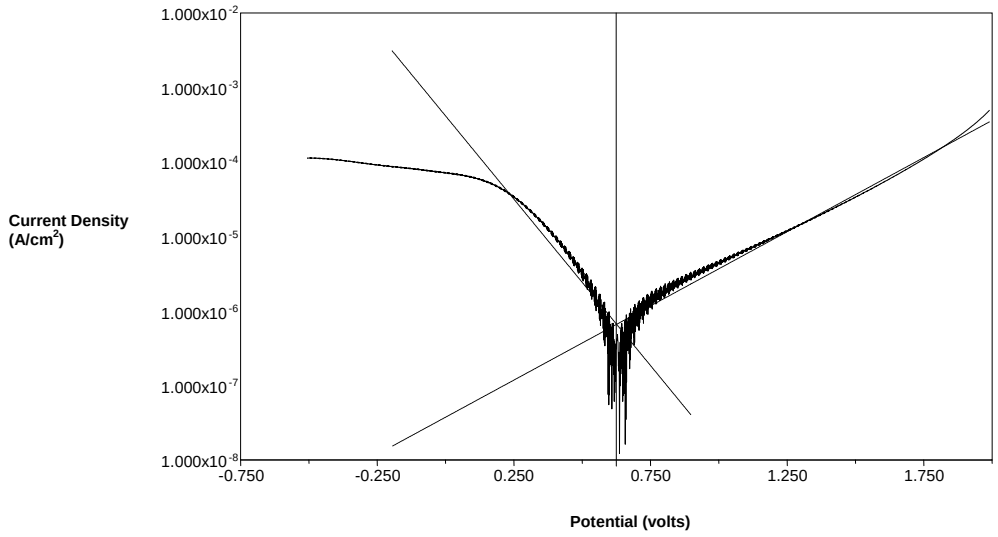

Figure 3-4: Corrosion process showing anodic and cathodic current components of Mo in NH_4NO_3/NH_3 system vs Ag/Ag^+.

The reaction at the anode is a corrosion reaction accompanied by the cathodic reduction reaction of NH_3 to hydrogen [156]. Oxidation of ammonia at molybdenum electrode in NH_4NO_3/NH_3 system is the most important reaction at potential +1.5 V. Table 3-3 shows the redox parameters with both the systems to give a comparison between potential and current density values. The current density values in the ionic liquid system are twice as in the ammonia-ammonium nitrate system. The potential range selected in the current-potential diagram shows more the mechanistic behavior of electrolyte rather than the metal dissolution and deposition process itself because metal starts to corrode at higher potential as shown in figure 3-2 from galvanostatic measurements.

Current-potential diagram for molybdenum in NH_4NO_3/NH_3 shows both the oxidation and reduction processes. Nitrogen production takes a route that is kinetically controlled at the surface of electrode while the production of hydrogen shows a mass transport mechanism after the depletion of the Nernst layer [157]. The negative potential region from 0 to -2 volts vs Pt shows electro-oxidation of NH_3 in NH_4NO_3/NH_3 system [158].

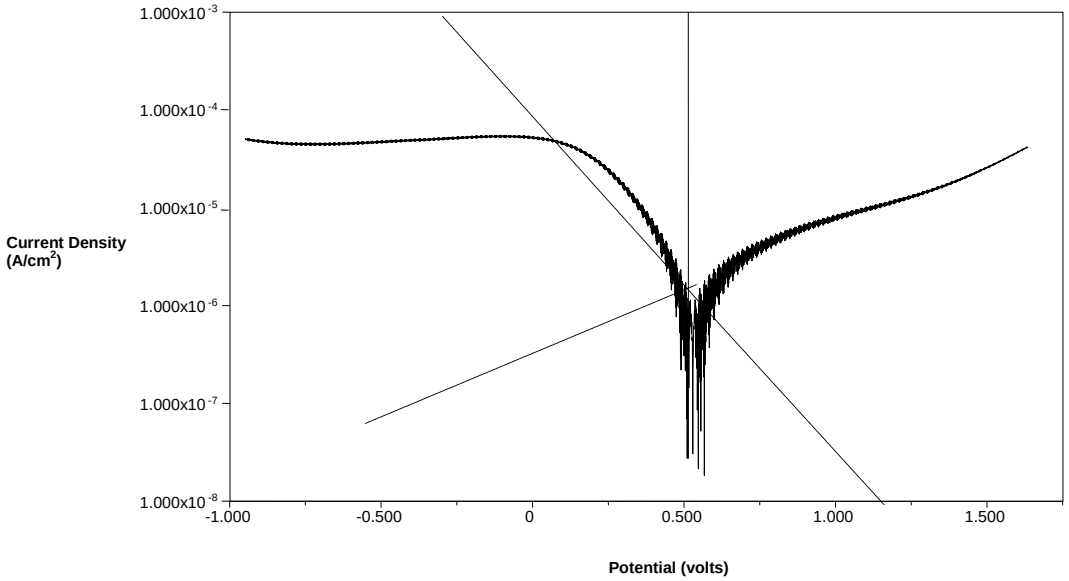

Figure 3-5: Corrosion process showing anodic and cathodic current components of Mo in $[Bmim]^+/CF_3SO_3^-$ system vs Ag/Ag^+.

Current-potential diagrams in figure 3-4 and 3-5 show the corrosion potential at a value of +0.6 volts for NH_4NO_3/NH_3 system while +0.5 volts for the ionic liquid

system. The current-potential diagrams also show the reaction in negative direction to be mass transport controlled from -0.25 volts onwards in negative direction, while it looks kinetically controlled or depends on charge transport from 0 to -0.25 volts. Metal oxidation in NH_4NO_3/NH_3 system takes place at 4.3 volts, while the region in positive direction from 0 to 2 volts shows the oxidation of electrolyte system. The corrosion process for both ionic liquid and NH_3/NH_4NO_3 systems indicates the hydrogen evolution at cathode by the reduction of ammonia at the surface of molybdenum. This is also indicated by the galvano-static measurements where there is an initial build up of oxidized gaseous species which requires higher potential to further dissolve it and finally the dissolution of metal anode (Mo) starts.

Polarization resistances of these systems are in the range of 10^4 Ω which is quite high as compared to the aqueous systems but it is comparable to the room temperature ionic liquids RTILs [159]. Higher value of the polarization suggests about viscosity and density of NH_4NO_3/NH_3 system to be high comparable with room temperature ionic liquids RTILs. Table 3-4 shows a comparison between the kinetic parameters of both the systems used and gives a nice picture about the ability of NH_3/NH_4NO_3 system to be used as an alternate of ionic liquids.

	Icorr (A/cm^2)	Ecorr (obs)	Ecorr (calc)	bc (V/dec)	ba (V/dec)	Rp (Ω)	Corrosion Rate (mm/year)
NH_4NO_3/NH_3	6.7×10^{-7}	0.6V	0.62V	0.22	0.51	7.2×10^{4}	2.12×10^{-2}
EMIM/TFSO	1.5×10^{-6}	0.5V	0.51V	0.28	0.77	6.42×10^{4}	4.6×10^{-2}

Table 3-4: Kinetic parameters of NH_3/NH_4NO_3 and $[Bmim]^+/CF_3SO_3^-$ systems.

As described by Beata Zawisza and Rafał Sitko [160], lower detection limits of analytes can be determined by the use of X-ray florescence (XRF). NH_4NO_3/NH_3 solution containing electrochemically dissolved molybdenum was further investigated by XRF analysis to check the presence of molybdenum in electrolytic residue. Figure 3-6 shows the presence of molybdenum in the residue as major component that indicates the possibility to form some molybdenum compound during electrochemical reaction.

From the experimental results obtained through XRF analysis, the most abundant specie inside the residue is Mo. But it is not possible to fully know about the

chemistry of dissolved molybdenum. Molybdenum might be present in the form of a complex as described later.

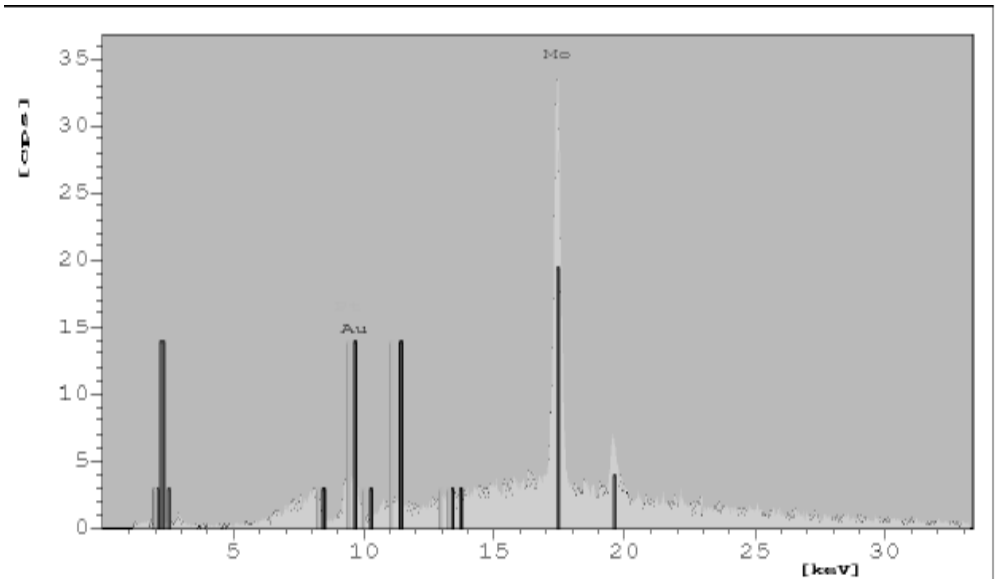

Figure 3-6: XRF analysis performed on the residue filtered and analyzed after electrochemical treatment.

B.D. Cullity [161] discussed in detail about elements in the low concentration range to show their evidences in x-ray diffraction. XRD in figure 3-7 was performed on the remaining residue after electrochemical treatment, filtering and washing with methanol. XRD diagram shows presence of molybdenum in two shoulder peaks. These shoulders peaks are important because same sample showed big peak belonging to molybdenum in XRF analysis.

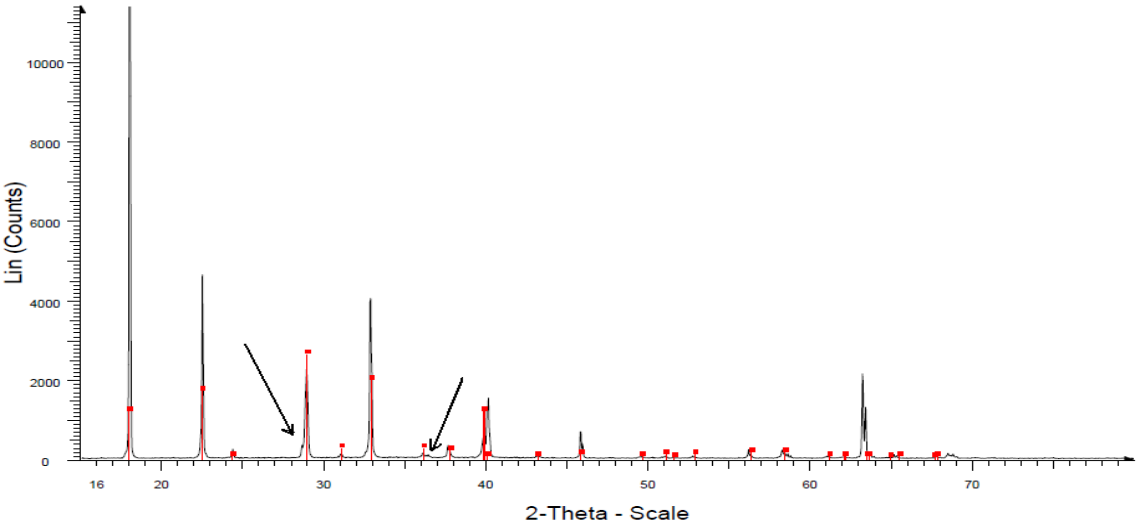

Figure 3-7: XRD shows the presence of Mo complex after electrochemical treatment, arrows indicate the shoulder peaks.

3.1.1 Discussion of Molybdenum Complexing Reaction

Primary dissolution products from the electrochemical dissolution of molybdenum in aqueous electrolytes usually end up, independent of the initial oxidation state as a suspension of particles consisting of hydrated MoO_2 [162-164].

In anodic dissolution molybdenum is allowed to oxidize and subsequently forms complex with NH_3 giving the following general reaction [165].

$$M + xNH_3 \longrightarrow [M(NH_3)x]^{z+} + ze^- \qquad (3\text{-}1)$$

Under non-aqueous conditions where molybdenum dissolves in +5 oxidation state, the possible reactions are as follows:

$$Mo + 5NH_3 \longrightarrow [Mo(NH_3)_5]^{5+} \rightleftharpoons [Mo(NH_3)_5NO_3]^{4+} \qquad (3\text{-}2)$$

According to our assumption from the color change during electrochemical reaction, $[Mo(NH_3)_5]^{5+}$ is formed which is dark brown. $[Mo(NH_3)_5]^{5+}$ further reacts chemically to form $[Mo(NH_3)_5NO_3]^{4+}$ which is light yellow in color and a color

change after the anodic reaction takes place in the bulk of solution suggesting an electrochemical reaction at the surface of electrode followed by chemical reactions.

Molybdenum has electronic configuration of (Kr) $5s^1$, $4d^5$ [166]. It is assumed that molybdenum dissolves in non aqueous media in oxidation state of +5 releasing all the electrons in 'd' sub shell thus leaving the vacancy for 10 electrons in empty d orbitals. Dark brown product formed by the electrolysis of NH_4NO_3/NH_3 system is probably the coordinated compound of Mo with NH_3 as ligand and later NO_3^- ions attach to form light yellow product $[Mo(NH_3)_5NO_3]^{+4}$.

Electrochemical experiments of molybdenum as working electrode in $[Bmim]^+/CF_3SO_3^-$ system yielded yellow color at electrode surface which might be due to the formation of complex of molybdenum with $CF_3SO_3^-$ anions but a real chemistry is unknown. Change in color at the surface of electrode was observed on anodic scan at +1.5V. However, the dissolution amount and hence current efficiency measurements are yet to be performed.

3.1.2 Electrodeposition of Mo in NH_4NO_3/NH_3 system.

Based on the results obtained from cyclic voltammetry and molybdenum complex analysis using XRF and XRD, electrodeposition of molybdenum was investigated on parent electrode. Same experimental setup of two electrode systems with double jacket corrosion cell and a DC power supply was used. Molybdenum anode was dissolved in NH_4NO_3/NH_3 system at 100 mA/cm^2. Dissolved molybdenum forming a complex with the ligands in +5 oxidation state was also able to deposit on molybdenum cathode.

Following table 3-5 shows the weight gained by molybdenum cathode during deposition experiments. The amount of electrochemically dissolved molybdenum in NH4NO3/NH3 system was 0.095 g. The dissolved molybdenum was able to redeposit up to 76% which shows the ability of NH_4NO_3/NH_3 system to be a good option for the recycling of molybdenum.

Current density (mA/cm^2)	Anode Material	Cathode Material	Weight of cathode before exp	Weight of cathode after exp	Weight gain at cathode	%age of deposited Mo
100	Mo	Mo	4.210 g	4.2638 g	0.0538 g	75%
100	Mo	Mo	4.200 g	4.2548 g	0.0548 g	76%
100	Mo	Mo	4.195 g	4.2498 g	0.0548 g	76%

Table 3-5: Redeposition of dissolved Mo at parent electrode in NH_4NO_3/NH_3 system containing 0.0722 g of dissolved Mo for each measurement.

The electrodeposition results of molybdenum in NH_4NO_3/NH_3 system indicate the presence of Mo^{+5} in comparison to the Mo^{+6} in aqueous systems. As previously described, that Mo usually exists in +6 oxidation state which forms complexes with hydroxyl ions making it hard to redeposit while in our experiments, we are able to conclude that Mo is present in +5 oxidation state. Although the experiments for such kind of deposition require extra labor and care at low temperature, yet further investigations in this field can lead to processes where molybdenum like refractory metals can be deposited from spent material at low temperatures.

3.2 Weight loss analysis in choline chloride based binary mixtures.

The faradaic weight loss efficicnecy was calculated by calculating the percentage weight loss according to the Faraday Law assuming the valency of molybdenum and tungsten as +5 [167]. Weight loss experiments indicated the strong corrosive property of choline chloride based binary mixtures. Anodic dissolution of molybdenum and tungsten as anode is shown in the graphs given below. The graphs have been discussed according to the type and nature of electrolytic system used for anodic dissolution process. Dissolution efficiency went up to 85% for choline chloride and glycerin (CC/Gly) mixture at lower current densities as discussed later on. An increase in the dissolution of Mo at lower current densities was observed. Dissolution efficiency stayed constant independent of current density values at higher current densities.

It was assumed based on this observation that at higher current densities dissolution mechanism is mass transport controlled while at lower current densities dissolution is kinetically controlled. At higher current density the species like metal

chlorides are formed near the surface of electrode that passivate the electrode surface and would make the further transport mechanism of these species into solution difficult and on the other hand at lower current densities small amount of the product is formed at electrode surface that dissolves away quickly making the surface available for further metal dissolution.

3.2.1 Weight loss in choline chloride and urea system

Choline chloride based binary mixture with urea form an ideal deep eutectic solvent which is liquid at 30^{o}C and was used as electrolyte to check the anodic dissolution of molybdenum. The binary mixture is stabilized by the hydrogen bond donor group of urea [168]. When molybdenum is dissolved anodically, it dissolves more at low current density indicating the diffusion controlled dissolution process. MoO_2 formed at the surface allows the molybdenum ions to pass through it. Oxide layer formed at the surface is thick at lower current densities and hence makes possible the slow and efficient dissolution of molybdenum. Addition of KCl to the urea based binary mixture did not change the dissolution efficiency at any current density value. At higher current density rate of molybdenum dissolution is independent of the current density which indicated the formation of thick oxide later followed by metal chloride layer, which would hinder the dissolution efficiency.

Current Density (mA/cm^2)	Cathode	Anode	Mass of Mo anode before A.D	Mass of Mo anode after A.D	Mass of Mo Dissolved	Weight Loss Efficiency (%age)
5	W	Mo	5.178 g	5.1759 g	0.00204 g	57
10	W	Mo	5.092 g	5.0891 g	0.00286 g	40
15	W	Mo	5.041 g	5.0377 g	0.00321 g	30
20	W	Mo	4.987 g	4.9827 g	0.00429 g	30
30	W	Mo	4.902 g	4.8967 g	0.00528 g	24.7
50	W	Mo	4.857 g	4.8497 g	0.00730 g	20.4
100	W	Mo	4.831 g	4.8182 g	0.01280 g	18
150	W	Mo	4.809 g	4.7866 g	0.02230 g	20.8

Table 3-6: Weight loss efficiency of Mo in CC/urea system at 100 mA/cm^2 calculated by using Faraday's law. *A.D stands for anodic dissolution.

Current Density (mA/cm^2)	Cathode	Anode	Mass of Mo anode before A.D	Mass of Mo anode after A.D	Mass of Mo Dissolved	Weight Loss Efficiency (%age)
1	W	Mo	3.575 g	3.5746 g	0.0004 g	56
5	W	Mo	3.512 g	3.5100 g	0.0020 g	56
10	W	Mo	3.472 g	3.4693 g	0.0027 g	38
15	W	Mo	3.438 g	3.4349 g	0.0031 g	29
20	W	Mo	3.419 g	3.4156 g	0.0034 g	24
30	W	Mo	3.381 g	3.3763 g	0.0047 g	22
50	W	Mo	3.350 g	3.3440 g	0.0060 g	17
100	W	Mo	3.326 g	3.3139 g	0.0121 g	17
150	W	Mo	3.291 g	3.2728 g	0.0182 g	17

Table 3-7: Weight loss efficiency of Mo in CC/urea/KCl system at 100 mA/cm^2 calculated by using Faraday's law. *A.D stands for anodic dissolution.

Table 3-6 and table 3-7 show the percentage weight loss efficiency of molybdenum in two deep eutectic mixtures. It is clear that anodic dissolution of molybdenum is higher at small current densities while becomes lower and attains a constant value at high current density. At high current densities, the formation of thick passive layer immediatly after the anodic polarization hinders the dissolution process.

It is also important to note that dissolution efficiency is quite low as compared to other mixtures. The maximum is 60% at low current density and this is due to the highly viscous binary mixture of urea with choline chloride.

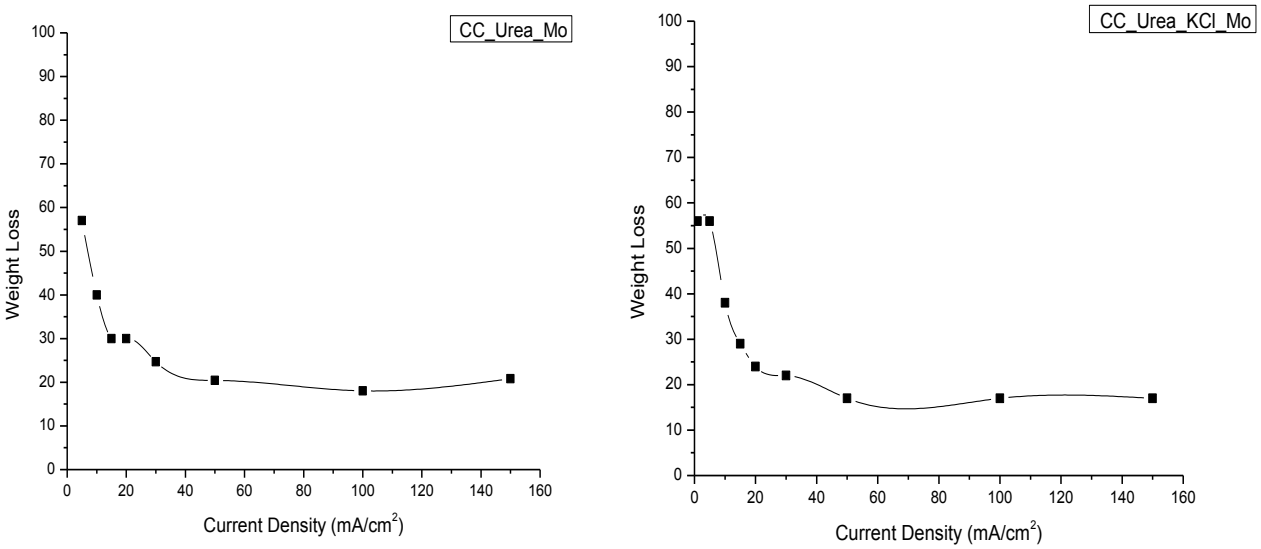

Figure 3-8: Graph showing the percentage weight loss at anode versus current density for Mo and W in choline chloride and urea based binary mixtures.

High viscosity of electrolytic system hinders the transporation of oxidised species to the bulk of the solution and making it hard to clear the electrode surface. This is the reason due to which electrode surface is not available for further oxidation. Graphs in figure 3-8 show the dissolution behavior of Mo in CC/urea and CC/urea/KCl systems. The dissolution efficiency at lower current densities is compared to the normal dissolution as observed in other systems described later on. The low viscosity and high conductivity make those electrolytic systems highly corrosive as CC/DMSO system gave the dissolution efficiency of 80% which is comparable to that of CC/Gly system. While CC/DMF system also showed the dissolution efficiency in the range of 50% to 60%. The dissolution efficiency is not affected by the current density and remains constant over a long range of current density. Since CC/urea system has high viscosity compared to other deep eutectic systems, that causes problem in the over diffusion process of dissolved species from electrode surface.

3.2.2. Weight Loss in choline chloride with ethylene glycol and glycerol systems

Choline chloride based binary mixtures with ethylene glycol (EG) and glycerol (Gly) is well known deep eutetic mixtures which are liquid at room temperature. Many investigators used these mixtures for electropolishing and electrodeposition of metals [169]. Molybdenum anodic dissolution is not affected by the current density. Dissolution efficiency of molybdenum is highest in CC/Gly mixture than any other deep eutectic solvent including CC/EG system. This shows the dependance of anodic dissolution on the stability of dissolved molybdenum ions. Molybdenum ions (Mo^{+5}) formed at the surface of electrode are more stabilised in glycerol system due to the presence of more –OH groups in glycerol molecule. The stability factor matters so much that molybdenum dissolves with highest faradaic dissolution efficiency in glycerol/choline chloride system than any other system.

Current Density (mA/cm^2)	Cathode	Anode	Mass of Mo anode before A.D	Mass of Mo anode after A.D	Mass of Mo Dissolved	Weight Loss Efficiency (%age)
1	W	Mo	5.464 g	5.4637 g	0.0003 g	42
10	W	Mo	5.431 g	5.4262 g	0.0048 g	68
30	W	Mo	5.419 g	5.4103 g	0.0087 g	41
50	W	Mo	5.352 g	5.3406 g	0.0114 g	32
100	W	Mo	5.311 g	5.2903 g	0.0207 g	29
150	W	Mo	5.252 g	5.2242 g	0.0278 g	26

Table 3-8: Weight loss efficiency of Mo in CC/EG at 100 mA/cm^2 calculated by using Faraday's law. *A.D stands for anodic dissolution.

Weight loss efficiency on the average remains between 30% to 40% but at lower current density e.g. at 10 mA/cm^2 dissolution goes up to 68% which is due to the mass transport effect of ionic species dissolved from molybdenum surface.

Current Density (mA/cm^2)	Cathode	Anode	Mass of Mo anode before A.D	Mass of Mo anode after A.D	Mass of Mo Dissolved	Weight Loss Efficiency (%age)
10	W	Mo	4.752 g	4.7460 g	0.0060 g	85
15	W	Mo	4.719 g	4.7104 g	0.0086 g	81
20	W	Mo	4.689 g	4.6780 g	0.0111 g	78
30	W	Mo	4.428 g	4.4094 g	0.0186 g	87
50	W	Mo	4.312 g	4.2827 g	0.0293 g	82
100	W	Mo	4.218 g	4.1586 g	0.0594 g	83
150	W	Mo	4.107 g	4.0276 g	0.0794 g	74

Table 3-9: Weight loss efficiency of Mo in CC/Gly at 100 mA/cm^2 calculated by using Faraday's law. *A.D stands for anodic dissolution.

Faradaic dissolution efficiency for Mo stays in the range of 80% for CC/Gly. This is due to the good solvation effect of $MoCl_5$ species formed as a result of dissolition of molybdenum. In case of CC/Gly system, molybdenum dissolution is high at lower current density and becomes low towards higher current densities which is usual phenomenon described earlier. Table 3-10 shows the dissolution efficiency of tungsten in CC/EG system, which is low at lower current densities and increases with the increase in current density until it gets a constant value.

Current Density (mA/cm^2)	Cathode	Anode	Mass of Mo anode before A.D	Mass of Mo anode after A.D	Mass of Mo Dissolved	Weight Loss Efficiency (%age)
1	Pt	W	3.918 g	3.9179 g	0.00001 g	1
10	Pt	W	3.851 g	3.8506 g	0.0004 g	3
30	Pt	W	3.792 g	3.7863 g	0.0057 g	14
50	Pt	W	3.741 g	3.7130 g	0.0280 g	41
100	Pt	W	3.708 g	3.6491 g	0.0589 g	43
150	Pt	W	3.683 g	3.5884 g	0.0946 g	46

Table 3-10: Weight loss efficiency of W in CC/EG at 100 mA/cm^2 calculated by using Faraday's law. *A.D stands for anodic dissolution.

Difference in the dissolution efficiency of W and Mo in CC/EG system might be due to the difference in crystal lattice and the stabilization energies of complexes formed after dissolution in electrolyte. Figure 3-9 shows the faradaic weight loss efficiency of molybdenum in CC/EG and CC/Gly system and also faradaic dissolution efficiency of tungsten in CC/EG system. It can be noticed that molybdenum dissolved to over 80% efficiency in CC/Gly system.

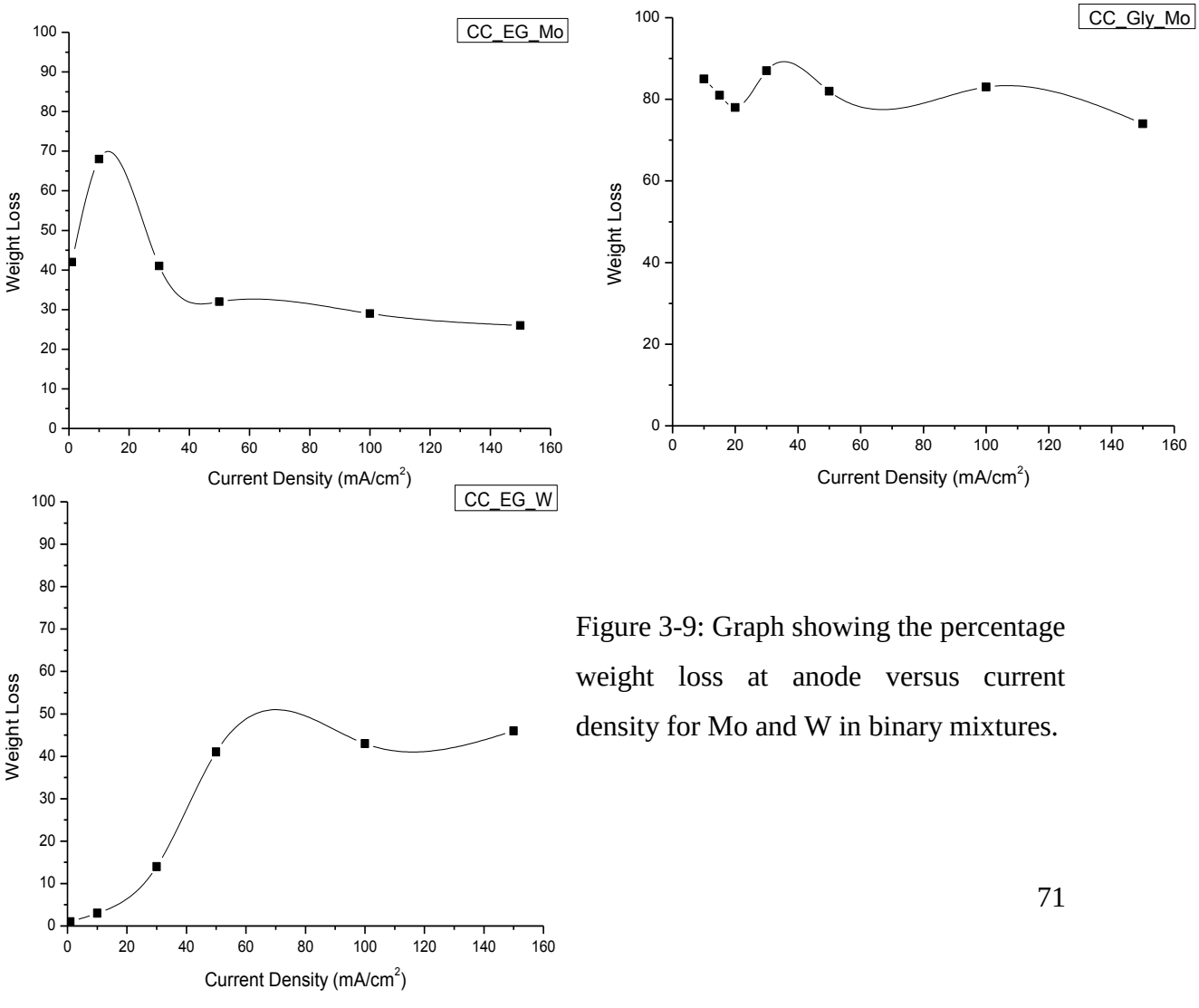

Figure 3-9: Graph showing the percentage weight loss at anode versus current density for Mo and W in binary mixtures.

Both Mo and W dissolve to 50% efficiency in CC/EG system. The difference is, molybdenum dissolution is independent of the current density applied for the dissolution, which is most probably due to the nature of oxide layer formed at the surface of electrode. While in case of tungsten, it dissolved in low percentage at lower current densities and as the current density was increased, the dissolution efficiency also increased.

3.2.2 Weight loss in choline chloride and polar aprotic systems

Polar aprotic systems are the one which have strong ion dissolving power, but they do not display hydrogen bonding but still they are able to stabilize ions [170]. Dimethyle sulfoxide (DMSO) and dimethyl formamide (DMF) were used with choline chloride. Due to the good stability of dissociated choline cations and chloride anions in both DMSO and DMF solution, conductivity of electrolyte is fairly high. Another factor is the low viscosity of the electrolyte due to DMSO and DMF.

Current Density (mA/cm^2)	Cathode	Anode	Mass of Mo anode before A.D	Mass of Mo anode after A.D	Mass of Mo Dissolved	Weight Loss Efficiency (%age)
1	W	Mo	5.141 g	5.1406 g	0.00057 g	80
5	W	Mo	5.119 g	5.1161 g	0.0029 g	83
10	W	Mo	5.074 g	5.0683 g	0.0057 g	80
15	W	Mo	5.021 g	5.0121 g	0.0089 g	84
20	W	Mo	4.982 g	4.9708 g	0.0112 g	79
30	W	Mo	4.941 g	4.9235 g	0.0175 g	82
50	W	Mo	4.906 g	4.8767 g	0.0293 g	81
100	W	Mo	4.849 g	4.7903 g	0.0587 g	82
150	W	Mo	4.761 g	4.6720 g	0.0890 g	83

Table 3-11: Weight loss efficiency of Mo in CC/DMSO at 100 mA/cm^2 calculated by using Faraday's law. *A.D stands for anodic dissolution.

The dissolution efficiency of molybdenum in CC/DMSO system is shown in table 3-11 which is comparable to the dissolution efficiency in CC/Gly system. Low viscosity of this binary mixture eases the transport of dissolved species from electrode surface into the bulk solution making electrode surface available again for dissolution. Another important aspect can be the stability of $MoCl_5$ inside the solution which also

important for the good dissolution of molybdenum. The dissolution efficiency stays around 80% both at low and high current densities.

Current Density (mA/cm^2)	Cathode	Anode	Mass of Mo anode before A.D	Mass of Mo anode after A.D	Mass of Mo Dissolved	Weight Loss Efficiency (%age)
1	W	Mo	4.521 g	4.5206 g	0.00037 g	52
5	W	Mo	4.478 g	4.4764 g	0.0016 g	46
10	W	Mo	4.431 g	4.4280 g	0.0030 g	43
15	W	Mo	4.389 g	4.3836 g	0.0054 g	51
20	W	Mo	4.324 g	4.3158 g	0.0082 g	58
30	W	Mo	4.268 g	4.2533 g	0.0147 g	69
50	W	Mo	4.201 g	4.1746 g	0.0267 g	74
100	W	Mo	4.105 g	4.0464 g	0.0587 g	82
150	W	Mo	3.981 g	3.9253 g	0.0557 g	52

Table 3-12: Weight loss efficiency of Mo in CC/DMF at 100 mA/cm^2 calculated by using Faraday's law. *A.D stands for anodic dissolution.

Weight loss of molybdenum in CC/DMF is more variable versus current density as compared to that in CC/DMSO system shown in figure 3-10. Dissolution efficiency goes from lower to higher value with the increase in current density for CC/DMF system. It can be said that dissolution in CC/DMF is more controlled by mass transport of dissolved species than in CC/DMSO.

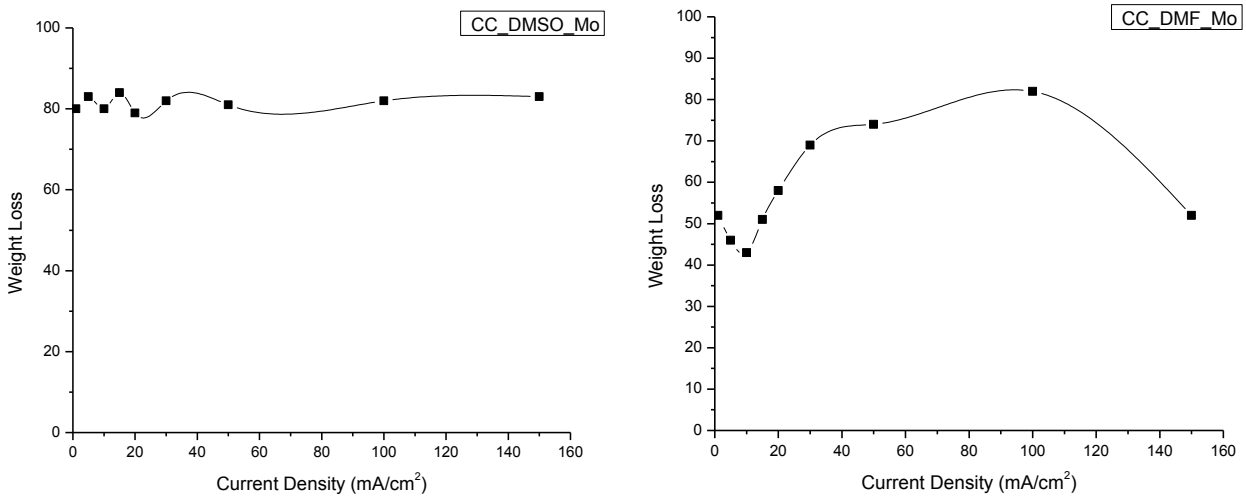

Figure 3-10: Graph showing the percentage weight loss at anode versus current density for Mo and W in CC/DMSO and CC/DMF binary mixtures.

3.2.3 Weight loss in choline chloride and acetic acid system

Acetic acid is one of the simplest carboxylic acids, whose pure and concentrated form is highly corrosive in character. Acetic acid is polar protic solvent similar to ethanol and water. Due to moderate dielectric constant, acetic acid can dissolve salts like choline chloride very easily making the binary mixture a highly corrosive electrolyte [171]. Choline chloride and acetic acid mixture is stable liquid at room temperature and was used to anodically dissolve molybdenum. The faradaic dissolution efficiency at both low and high current density is 70% to 75% which is fairly high. The electolyte turned black after electrolysis which is an indication of formation of complex of dissolved molybdenum with acetate ions present in the solution.

Current Density (mA/cm^2)	Cathode	Anode	Mass of Mo anode before A.D	Mass of Mo anode after A.D	Mass of Mo Dissolved	Weight Loss Efficiency (%age)
1	W	Mo	3.752 g	3.7515 g	0.0005 g	72
10	W	Mo	3.712 g	3.7068 g	0.0052 g	74
15	W	Mo	3.668 g	3.6597 g	0.0083 g	78
20	W	Mo	3.624 g	3.6135 g	0.0105 g	74
30	W	Mo	3.539 g	3.5224 g	0.0166 g	78
50	W	Mo	3.488 g	3.4619 g	0.0261 g	73
100	W	Mo	3.412 g	3.3598 g	0.0522 g	73
150	W	Mo	3.311 g	3.2274 g	0.0836 g	78

Table 3-13: Weight loss efficiency of Mo in CC/Acetic Acid at 100 mA/cm^2 calculated by using Faraday's law. *A.D stands for anodic dissolution.

Weight loss efficiency of Mo in CC/acetic acid as shown in table 3-13 and then described by figure 3-11 is 72% to 78% which is almost constant. High efficiency is due to the low viscosity of the binary mixture and good stability of the molybdenum complex formed after dissolution. It is obvious that dissolution is independent of current density value which shows that the anodic dissolution process is not controlled by the transport of species from electrode surface.

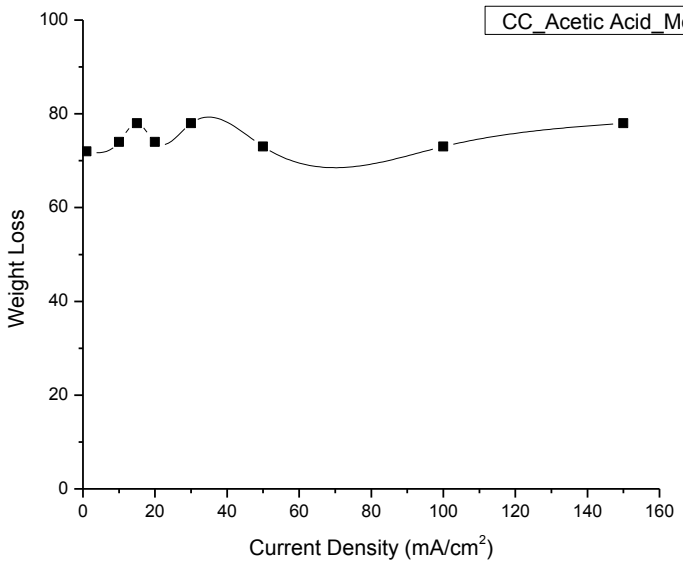

Figure 3-11: Graph showing the percentage weight loss at anode versus current density for Mo in CC/acetic acid binary mixtures.

The most important feature of the anodic dissolution of molybdenum and tungsten which is further discussed in the next section is the dependence of faradaic dissolution efficiency on the concentration of chloride ions. As the concentration of chloride ions increases, dissolution efficiency decreases reaching a plateau. The dissolution efficiency increases with a decrease in chloride ion concentration until the graph reaches a plateau.

3.3 Anodic Dissolution of Molybdenum and Tungsten

Dissolution is better at the low current density which is the case mostly in Mo and not for W, the reaction is kinetically controlled; the product formed at the surface in this case has more time to move away from the electrode surface into the bulk electrolyte. At high current density values the reaction remains a transport controlled process because the product is accumulating the electrode surface and dissolution curve shows a steady state. This is the case for all dissolution processes of W and Mo with binary mixtures. Dissolution at lower current densities is kinetically controlled and at higher current densities dissolution appears a straight line indicating the accumulation of the dissolution products at the surface, lowering the dissolution rate and making it almost a constant value.

The graph of percentage weight loss versus current density for W and Mo for different ratios of choline chloride containing binary mixtures shows interesting results. The binary mixtures containing alcohols of high number of –OH groups dissolve more metal than the one with low number of –OH groups and the comparison here is between EG and Glycerol. For Mo, EG shows percentage dissolution of 40% on the average for various current densities while for Glycerol the percentage weight loss is close to 80% which is quite high.

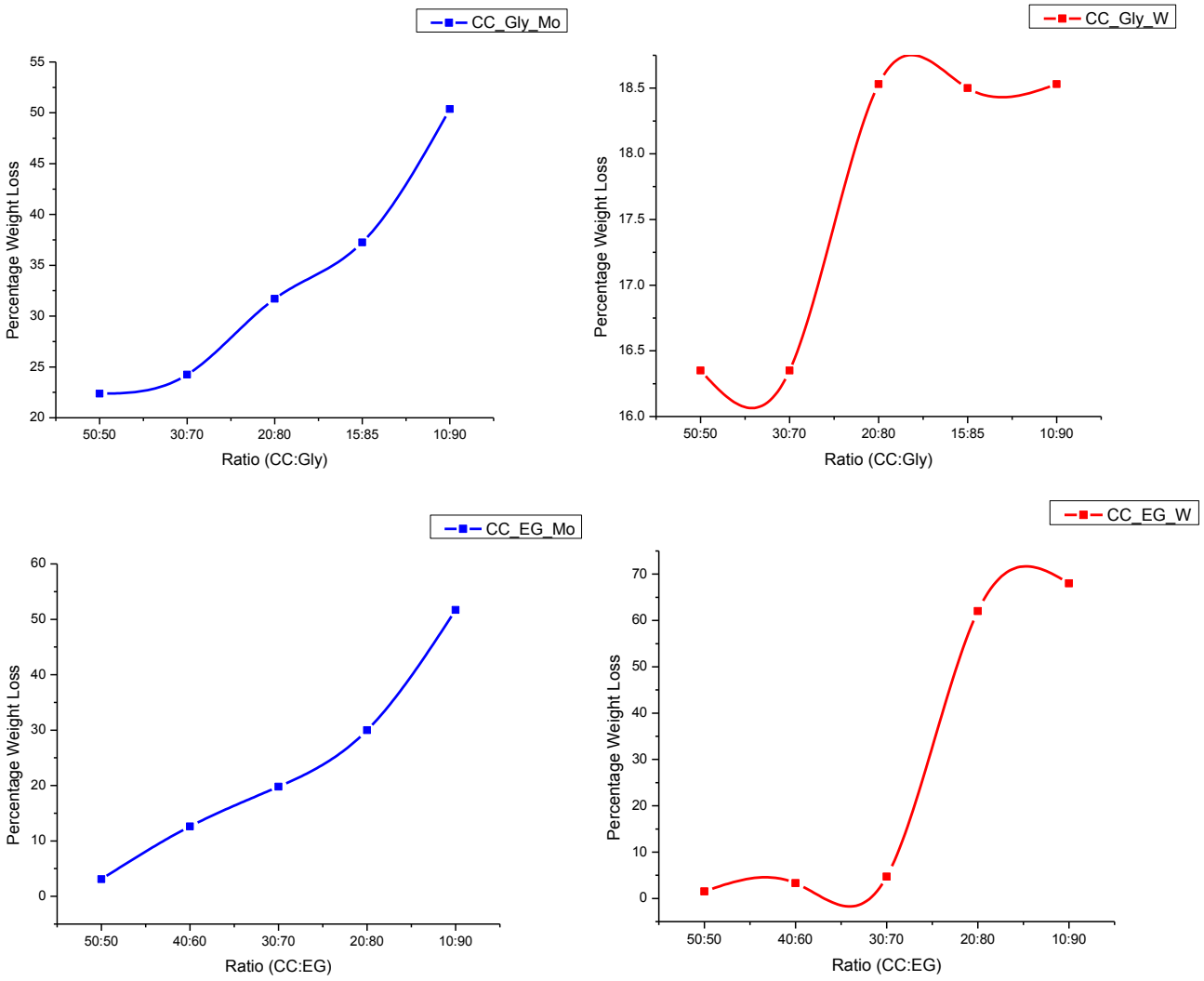

Figure 3-12: Percentage weight loss of Mo and W in mixtures of different ratios between choline chloride and HBDs (EG and Glycerin) at 150 mA/cm^2.

This graph 3-4 indicates the dissolution of Mo in choline chloride mixture with Urea where the percentage weight loss stays around 20% on the average. Which is due to absence of –OH groups and instead there are two –NH2 groups in Urea which have low ability to stabilize metal chloride formed after dissolution of metal.

The weight loss curves for both Mo and W in CC/EG system of different concentrations of chloride ions is given above. The weight loss in case of Mo has linear increase in dissolution as chloride ions concentration decreases in the binary mixture of CC & EG which means choline chloride proportion is decreasing. While in case of W, the weight loss remains small and almost constant on same line until chloride ions concentration decreases to a specific lower value. At this point there is sharp increase in the dissolution of W which continues to increase until some specific lower concentration of chloride ions and then once again becomes constant. The important point here is the effect of chloride ions concentration on the dissolution of these two metals which varies with decreasing chloride ions concentration.

Ratio of CC/EG	Mo Dissolved (g)	W dissolved (g)
50/50	0.0036	0.002
	0.002	0.002
	0.0045	0.003
average	0.003367	0.002333
40/60	0.0112	0.0037
	0.0139	0.0052
	0.0157	0.0067
average	0.0136	0.0052
30/70	0.0176	0.0081
	0.0222	0.0061
	0.0242	0.0079
average	0.021333	0.007367
20/80	0.0282	0.0812
	0.0322	0.1143
	0.0371	0.0934
average	0.0325	0.0963
10/90	0.0546	0.1121
	0.0545	0.0932
	0.0574	0.1141
average	0.0555	0.106467

Table 3-14: Effect of the concentration of HBD on the dissolution of Mo and W. Average value of dissolved amount was taken after repeating the experiment three times.

Molybdenum (Mo) seems to form one type of chloride complex which might be $MoCl_5$, the formation of this complex depends on the solubility product of this salt

in the chloride containing electrolyte [172-173]. As the concentration of chloride ions increases in the electrolyte the dissolution of molybdenum is suppressed and vice versa. Formation of $MoCl_5$ is kinetically controlled process as this depends on the release of chloride ions from HBDs near the electrode surface. In case of tungsten (W), there seems formation of different complex salts at different concentrations of chloride ions. In the present experiment there seems formation of WCl_5 and other might be WCl_2. It depends on the solubility constants of newly formed salt as the slope in the region between 30:70 and 20:80 is high while at the beginning we observe a small slope.

More than one type complex are formed in this region, which seem to be readily soluble at this chloride concentration and thus allows the dissolution of tungsten in large amounts. The middle part of the graph indicates formation of intermediates which have two possible reaction pathways both of which might be of chemical nature and not electrochemical nature. In high chloride ion conc. region, the single complex salt of very low solubility is formed and in low chloride ion conc. region single complex salt of high solubility is formed.

For tungsten (W) there are two parts of the weight loss graphs, first part where dissolution of metal is almost constant and low and second part where dissolution is again almost constant but higher. Between the low and high dissolution is an intermediate point or point of critical concentration of –OH and chloride ions. The presence of more –OH groups in second part can be related to higher dissolution. In both the curves, 20:80 ratio shows a critical –OH concentration where the dissolution of both the metals increases exponentially. The reason for this is the low –OH concentration region as compared to chloride ions, the higher oxidized products are formed and hence large complex is formed which requires high energy for stabilization and hence is not easy to move away from the surface, while in the mixtures of high –OH than chloride ion concentration, the lower oxidized products and hence the lower chlorides are formed which are transported away from the surface quite easily and the electrode surface becomes fresh.

In the case of Mo, only one kind of complex seems to form and if there is any other oxidized product, it is less in amount, there are two linear regions in Mo weight loss curve for different CC and EG compositions. The complex formed in the low –OH region is not much stabilized while in high –OH concentration it is easily transported and leaves behind the free surface. Similar results were obtained for PEG200 where

dissolution reached up to 87%. These experimental observations support our view point about the contribution of –OH group in the stability of incipient metal chloride and hence the overall dissolution process.

3.3.1 Anodic Polarization

When potential is applied on Mo, current varied more or less linearly as compared to W where there is an upward curve in the potential in first scan but at repeating the potential again this peak or curve disappears and starts disappearing from the second to onward scans. In case of Mo the peak is smaller indicating small potential increase which means low amount of current is utilized, showing almost a linear behavior while the W potential-current diagram tends to remain flat for most part of the scan, from -1.5V to 1.0V, then comes the peak which is developed on the fresh electrode surface and disappears on repeated scans and after few potential scans on the W electrode a flat potential-current line can be observed from -1.5 to 2.5 V.

Any peak in anodic polarization curve of W as working electrode is due to the oxidation of metal where metal chloride is formed at the surface of electrode which seems the most probable case here. This newly formed metal chloride requires second component to stabilize it, otherwise metal chloride will be adsorbed at the surface of electrode and hence hindering further dissolution process by blocking the surface. If metal chloride is stable enough, it can move away from the metal surface and diffuse into the electrolyte making fresh metal surface available.

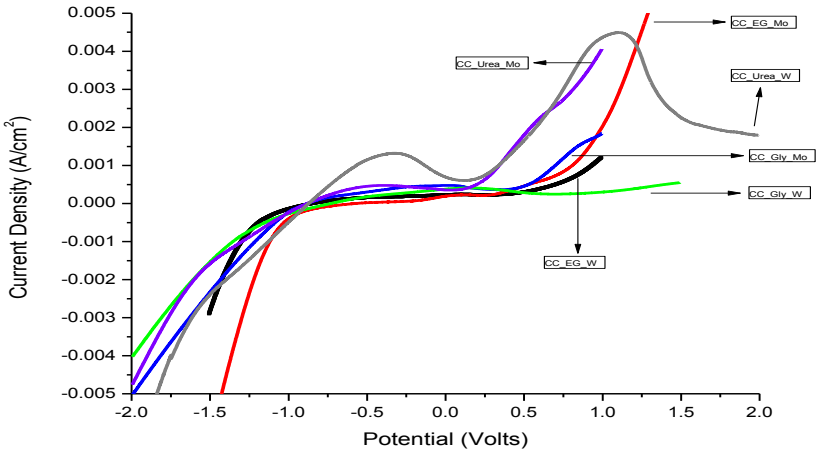

Figure 3-13: Anodic polarization curves of tungsten (W) and molybdenum (Mo) in choline chloride based binary mixtures.

It was further confirmed that the dissolution of the metal increased with low chloride ions concentration and more HBD concentration in binary mixture electrolyte. The higher the number of –OH groups on HBD the more is the dissolution, hence the presence of the –OH group seems to be the factor affecting the rate and amount of metal dissolution. This might be due the mobility of the-OH containing compound (HBD in this case) that the dissolution increases as the concentration is increased or the number of available –OH groups are increased. Further experiments were conducted with PEG200 and it confirmed even higher dissolution rates as compared to EG and Glycerin. Stability of chloride ions by the –OH group of HBDs in choline chloride based binary mixtures and an influence of the –OH group on metal chlorides is also important because the metal chlorides have always a polarity by metal part being positive and chloride part being negative [174].

It depends on the symmetry and structure of the metal chloride and if there is polarity then it is possible that the –OH group influences dissolution process by controlling the further chemical process in electrolyte after initial electrochemical dissolution of the metal from metal surface [175-176]. Anodic polarization curve is straight line over a wide range of potential indicating the stability of the electrolyte which is close to 2.5 volts at W electrode. The stability of CC/EG electrolyte makes it benign green electrolyte in this potential range and can be applicable in various fields of electrochemistry and chemistry in general. Anodic polarization curve for W shows passivation in the region of -1.1 to -0.5 V where then passivated layer is dissolved.

3.3.2 Galvano-static measurements at shorter times

In galvano-static experiments potential varied with time, for 10 sec experiments (shown in figure 3-14a) a rise in potential immediately after the start of experiment was observed on both Mo and W electrodes. In short time experiment there is an increase in potential with time which indicates the formation of oxide layer at the surface of electrode initially and it is formed for short period of time as Mo metal atoms are dispatched from the surface [177-178]. This oxide species which is most probably the MoO_2 species [179-180] or Mo_2O_5 species [181-182], either of which seems to live a short life in the diffusion layer near electrode surface and is attacked by

the chloride ions present in the bulk and near the surface. This is evidenced by the energy comparison of Mo-O and Mo-Cl bond [183].

Dissolution of Mo atoms from the surface seems to be a diffusion controlled process. As soon as chloride ions stabilized by HBDs are available, metal atoms start to leave bulk metal forming metal chloride. The possibility is the formation of metal oxide in any stoichiometric ratio at the surface, which then near the surface of electrode looses oxygen and accepts chloride making $MoCl_5$ or Mo_2Cl_{10}. For long time experiment (100sec in figure 3-14b, 1000 sec in figure 3-14c) the potential for Mo and W oscillates between two values for each electrolytic system. First a drop in potential for longer time experiments as compared to the short time experiments and then an oscillation in potential over longer time at constant current give an idea about the surface phenomena.

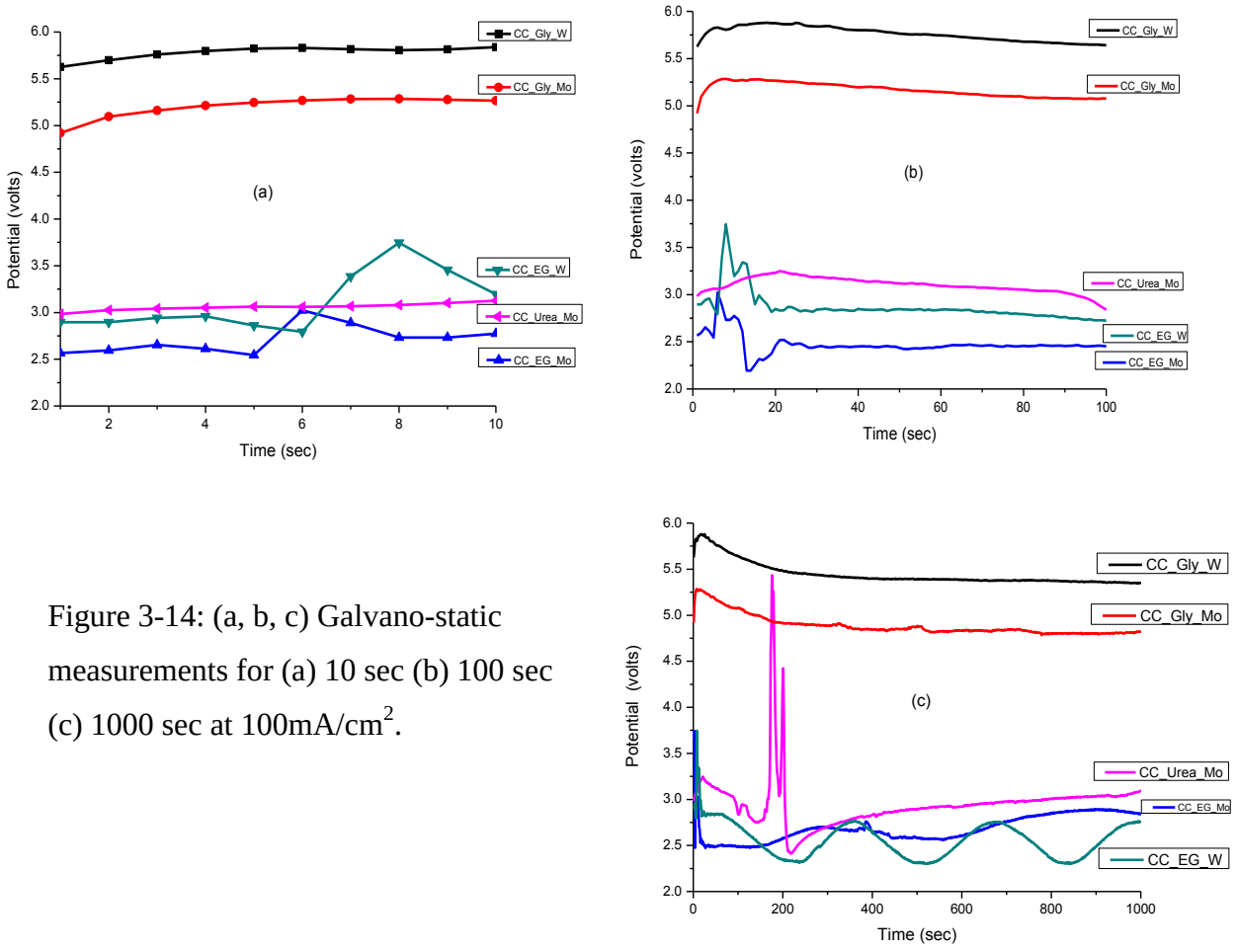

Figure 3-14: (a, b, c) Galvano-static measurements for (a) 10 sec (b) 100 sec (c) 1000 sec at 100mA/cm^2.

The oxide layer at the surface is attacked by chloride ions and initially it was thick but after few seconds the thickness of this oxide layer is decreased due to the presence of chloride ions. So a first drop in potential with passage of time shows the depletion of oxide layer at the surface and then potential oscillates between two values over longer period of time for almost all experiments showing periodic behavior of formation and depletion of oxide layer at the surface of electrode.

3.3.3 Anodic Dissolution at longer time in different electrolytic systems

Molybdenum and tungsten were polarized galvanostatically in choline chloride based binary mixtures for 1 hour at 100 mA/cm^2. The purpose was to analyse the variation in potential at constant current with the passage of time.

3.3.3.1 Choline chloride and ethylene glycol system

Choline chloride and ethylene glycol based binary mixture has good conductivity and display high corrosive ability [20]. Galvanostatic dissolution at 100 mA shows the potential for molybdenum in the range of 2.5 V to 3.0 V. The oxide layer formed at the surface of anode lasts for few seconds and is dirupted by the further potential. This is the reason why early passivation and an increase in the potential is observed at the start. After the oxide layer is ruptured or damaged, the potential stays at a constant value. The high conductivity and moderate viscosity of choline chloride and ethylene glycol system play an important role in getting the electropolished surface of molybdenum and tungsten.

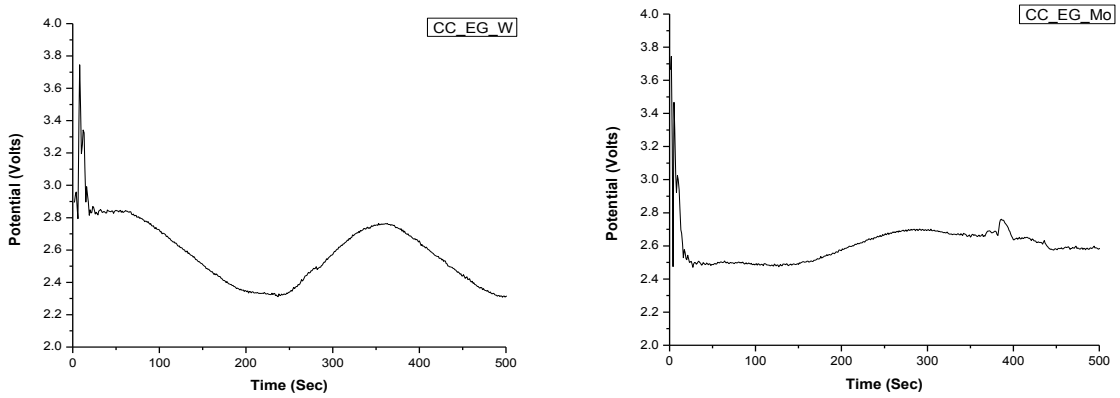

Figure 3-15: Galvanostatic dissolution of molybdenum and tungsten in CC/EG system at 100 mA/cm^2.

3.3.3.2 Choline chloride and polar aprotic systems

Choline chloride mixtures with polar aprotic solvents have been reported in our work [138]. Good conductivity of these mixtures makes them a good choice to be used in future as electrolytes. Anodic dissolution at 100 mA/cm^2 shows that after early stage passivation for the start of the experiment caused by the oxide layer at electrode surface, potential stays at a constant vlaue. After the intial passivation potential oscillates between a minimum and a maximum which indicates the formation and dissolution of metal chloride layer at the surface of electrode periodically. The potential for 100 mA for CC/DMSO system is fairly high indicating the polarization due to bulk electrolyte and also due to diffusion of larger complex species at the surface of electrode.

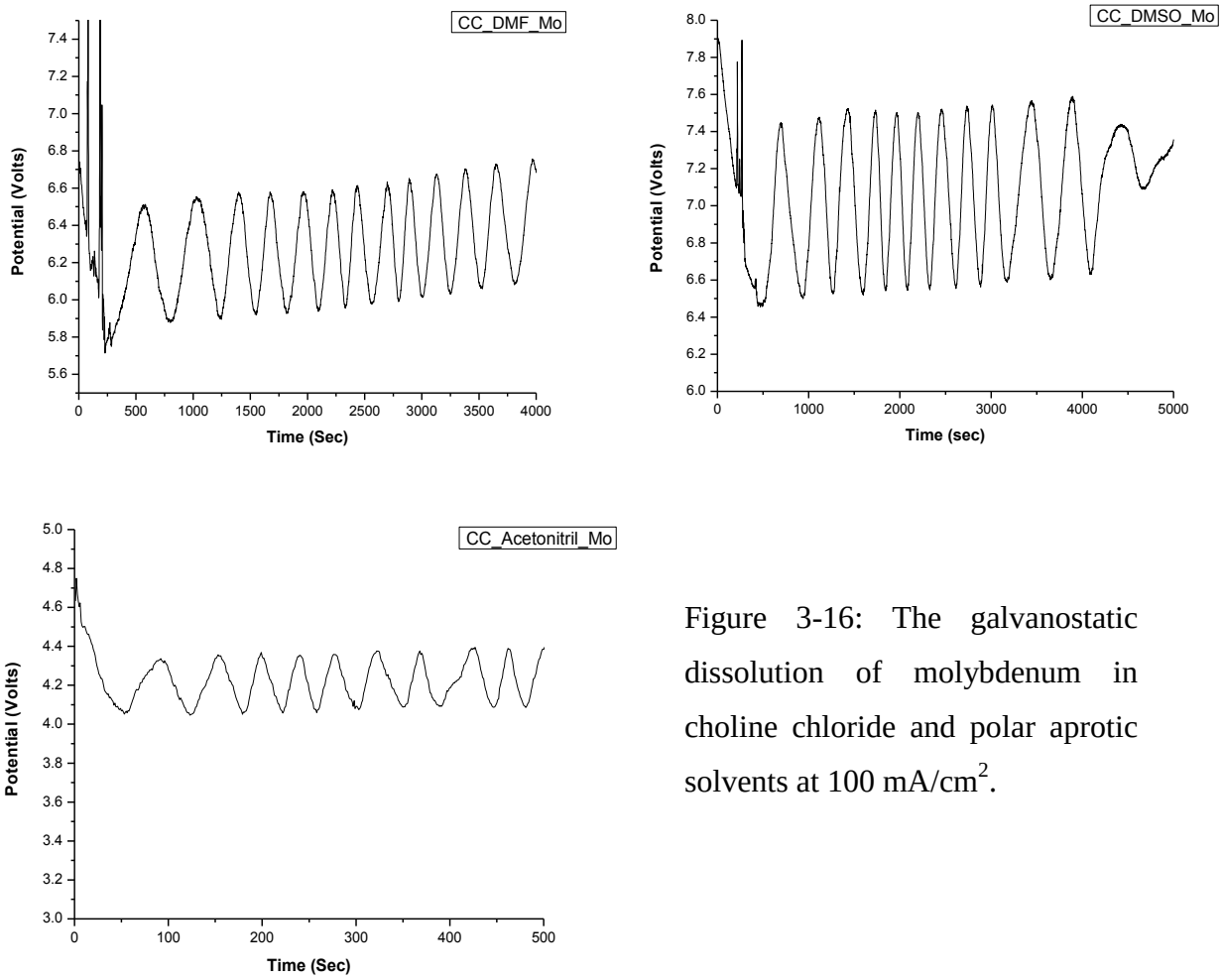

Figure 3-16: The galvanostatic dissolution of molybdenum in choline chloride and polar aprotic solvents at 100 mA/cm^2.

Figure 3-16 shows the cell potential of all three polar aprotic systems with choline chloride at molybdenum electrode measured versus Ag/Ag^{+}. The minimum potential of these systems is that of acetonitril with choline chloride which is 4.2 V oscillating between two values 4.0 V and 4.4 V. The solution of choline chloride in DMF shows the similar trend as in other aprotic systems. The potential oscillates between two values after a passive layer is dissolved. The potential value change between two values might be due to the week metal complex formation which passes through a reversible reaction at electrode surface.

3.3.3.3 Choline chloride with glycerol and urea

Choline chloride based deep eutectic solvent with urea and glycerol has been reported [138]. The solutions are stable liquids and are used as electrolytic medium in electropolishing and electrodeposition processes. In our work, CC/gly system is more efficient in giving polished surface than the CC/urea system. The reason might be the stability of dissolved species from electrode surface and their diffusion from surface into the bulk of solution.

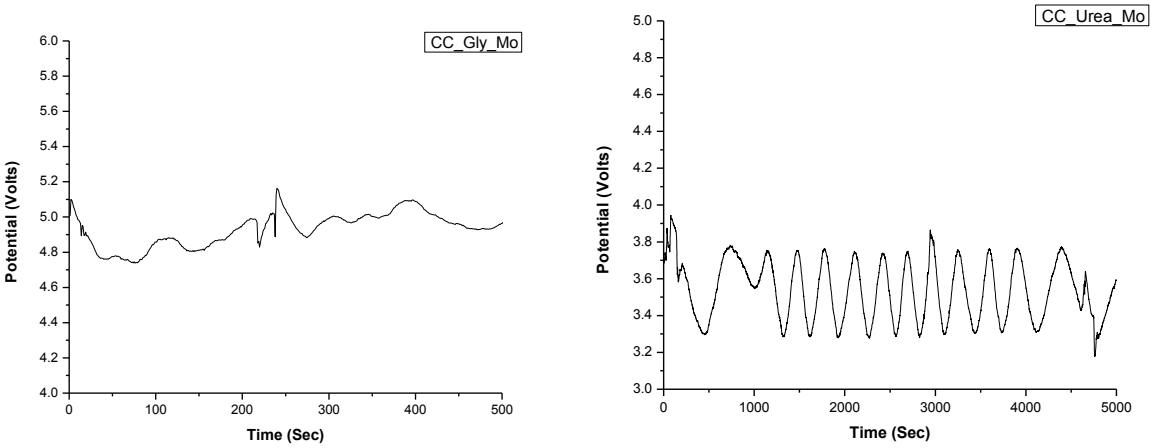

Figure 3-17: The galvanostatic curves of Mo in CC/Gly and CC/urea the systems at 100 mA/cm^2.

CC/gly system shows the potential between 4.8 V and 5.0 V which is normal value, giving the idea that this system can be used as electrolytic system for polishing of molybdenum and other refractory metals. In case of CC/urea system, although open circuit potential is not high, and the potential value oscillates between the two values,

still not much of the polished surface is obtained. The important factor involved might be the stability of dissolved molybdenum species at the electrode surface. We have not been able to analyse the nature and stability parameters of the molybdenum complex formed at electrode surface so far. But the most probable complex is the molybdenum chloride formed while molybdenum is in +5 oxidation state, so $MoCl_5$ is formed.

3.3.3.4 Choline chloride with organic acids

Organic acids are weak acids and do not dissociate completely and most organic acids are very soluble in organic solvents. Exceptions to these solubility characteristics exist in the presence of other substituents that affect the polarity of the compound [184]. Binary mixtures of choline chloride with oxalic acid, citric acid, maliac acid, melonic acid and citric acid are stable liquids at room temperature. And the preparation of these liquids has been discussed in our work [138].

As compared to the previously discussed binary mixtures where potential oscillates between minimum and maximum values without much increase in the start of polarization, choline chloride based binary mixtures with organic acids display a totally different behaviour on molybdenum electrode. At the start potential increases gradually with the passage of time and oscillating at the same time. The gradual increase in the potential and oscillation are an indication of two processes going on at the surface of molybdenum. Oscillation as discussed earlier is due to the formation and breakage of passive layer with the passage of time. Since $MoCl_5$ which is formed along with oxides of molybdenum cover the surface a slight increase in potential is required to remove the layer and making electrode surface fresh for further electrochemical process.

The gradual increase in potential along with oscillation is due to the accumulation of the oxidised species at molybdenum electrode. These oxidised species are formed due to the oxidation of organic acids at electrode surface and are unable to move into bulk solution. This is the reason that potential oscillation is irregular and with big wave in the intial region. Later on when the potential is high enough to remove all the species from electrode surface, oscillation of potential becomes regular and has smaller waves. Behavior of CC/oxalic acid and CC/succinic acid binary

mixtures looks more close to those of ealier discussed binary mixtures, which may be due to low viscosity and good stabilization ability of dissolved molybdenum complex.

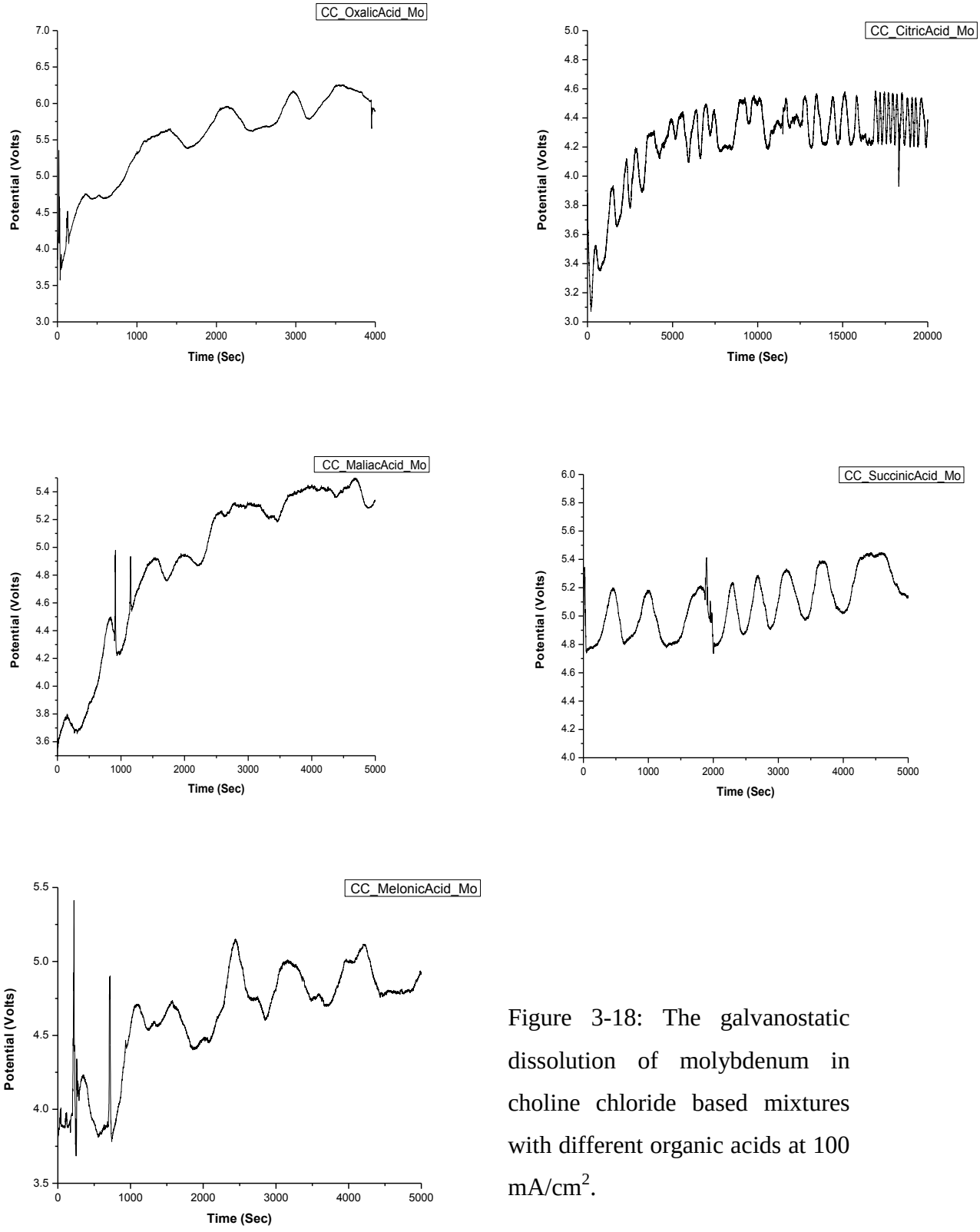

Figure 3-18: The galvanostatic dissolution of molybdenum in choline chloride based mixtures with different organic acids at 100 mA/cm^2.

Except CC/melonic acid system which did not display good physical properties as an electrolyte, rest of the choline chloride based binary mixtures with oxalic acid, maliac acid, citric acid and succenic acid gave liquids at room temperature. Anodic dissolution of molybdenum shows a gradual increase in potential with the passage of time for longer time experiments at 100 mA. This gradual increase in potential can be attributed to the accumulation of oxidation products at the surface of molybdenum electrode. At the continuous application of current the potential attained a plateau which is an indication of unavailability of electrode surface for oxidation of undissociated acid.

3.3.3.5 Choline chloride with acetonitril

Acetonitrile is simplest organic nitrile used as polar aprotic solvent. It is widely used in battery applications because it has high dielectric constant and ability to dissolve electrolytes. This is the reason it is used in cyclic voltammetry as well. Due to low viscosity, when a salt like choline chloride was dissolved in it, a good conductive electrolyte was prepared [138]. CC/acetonitrile system exhibit good conductive and at 100 mA it showed potential between 4.0 V to 4.2 V which is comparable to good conductive deep eutectic solvents. The potential oscillates between two values, a minimum and a maximum value which is an indication of the formation of species which form and diffuse away from the surface of electrode periodically.

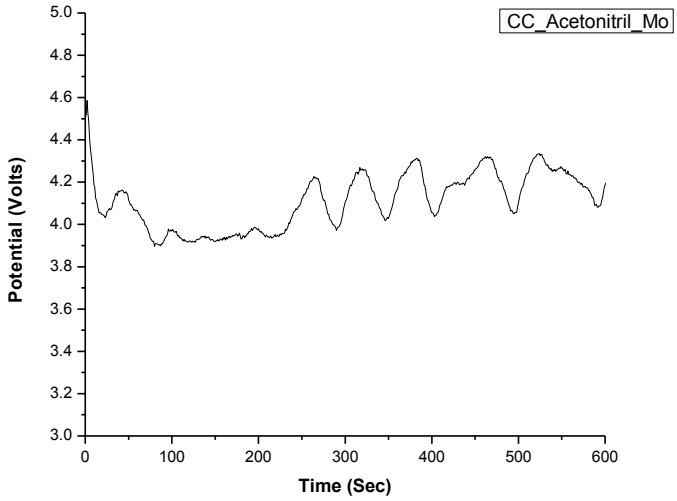

Figure 3-19: The galvanostatic dissolution of molybdenum in choline chloride and acetonitril mixture.

3.4 Anodic Dissolution versus Molecular Properties

Different molecular properties considering both inter-molecular and intra-molecular interactions affect the solvent properties to great deal. Anodic dissolution of molybdenum is greatly affected by the solvent properties of electrolyte. Dipole moment, hydrogen bonding, qualitative properties like lewis acidity and basicity are the important factors which can affect the anodic dissolution of a molybdenum. Following are the different properties of the solvent which affect the anodic dissolution, however a true nature and exact explaination of of the amount of affect in still unknown.

3.4.1 Dipole Moment and anodic dissolution

Dipole moment arises due to the non-uniform distribution of positive and negative charges on the various atoms. This is same for the molecules as well [185]. A correlation between dipole moments of solvents used versus the anodic dissolution of molybdenum was tried. It was not possible to fully understand the relationship if any, between anodic dissolution of molybdenum and the dipole moments of the solvents used with choline chloride. However, it is important to note that the species dissolved from electrode surface are influced by the dipole moments of the solvent molecules. Figure 3-20 shows the grpah between percentage anodic dissolution with dipole moments of few solvents used with choline chloride.

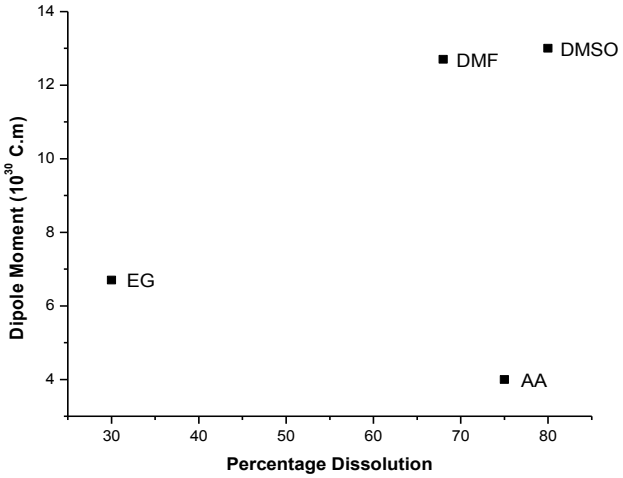

Figure 3-20: Anodic dissolution of molybdenum versus the dipole moments of hydrogen bond donors.

3.4.2 Boiling point and anodic dissolution

Addition of organic or inorganic salts to a solvent affects the boiling point of solvent. Intermolecular forces also interact with the ionic species dissolved in that solvent [186]. A try has been made to check the correlation in figure 3-21. It was noticed that that a relation between the boiling point of the solvent and the anodic dissolution hardly exists. However, the solvents like DMSO, DMF, 2-propanol show more dissolution due to low viscosity and good solvation ability of dissolved species as compared to the ethylene glycol.

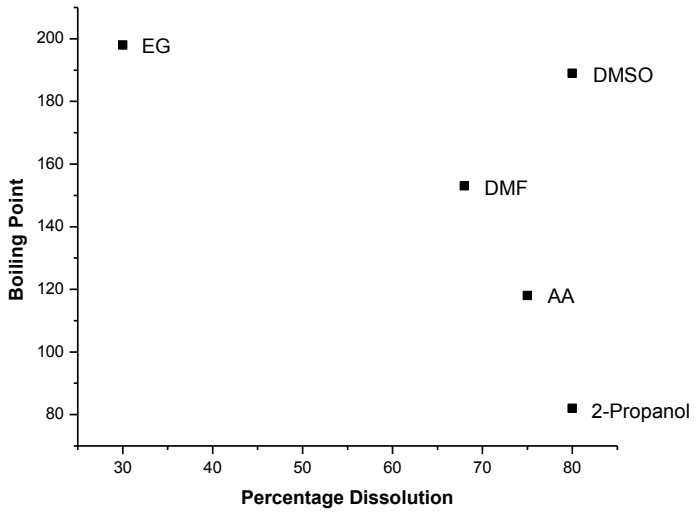

Figure 3-21: Anodic dissolution of molybdenum versus the boiling points of hydrogen bond donors.

3.4.3 Molecular Polarity and anodic dissolution

Polarity in a molecule arises due to the uneven partial distribution of charges between atoms. In choline chloride and in hydrogen bond donors used, there are a number of atoms like nitrogen, oxygen and chloride which are more electronegative and would create partial negative charges on themselves creating partial positive charges on atoms like hydrogen and carbon. This interaction would vary with the nature of molecules. Molecular polarity also has an influence in creating the polarizability which is induced polarity in a molecule by an external source. The graph in figure 3-22 of anodic dissolution versus the polarity of molecules shows that even with high polarity

EG has low anodic dissolution. This shows that there are other factors like viscosity which influence the transport of the molecular species within electrolyte.

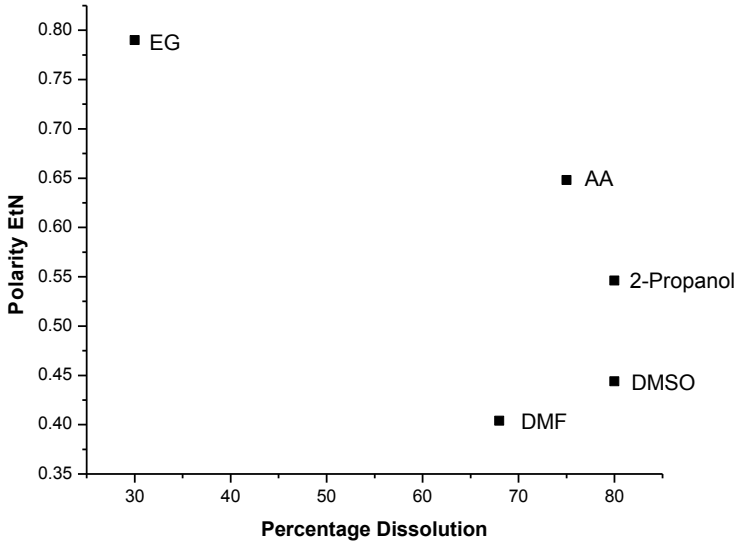

Figure 3-22: Anodic dissolution of molybdenum versus the polarity of hydrogen bond donors.

3.4.4 Donor and acceptor number versus anodic dissolution

Donor number is the measure of the ability of a solvent to solvate cations and lewis acids so donor number is a quantitative measure of lewis basicity [187]. On the other hand acceptor number is the quantitative measure of lewis acidity. Figure 3-23 shows the graphs of acceptor number and donor number of HBD in electrolyte versus anodic dissolution of molybdenum. Acetic acid has high acceptor number and shows dissolution to good extent. But overall there is hardly a good relationship between the acceptor number of HBD and the anodic dissolution of molybdenum.

On the other hand, in second graph, anodic dissolution versus donor number of HBD, the donor ability of solvent overcomes the physical properties like viscosity. In second graph, donor number of solvents like DMF, DMSO and 2-propanol increase and there is gradual increase in the percentage dissolution of molybdenum. This is an indication of the importance of donor number. The higher the donor number of a solvent, the higher is the hydrogen bond donor ability of the solvent and hence the strong interaction of molecular species make the electrolyte conductive and low

viscosity values add in the good transport ability of species. Hence the newly formed species and dissolved molybdenum ions can move away into the bulk sloution easily.

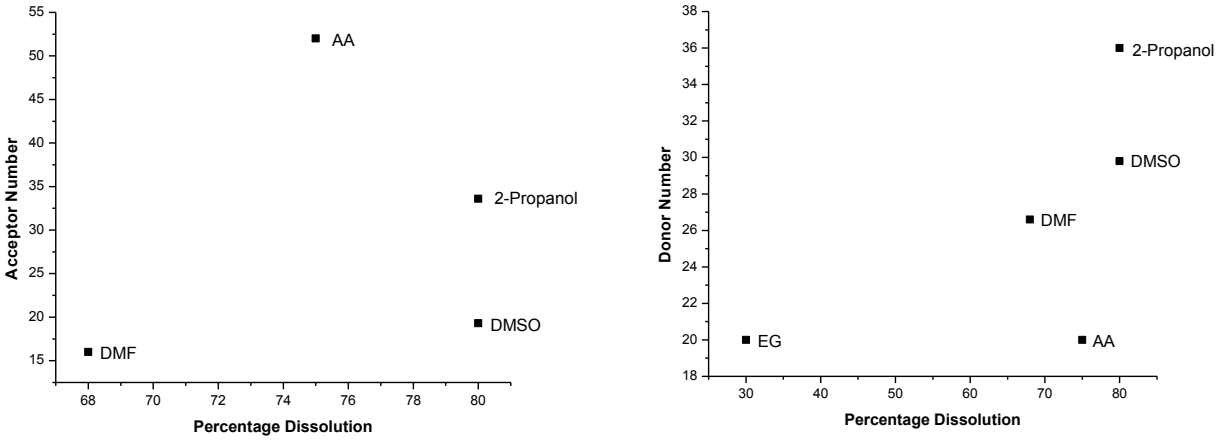

Figure 3-23: Anodic dissolution of molybdenum versus the acceptor numbers (left) and the donor numbers (right) of hydrogen bond donors.

3.4.5 Kamlet and Taft solvent parameters versus anodic dissolution

Kamlet, Abboud and Taft (Ref) described a number of observed solvent effects upon reactions. The general linear free energy function in equation relates the three Kamlet-Taft numbers for a solvent to observable property P and its specified reference state P_0.

$$P = P_0 + a\alpha + b\beta + s\pi^* \qquad (3\text{-}3)$$

The variables related to the solvents are: α, the hydrogen bond donor acidity: β, the hydrogen bond acceptor basicity: and π*, a measure of the interinsic polarity-polarizability characteristics of the solvent at molecular level [188]. The graph of acceptor number versus anodic dissolution represent the same trend as the acceptor number in section 3.6.4. This shows that there no clear relationship between anodic dissolution of molybdenum and the acceptor number of solvent molecules. The graph on left side shows that dissolution is more dependent on other properties like viscosity and solvent donor ability than the acceptor ability.

The graph on left side shows a relation between anodic dissolution and donor ability of solvent molecules. It has been noticed that β values behave in similar way

versus anodic dissolition as the donor numbers do. Increase in the trend of anodic dissolution with an increase in β values shows the strong impact of hydrogen bond donor ability of solvent on the overall solvent behavior. The more strong is the interaction among molecular species of solvent more will be the stability of inorganic species being dissolved anodically. The values of α and β were taken from literature [189].

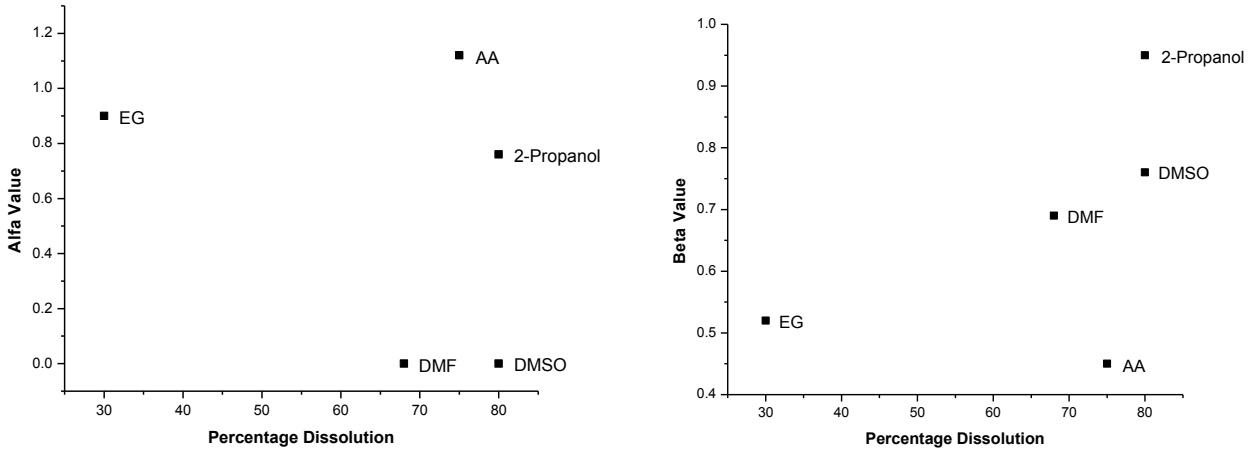

Figure 3-24: Anodic dissolution of molybdenum versus the alfa values (left) and the beta values (right) of hydrogen bond donors.

3.5 Surface Analysis of Molybdenum

Surface analysis of molybdenum before and after the anodic dissolution in choline chloride based binary mixtures give an insight into the possible reaction products. Scanning electron microscopy was used to analyse molybdenum electrode surface. Figure 3-25 shows the comparison of two electrode surfaces, right hand side figure shows the suface of molybdenum electrode before it is put into the cell, while the left hand side figure shows the surface of electrochemically polished surface. A normal molybdenum surface is rough in structure and has several crests and troughs which are usually formed during metal fabrication.

The polished surface is obtained by anodically dissolving the molybdenum surface, giving rise to a uniform and bright surface. Surface analysis of polished molybdenum shows the presence of black spots scattered on the electrode surface. EDX diagram shown in figure 3-26 show the presence of carbon on the

electrochemically polished surface. The presence of carbon might be due to the oxidation of ethylene glycol at the electrode surface. It has been known that materials like platinum and tungsten are used to oxidise compounds like ethylene glycol [190]. The oxidation of organic compounds can produce carbon under low oxygen concentrations.

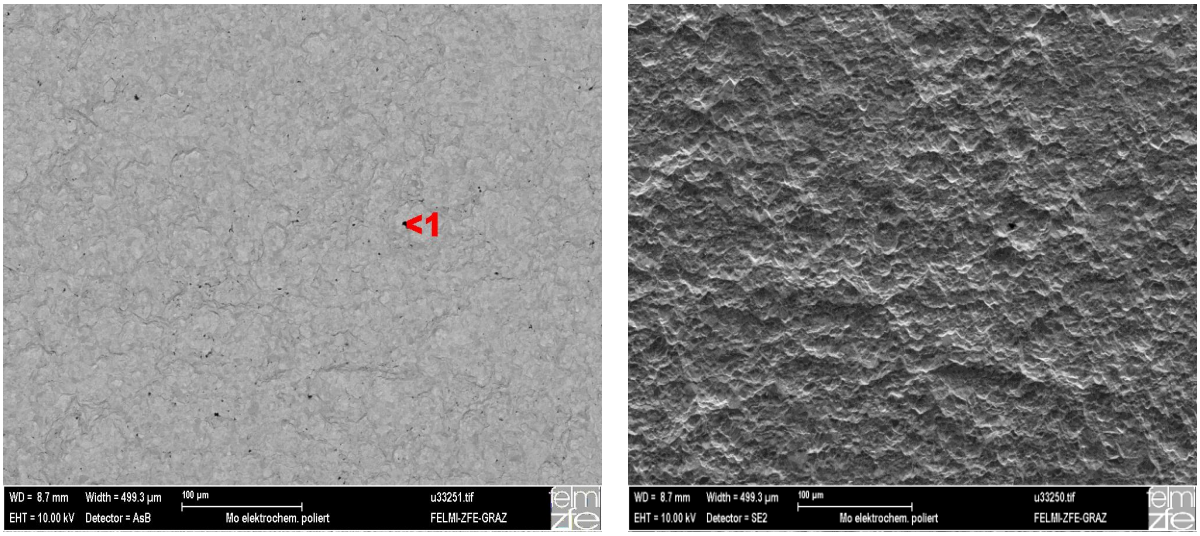

Figure 3-25: SEM images of normal molybdenum surface (right) and electrochemically polished molybdenum surface (left). The presence of dark spots at electrode surface on the left side are carbon particles produced due to oxidation of ethylene glycol.

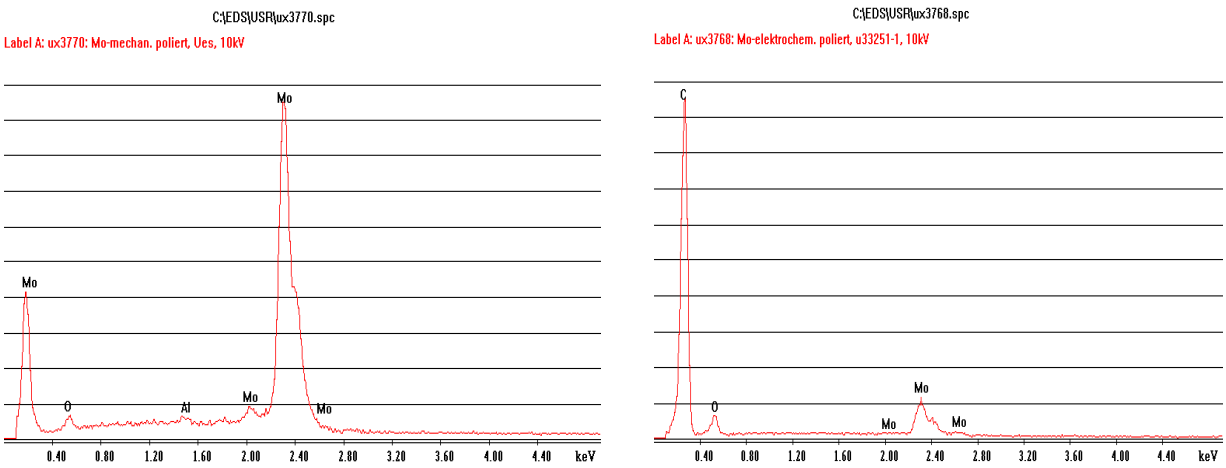

Figure 3-26: EDX diagram showing the unpolished molybdenum surface (left) and a polished surface with carbon material on it (right).

Choline chloride based binary mixture with ethylene glycol (CC/EG) and with glycerol (CC/Gly) can be a potential candidates in future to be used as polishing medium for the electrochemical polishing of molybdenum like hard metals. A comparison of molybdenum polished surface in CC/EG and in CC/Gly shows difference in surface brightness. A molybdenum surface obtained after electrochemical dissolution in CC/Gly is more bright and shiny than the one obtained in CC/EG. This might be due to the viscosity difference between two hydrogen bond donors. CC/Gly system is more viscous than CC/EG system due to high viscosity of glycerol than ethylene glycol. This high viscosity of CC/Gly system causes the formation of thick viscous layer at the electrode surface hence making the molybdenum dissolution process more uniform.

As has been described earlier, thick viscous layer causes uniform metal dissolution process. At the same time thick viscous layer at electrode surface causes the high dissolution rate of molybdenum as well. This is the reason that CC/Gly system has the highest dissolution efficiency of molybdenum which is more than 80%. Such viscous solutions having one component of choline chloride and other a good hydrogen bond donor can be good option for getting good polished surface of refractory metals.

4 Conclusions

NH_4NO_3/NH_3 system has fairly good conductivity that is comparable with ionic liquids and shows high corrosion current density at -35 ^oC with molybdenum metal. Molybdenum dissolves in NH_4NO_3/NH_3 system with weight loss efficiency of 79% under non-aqueous conditions. In NH_4NO_3/NH_3 system it is possible to redeposit molybdenum on parent electrode with an efficiency as high as 76%. High dissolution and redeposition ability of Mo in and from NH_4NO_3/NH_3 system respectively suggests that this electrolyte system can be used for recycling molybdenum from molybdenum scrap. From the observation and comparison of electrochemical behavior of Mo in NH_4NO_3/NH_3 system and in $[Bmim]^+/CF_3SO_3^-$, it can be safely suggested that the ionic liquids of imidazolium series can be used for the electrochemical dissolution and deposition of refractory metals like Mo at room temperature.

Karl Fischer titration was used to determine the water contents of three choline chloride based binary mixtures. It was possible to bring the water content level down to 200 ppm to 250 ppm by carefully drying choline chloride under vacuum but this amount of water is still high. Infrared spectroscopy enables to look into the bonding mechanism of these binary mixtures giving evidences of O-H…Cl^- and C-H…Cl^- interactions due to hydrogen bonding. ESR experiments of the electrolyte containing dissolved molybdenum suggest that molybdenum is present as Mo^{+5} in the electrolyte.

Electrochemical behavior of ferrocene has been investigated in CC/PEG200 and CC/PEG600 systems by using cyclic voltammetry to check the ability of these two media for further electrochemical processes. Peak current (i_p) values and peak potential shift (ΔE_p) give a good insight and understanding of the reaction mechanisms of electrochemical reactions. Fairly high diffusion coefficient and rate constants of ferrocene redox process in CC/EG, CC/PEG200 and CC/PEG600 systems make these liquids, good future candidates as potential reaction media for various electrochemical processes. A comparison has been made among previously reported systems and newly reported CC/PEG200 and CC/PEG600 systems. From this a correlation of rate constants and diffusion coefficients with PEG chain length, viscosity and hydrogen donor bonding was found.

Thermogravimetric analysis (TGA) and differential scanning calorimetry (DSC) analysis show that choline chloride based binary mixtures with ethylene glycol, glycerol, urea, acetic acid, are stable up to 300 $^{\circ}$C. Among these systems choline chloride and ethylene glycol system was found to be more stable, having properties close to room temperature ionic liquids (RTILs). Choline chloride and DMSO mixture showed decomposition below 100 $^{\circ}$C. Electrochemical investigations at platinum (Pt) and tungsten (W) electrodes show that these binary systems possess reasonably wide electrochemical potential window and hence can be applied in different electrochemical reactions. Nevertheless these binary mixtures are good room temperature liquids to carry out various chemical and electrochemical processes.

Choline chloride based binary mixtures have good conductivity which is comparable to that of ionic liquids. Refractory metals like molybdenum and tungsten dissolve in these systems up to 80% dissolution efficiency. Electrochemical dissolution efficiency in these eutectic mixtures can be used to polish the hardest metals like Mo and W. Dissolution of these metals is affected by different factors and in our work we have analyzed that dissolution efficiency depends on the amount of available chloride ions. It is also assumed that the release of chloride ions from HBDs is the factor affecting dissolution process and overall mechanism is kinetically controlled. While the weight loss in Mo and W is also dependent on the current density, at higher current densities dissolution is mass transport controlled while at low current densities it is kinetically controlled giving higher weight losses at lower current density values. The presence of –OH group on the HBDs is also a factor that affects the movement of species towards and away from the electrode surface. It was noticed that more the number of –OH groups present, it enhances the dissolution of Mo and W. Such eutectic mixtures can also be a good option under non-aqueous conditions for the electrochemical deposition of non-reactive metals like Mo and W.

The molybdenum surface analysis by using scanning electron microscopy (SEM) and energy dispersive X-ray analysis shows that organic material is oxidized during galvanostatic polarization and carbon spots can be clearly seen. A polished and bright metal surface with smooth morphology of molybdenum can be obtained by using choline chloride based binary mixtures at room temperature.

Reference:

1. Hoar, T. P. "The production and breakdown of the passivity of metals." Corrosion Science **7**(6): 341-355.
2. Mao, K.-W., M. A. LaBoda, et al. "Anodic Film Studies on Steel in Nitrate-Based Electrolytes for Electrochemical Machining." Journal of the Electrochemical Society **119**(4): 419-427.
3. Hoare, J. P. and K.-W. Mao. "Anion Effects on the Dissolution of Steel in ECM Binary Electrolyte Systems." Journal of the Electrochemical Society **120**(11): 1452-1456.
4. Figour, H. and P. A. Jacquet. French Patent **707526**.
5. Jacquet, P. A. Sheet Metal Industry **24**: 2015.
6. Fedot'ev and S. Y. Grilikhes (1959). Electropolishing, Anodizing, and Electrolytic Pickling of Metals. Teddington, England, Robert Draper Ltd.
7. Zmeskal, O. (1945). Metal Progress **47**: 729.
8. Schaefer, C. (1940). Metal Industry **38**: 22.
9. Young, C. B. F. and W. L. Brytczuk (1942). Metal Finishing **40**: 237.
10. Mondon, R. (1963). Metal Progress **63**(1): 95.
11. Edwards, J. (1953). "The Mechanism of Electropoiishing of Copper in Phosphoric Acid Solutions." Journal of the Electrochemical Society **100**(7): 189C-194C.
12. Mondon, R. (1955). Sheet Metal Industry **32**: 923.
13. Bellucci, F., C. A. Farina, et al. "The anodic dissolution of nickel and molybdenum in methanol and water-methanol mixtures." Materials Chemistry **5**(3): 185-198.
14. Rybalka, K. V. and L. A. Beketaeva (1993). "Anodic dissolution of aluminium in nonaqueous electrolytes." Journal of Power Sources **42**(3): 377-380.
15. Biallozor, S. (1978). "Kinetics and mechanism of cadmium anodic dissolution in organic solvents - I." Electrochimica Acta **23**(12): 1309-1312.
16. Fushimi, K., H. Kondo, et al. (2009). "Anodic dissolution of titanium in chloride-containing ethylene glycol solution." Electrochimica Acta **55**(1): 258-264.

17. Zamin, M., P. Mayer, et al. (1977). "On the Electropolishing of Molybdenum." Journal of the Electrochemical Society **124**(10): 1558-1562.
18. Hoar, T. P. (1967). "The production and breakdown of the passivity of metals." Corrosion Science **7**(6): 341-355.
19. Abbott, A. P., G. Capper, et al. (2003). "Electrochemical studies of ambient temperature ionic liquids based on choline chloride." Ionic Liquids as Green Solvents: Progress and Prospects **856**: 439-452.
20. Abbas, Q. and L. Binder (2011). "Anodic Dissolution of Refractory Metals in Choline Chloride Based Binary Mixtures." Ecs transactions **33**(30): 57-67.
21. "Properties of Molybdenum". *Integral Scientist Periodic Table*. Qivx, Inc.. 2003. Retrieved 2007-06-10.
22. Davis, Joseph R. (1997). *Heat-resistant materials*. ASM International. p. 365. ISBN 0871705966.
23. Holleman, Arnold F.; Wiberg, Egon; Wiberg, Nils (1985). *Lehrbuch der Anorganischen Chemie* (91–100 ed.). Walter de Gruyter. pp. 1096–1104. ISBN 3-11-007511-3.
24. Pope, Michael T.; Müller, Achim (1997). "Polyoxometalate Chemistry: An Old Field with New Dimensions in Several Disciplines". *Angewandte Chemie International Edition* **30**: 34. doi:10.1002/anie.199100341.
25. Binder L, Rathwallner G, Mollay B, Nauer G. The Electrochemical dissolution of molybdenum. Proceedings 55th ISE Meeting 2004:Abstract No S7FP3.
26. Binder L. Electrochemical machining of tungsten, molybdenum and tantalum. The Electrochem Society Proceedings 1988; 88-23.
27. Hull, M. N. (1972). Electroana. Chem. **38**: 143.
28. Bellucci, F., C. A. Farina, et al. "The anodic dissolution of nickel and molybdenum in methanol and water-methanol mixtures." Materials Chemistry **5**(3): 185-198.
29. Turnbull, A., M. Ryan, et al. (2003). "Corrosion and electrochemical behaviour of 316L stainless steel in acetic acid solutions." Corrosion Science **45**(5): 1051-1072.
30. Besson, J. and G. Drautzburg (1960). "Das anodische verhalten der metalle molybdän und wolfram." Electrochimica Acta **3**(1-2): 158-168.
31. Wikstrom, L. L. and K. Nobe (1969). "The Electrochemical Behavior of Molybdenum." Journal of the Electrochemical Society **116**(4): 525-530.

32. Badawy, W. A., A. G. Gad-Allah, et al. (1987). "On the stability of anodic oxide films formed on molybdenum in various aqueous solutions." Surface and Coatings Technology **30**(4): 365-373.
33. Domka, F. and I. Wolska (1986). "Porous structure of an iron (III) oxide-thoria catalyst for the water gas shift conversion." Surface and Coatings Technology **28**(2): 187-200.
34. Povey, A. F. and A. A. Metcalfe (1977). "The anodic dissolution of molybdenum in alkaline solutions -- X-ray photoelectron spectroscopic studies." Journal of Electroanalytical Chemistry and Interfacial Electrochemistry **84**(1): 73-81.
35. Bojinov, M., I. Betova, et al. (1996). "Kinetics of formation and properties of a barrier oxide film on molybdenum." Journal of Electroanalytical Chemistry **411**(1-2): 37-42.
36. Petrova, M., M. Bojinov, et al. "Mechanism of anodic oxidation of molybdenum in nearly-neutral electrolytes studied by electrochemical impedance spectroscopy and X-ray photoelectron spectroscopy." Electrochimica Acta **In Press, Corrected Proof**.
37. Bojinov, M., I. Betova, et al. (1995). "Transpassivity of molybdenum in H2SO4 solution." Journal of Electroanalytical Chemistry **381**(1-2): 123-131.
38. Badawy, W. A. and F. M. Al-Kharafi (1998). "Corrosion and passivation behaviors of molybdenum in aqueous solutions of different pH." Electrochimica Acta **44**(4): 693-702.
39. Daintith, John (2005). *Facts on File Dictionary of Chemistry* (4th ed.). New York: Checkmark Books. ISBN 0816056498.
40. Emsley, John E. (1991). *The elements* (2nd ed.). New York: Oxford University Press. ISBN 0198555695.
41. Morse, P. M.; Shelby, Q. D.; Kim, D. Y.; Girolami, G. S. (2008). "Ethylene Complexes of the Early Transition Metals: Crystal Structures of $[HfEt_4(C_2H_4)^{2-}]$ and the Negative-Oxidation-State Species $[TaHEt(C_2H_4)_3^{3-}]$ and $[WH(C_2H_4)_4^{3-}]$". *Organometallics* **27** (5): 984–993. doi:10.1021/om701189e.
42. Koerner, W. E. (1917). Trans. Electrochem. Soc., **31**: 221.

43. Besson, J. and G. Drautzburg (1960). "Das anodische verhalten der metalle molybdän und wolfram." Electrochimica Acta **3**(1-2): 158-168.
44. Johnson, J. W. and C. L. Wu (1971). "The Anodic Dissolution of Tungsten." Journal of the Electrochemical Society **118**(12): 1909-1912.
45. R. S. Lillard, G. S. Kanner, and D. P. Butt, *J. Electrochem. Soc.*, **145**, 2718 (1998).
46. Bojinov, M. (1997). "The ability of a surface charge approach to describe barrier film growth on tungsten in acidic solutions." Electrochimica Acta **42**(23-24): 3489-3498.
47. Macdonald, D. D., E. Sikora, et al. (1998). "The kinetics of growth of the passive film on tungsten in acidic phosphate solutions." Electrochimica Acta **43**(19-20): 2851-2861.
48. Sikora, J., E. Sikora, et al. (2000). "The electronic structure of the passive film on tungsten." Electrochimica Acta **45**(12): 1875-1883.
49. Seo, Y.-J., N.-H. Kim, et al. (2006). "Electrochemical corrosion effects and chemical mechanical polishing characteristics of tungsten film using mixed oxidizers." Microelectronic Engineering **83**(3): 428-433.
50. Antolini, E. and E. R. Gonzalez (2010). "Tungsten-based materials for fuel cell applications." Applied Catalysis B: Environmental **96**(3-4): 245-266.
51. Vergé, M. G., C. O. A. Olsson, et al. (2004). "Anodic oxide growth on tungsten studied by EQCM, EIS and AES." Corrosion Science **46**(10): 2583-2600.
52. Anik, M. (2006). "Effect of concentration gradient on the anodic behavior of tungsten." Corrosion Science **48**(12): 4158-4173.
53. Anik, M. (2010). "Anodic reaction characteristics of tungsten in basic phosphate solutions." Corrosion Science **52**(9): 3109-3117.
A. P. Abbot, G. Capper, D. L. Davies, K. Raymond, R. K. Rasheed, V. Tambyrajah, Chem. Comm., (2003) 70-71.
54. A. P. Abbot, G. Capper, D. L. Davies, R. K. Rasheed, V. Tambyrajah, Chem. Comm. (2001) 2010-2011.

55. H. Ohno (ed.), Electrochemical aspects of ionic liquids, New York, John Wiley and Sons, 2005.
56. P. Wasserscheid, T. Welton, Ionic Liquids in Synthesis, Weinhein, Wiley-VCH, 2003.
57. F. Endres, A. P. Abbott and D. R. MacFarlane, Electrodeposition of metals using ionic liquids, Weinheim, Wiley-VCH, 2008.
58. A. J. Bard and L. R. Faulkner, Electrochemical Methods: Fundamentals and Applications, New York: Wiley, 2nd ed, 2001.
59. H. Ti Tien, J. Phys. Chem. **88** (1984) 3172-3174.
60. P. M. Allemand, A. Koch, F. Wudl, Y. Rubin, F. Diederich, M. M. Alvarez, S. J. Anz, R. L. Whetten, J. Am. Chem. Soc. **113** (1991) 1050-1051.
61. H. A. Azab, L. Banci, M. Borsari, C. Luchinat, M. Sola, M. S. Viezzoli, Inorg. Chem. **31**(1992) 4649-4655.
62. N. Anicet, A. Anne, J. Moiroux, J. M Saveant. J. Am. Chem. Soc. **120** (1998) 7115-7116.
63. T. J. Kealy, P. L. Paulson, Nature **168** (1951) 1039-1040.
64. E. A. Seibold, L E. Sutton, J. Chem. Phys. **23** (1955) 1967-1967.
65. K. M. Kadish, C. H. Su, J. Am. Chem. Soc. **105** (1983) 177-180.
66. K. M. Kadish, C. H. Su, J. Am. Chem. Soc. **105** (1983) 177-180.
67. A. P. Abbot, G. Capper, D. L. Davies, K. Raymond, R. K. Rasheed, V. Tambyrajah, Chem. Comm., (2003) 70-71.
68. A. P. Abbot, G. Capper, D. L. Davies, R. K. Rasheed, V. Tambyrajah, Chem. Comm. (2001) 2010-2011.
69. H. Ohno (ed.), Electrochemical aspects of ionic liquids, New York, John Wiley and Sons, 2005.
70. P. Wasserscheid, T. Welton, Ionic Liquids in Synthesis, Weinhein, Wiley-VCH, 2003.
71. F. Endres, A. P. Abbott and D. R. MacFarlane, Electrodeposition of metals using ionic liquids, Weinheim, Wiley-VCH, 2008.
72. A. J. Bard and L. R. Faulkner, Electrochemical Methods: Fundamentals and Applications, New York: Wiley, 2nd ed, 2001.
73. H. Ti Tien, J. Phys. Chem. **88** (1984) 3172-3174.

74. P. M. Allemand, A. Koch, F. Wudl, Y. Rubin, F. Diederich, M. M. Alvarez, S. J. Anz, R. L. Whetten, J. Am. Chem. Soc. **113** (1991) 1050-1051.
75. H. A. Azab, L. Banci, M. Borsari, C. Luchinat, M. Sola, M. S. Viezzoli, Inorg. Chem. **31**(1992) 4649-4655.
76. N. Anicet, A. Anne, J. Moiroux, J. M Saveant. J. Am. Chem. Soc. **120** (1998) 7115-7116.
77. T. J. Kealy, P. L. Paulson, Nature **168** (1951) 1039-1040.
78. E. A. Seibold, L E. Sutton, J. Chem. Phys. **23** (1955) 1967-1967.
79. K. M. Kadish, C. H. Su, J. Am. Chem. Soc. **105** (1983) 177-180.
80. N. Ito, T. Saji, S. Aoyagui, J. Organomet. Chem. **247** (1983) 301-305.
81. G. Gritzner, J. Kuta, Pure, Appl. Chem **56** (4) 461-466 (1984).
82. M. A. Vorotyntsev, V. A. Zinovyeva, D. V. Konev, M. Picquet, L. Gaillon, C. Rizzi,. J. Phys Chem B, **13** (2009) 1085-1099.
83. Marek Kosmulski, R. A. Osteryoung, M. Ciszkowska,. J. Elect. Soc. **147** (2000) 1454-1458.
84. Y. Guo, M. Kanakubo, et al. J. Electroanal. Chem. **639** (2010) 109-115.
85. N. Tachikawa, Y. Katayama, et al. ECS Trans. **16** (2000) 589-595.
86. H. Zhou, S. J. dong,. Electrochimica Acta. **42** (1997) 1801-1807.
87. H. Zhou, N. Gu, et al. J. Electroanal. Chem. **441** (1998) 153-160.
88. R. S. Nicholson, I. Shain, Anal. Chem. **36** (1964)706.
89. Holbrey J, Seddon K. Ionic Liquids. Clean Prod Proc **1** (1999) 223–236.
90. Welton T. Room temperature ionic liquids, solvents for synthesis and catalysis. Chem Rev **99** (1999) 2071.
91. Endres F, Ionic liquids, solvents for the electrodeposition of metals and semiconductors. ChemPhysChem **3** (2002) 144-154.
92. Lin Y, Wen Sun I. Electrodeposition of zinc from a Lewis acidic zinc chloride-1-ethyl-3-methylimidazolium chloride molten salt. Electrochim. Acta 44 (1999)2771–2777.
93. Takahashi S, Koura N, Kohara S, Saboungi M, Curtiss L. Technological and scientific issues of room-temperature molten salts. Plasmas Ions **2** (1999)91–105.
94. Brennecke J, Magin E. Ionic Liquids: Innovative Fluids for Chemical Processing. AIChE J **47** (2001)2384–2389.

95. Ue M, Takeda M, Toriumi A, Kominato A, Hagiwara R, Ito Y. Application of Low-Viscosity Ionic Liquid to the Electrolyte of Double-Layer Capacitors. J Electrochem Soc **150** (2003) 499.
96. Balducci A, Bardi U, Caporali S, Mastragostino M, Soavi F. Ionic liquids for hybrid supercapacitors. Electrochem. Commun. **6** (2004) 566–570.
97. Booth H, Merlub-Sobel M. Electrodeposition of metals from anhydrous ammonia. J Phys Chem Lett **35** (1931) 3303.
98. Mann, Halversen. Trans Am Electrochem Soc Lett **45** (1924) 493-508.
99. Huerta D, Zhouping A, Luo P, Heusler K. Electrochemical behavior of chromium, molybdenum and manganese in liquid ammonia. Electrochim Acta Lett **39** (1994) 2795-2797.
100. Heusler K, Kutzmutz S. The nickel electrode in liquid ammonia. J Electroanal Chem Lett **285** (1990) 93-101.
101. M. Zamin, P. Mayer, and M. K. Murthy, J. Electrochem. Soc., Volume 124, Issue 10, pp. (1977) 1558-1562.
102. T. Deguchi, K. Chikamori, K. Kyo, A. Ogawa, Proceedings of the 2003 Annual Meeting of the Japan Engineering. (2003) 338.
103. T. Deguchi, K. Chikamori, Proceedings of the 2005 Annual Meeting of the Japan Society for Precision Engineering. (2005) 539.
104. K. Fushimi, H. Habazaki, Electrochim. Acta. **53** (2008) 3371.
105. A. P. Abbot.; G. Capper.; D. L. Davies.; K. Raymond.; R. K. Rasheed.; V. Tambyrajah. Chem. Comm., (2003) 70-71.
106. A. P. Abbot.; G. Capper.; D. L. Davies.; R. K. Rasheed.; V. Tambyrajah. Chem. Comm., (2001) 2010-2011.
107. H. Ohno (ed.): 'Electrochemical aspects of ionic liquids'; New York, John Wiley and Sons, 2005.
108. L. Binder, G. Rathwallner, B. Mollay, G. E. Nauer, Proc. 55th ISE-Meeting., (2004) 19-24.
109. P. Wasserscheid, T. Welton: 'Ionic Liquids in Synthesis'; Weinhein, Wiley-VCH., 2003.
110. P.W. Atkins: "Physical Chemistry", Oxford University Press, chapters 11,12, 32; 2004.
111. M. L. Holt, *Trans. Electrochem. Soc.*, **66** (1934) 453; **71** (1937) 301.

112. P. Zanello, "Inorganic Electrochemistry: Theory, Practice and Application" The Royal Society of Chemistry 2003.
113. Nicholson, R. S. and I. Shain "Theory of Stationary Electrode Polarography" Analytical Chemistry **36** (1964) 706.
114. Lavagnini, I., R. Antiochia, et al. "An Extended Method for the Practical Evaluation of the Standard Rate Constant from Cyclic Voltammetric Data." Electroanalysis **16** (2004) 505-506.
115. Vorotyntsev, M. A., Zinovyeva,A., Konev, V. Picquet, M., "Electrochemical and Spectral Properties of Ferrocene (Fc) in Ionic Liquid: 1-Butyl-3-methylimidazolium Triflimide, [BMIM][NTf2]. Concentration Effects" J. Phys. Chem. B **113** (2009) 1085–1099.
116. Kosmulski, M. Osteryoung, R. A. Ciszkowska, M. "Diffusion Coefficients of Ferrocene in Composite Materials Containing Ambient Temperature Ionic Liquids" Journal of The Electrochemical Society, **147** (2000) 1454-1458.
117. Nagy, L., G. Gyetvai, et al. "Electrochemical behavior of ferrocene in ionic liquid media." Journal of Biochemical and Biophysical Methods **69** (2006) 121-132.
118. Tachikawa, N., Y. Katayama, et al. "Electrode Kinetics of Ferrocenium/ferrocene in Room-temperature ionic Liquids." Ecs transactions **16** (2000) 589-595.
119. Feng, G. "Cyclic voltammetry investigation of diffusion of ferrocene within propylene carbonate organogel formed by gelator" Electrochimica Acta **53** (2008) 8253–8257.
120. Zhou, H., N. Gu, et al. "Studies of ferrocene derivatives diffusion and heterogenous kinetics in polymer electrolyte by using microelectrode voltammetry." Journal of Electroanalytical Chemistry **441** (1998) 153-160.
121. L. D. Zusman, Chem. Phys. **49** (1980) 295.
122. D. F. Calef, P. G. Wolynes, J. Phys. Chem. **87** (1983) 3387.
123. P. G. Wolynes, J. Chem. Phys. **86** (1987) 5133.
124. A. Kapturkiewicz, B. Behr, J. Electroanal. Chem. **179** (1984) 187.
125. G. Grampp, A. Kapturkiewicz, W. Jaenicke, Ber. Bunsen-Ges. Phys. Chem. **94** (1990) 439.
126. R. A. Marcus, Chem. Phys, **43** (1965) 679.
127. M. J. Weaver, G. E. McManis, Acc. Chem. Res. **23** (1990) 294.

128. W. R. Fawcett, M. Opallo, Angew. Chem., Int. Ed. Engl. **33** (1994) 2131.
129. R. Pyati, R. W. Murray, J. Am. Chem. Soc. **118** (1996) 1743-1749.
130. A. I. Burshtein, E. I. Kapinus, I. Yu. Kucherova, V. A. Morozov, J. Lumin. **43** (1989) 291.
131. R. W. Murray, Annu. Rev. Mater. Sci. **14** (1984) 145.
132. R. M. Nielsen, G. E. McManis, M. N. Golovin, J. M. Weaver, J. Phys. Chem. **92** (1988) 3441.
133. T. T. Wooster, M. Watanabe, R. W. Murray, J. Phys. Chem. **96** (1992) 5886-5893.
134. T. T. Wooster, M. L. Longmire, M. Watanabe, R. W. Murray, J. Phys. Chem. **95** (1991) 5315-5321.
135. A. Fry, W. E. Britton, in *Laboratory Techniques in Electrochemical Chemistry* (P. T. Kissinger, W. R. Heineman eds.) Marcel Dekker, New York, 1984, chapter 13.
136. Rogers, E. I., B. Šljukić, et al. "Electrochemistry in Room-Temperature Ionic Liquids: Potential Windows at Mercury Electrodes." Journal of Chemical & Engineering Data **54** (2009) 2049-2053.
137. Barrosse-Antle, L. E., D. S. Silvester, et al. "Electroreduction of Sulfur Dioxide in Some Room-Temperature Ionic Liquids." The Journal of Physical Chemistry C **112** (2008) 3398-3404.
138. Q. Abbas and L. Binder "Synthesis and Characterization of Choline Chloride Based Binary Mixtures." Electrochemical Society Transactions **33** (2010) 49-59.
139. R. J. Silbey, R. A. Alberty, and M. G. Bawendi, Physical Chemistry 4th ed. Wiley, New York, 2004.
140. O. Zech, A. Stoppa, R. Buchner, W. Kunz, *J. Chem. Eng. Data* **55** (2010) 1774–1778.
141. T. Koeddermann, C. Wertz, A. Heintz, R. Ludwig, Angew. Chem. Int. Ed. **45** (2006) 3697-3702.
142. K. Fumino, A. Wulf, R. Ludwig, Angew. Chem. Int. Ed. **47** (2008) 8731-8734.
143. K. Fumino, A. Wulf, R. Ludwig, Angew. Chem. Int. Eg. **48** (2009) 3184-3186.
144. T. Koeddermann, C. Wertz, A. Heintz, R. Ludwig, ChemPhysChem **7** (2006) 1944-1949.

145. S. Tait, R. A. Osteryoung, Inorg. Chem. **23** (1984) 4352.
146. K. M. Dieter, C. J. Dymek, N. E. Heimer, J. W. Rowang, J. S. Wilkes, J. Am. Chem. Soc. **110** (1988) 2722.
147. C. J. Dymek, D. A. Grossie, A. V. Fratini, W. W. Adams, J. Mol. Struct. **213** (1989) 25.
148. N. Campbell, B. Williamson, R. Heyden,. Biology: Exploring Life. Boston, Massachusetts: Pearson Prentice Hall 2006.
149. J. Emsley, Chemical Society Reviews **9** (1980) 91.
150. A. V. Kuchernov, T. N. Kuchernova, A. A. Slinkin, Mesoporous Microporous Matter. **26** (1998).
151. A. V. Kuchernov, A. A. Slinkin, Catal. Lett. **64** (2000) 53.
152. Z. I. Usmanov and A. V. Il'yasov, J. Struct. Chem. **13** (1972) 728-730.
153. Strong, F. C. "Faraday's Laws in One Equation". *Journal of Chemical Education* **38** (1961) 98.
154. Bard A, Faulkner L. Electrochemical Methods: Fundamentals and Applications; Wiley John & Sons Inc 1980.
155. Binder L. Electrochemical machining of tungsten, molybdenum and tantalum. The Electrochem Society Proceedings (1988) 88-23.
156. Oswin H, Salomon M. The anodic oxidation of ammonia at platinum black electrodes in aqueous KOH electrolyte. Can J Chem **41** (1963) 1686.
157. Despic A, Drazic D, Raskin P. Kinetics of electrochemical oxidation of ammonia in alkaline solution. Electrochim Acta **11** (1966) 997.
158. Grischer H, Mauerer A, Untersuchungen zur anodischen oxidation von ammoniak an platinelektroden J Electroanal Chem **25** (1970) 421.
159. Perissi I, Bardi U, Caporali S, Lavacchi A. High temperature corrosion properties of ionic liquids. Corrosion Sci **48** (2006) 2349–2362.
160. Zawisza B, Sitko R. Determination of Te, Bi, Ni, Sb and Au by X-ray fluorescence spectrometry following electroenrichment on a copper cathode. Spectrochimica Acta **62** (2007) 1147–1152.
161. Cullity B. Elements of X-Ray Diffraction, 2nd edition Addison-Wesley Reading MA (1978) 379.
162. Binder L, The electrochemical dissolution of molybdenum. Proceedings 39th ISE-Meeting Glasgow/UK Abstract No 547 (1988).

163. Armstrong R, Bell M, Metcalfe A. The anodic dissolution of molybdenum in alkaline solutions electrochemical measurements. J Electroanal Chem **84** (1977) 61-72.
164. Hull M. On the anodic dissolution of molybdenum in acidic and alkaline electrolytes. J Electroanal Chem **38** (1972) 143-157.
165. Notten G. Corrosion Engineering Guide. KCI publishing 2008.
166. Cotton F, Wilkinson G. Advanced Inorganic Chemistry. John Wiley and Sons 1972.
167. P. W. Atkin and J. de Paula, Physical Chemistry (7^{th} edition) Oxford university press, Oxford, UK, 2002.
168. A. P. Abbott, A. V. Malkov, N. Zimmermann, J. B. Raynor, G. Ahmad, J. Steele, P. Kocovsky, Organometallics., **16** (1997) 3690-3695.
169. H. Ohno (ed.): 'Electrochemical aspects of ionic liquids'; New York, John Wiley and Sons, 2005.
170. Loudon, G. Mark. Organic Chemistry 4th ed. New York: Oxford University Press. p. 317 (2002).
171. Zieborak,K.;K. Olszewski *Bull.Acad.Pol.Sci.Ser.Sci.Chim.Geol.Geogr.* **6** (1958) 3315–22.
172. A. P. Abbott, A. V. Malkov, N. Zimmermann, J. B. Raynor, G. Ahmad, J. Steele, P. Kocovsky, Organometallics., **16** (1997) 3690-3695.
173. S. Senderoff, G. W. Mellors, J. Electrochem. Soc., **114** (1967) 556-560.
174. F. Endres, A. P. Abbott and D. R. MacFarlane: 'Electrodeposition of metals using ionic liquids'; Weinheim, Wiley-VCH 2008.
175. C. F. Baes, R. E. Mesmer, The Hydrolysis of Cations, Wiley, New York 1976.
176. Greenwood, Norman N.; Earnshaw, A., *Chemistry of the Elements* (2nd ed.), Oxford: Butterworth-Heinemann, p. 384 (1997).
177. A. A. Pozdeeva, E. I. Antonovskaya, A. M. Sukhotin, (Zashch. Metal. **1** (1965) 20/8; Prot. Metals. (USSR) **1** (1965) 15/21.
178. A. M. Sukhotin, A. A. Pozdeeva, E.I. Antonovskaya., Tr. Inst. Prikl. Khim. No. **67** (1971) 5/17.
179. T. Humann, G. Hauck., Z. Metallk. **56** (1965) 75/9.
180. T. Heumann, G. Hauck, Ber. Bunsenges. Physik. Chem., **71** (1967) 404/10.

181. J. W. Johnson, C. H. Chi, C. K. Chen, W. J. James., Corrosion [Houston] **26** (1970) 238/42
182. J. W. Johnson, M. S. Lee, W. J. James., Corrosion [Houston] **26** (1970) 507/10.
183. S. V. Sastri, L. C. Chuni, E. D. Willis., Canadian Journal of Chemistry, **47** (1969) 587.
184. Patton, S. J., Stone, B., et.al., " solubility of fatty acids and other hydrophobic molecules in liquid trioleoylglycerol" Journal of Lipid Research **25** (1984) 189-197.
185. G.M. Barrow *Physical chemistry*, 2d Edition McGraw Hill (1996).
186. Silderberg, M.S. "Chemistry - The Molecular Nature of Matter and Change", 3rd Edition, 2003, pp508-509.
187. V. Gutmann, Coord. Chem. Rev., **18** (1976) 225
188. Lee, J.-M., S. Ruckes, et al. "Solvent Polarities and Kamlet−Taft Parameters for Ionic Liquids Containing a Pyridinium Cation." The Journal of Physical Chemistry B **112** (2008) 1473-1476.
189. http://www.stenutz.eu/chem/solv26.php
190. Christensen, P. A. and A. Hamnett "The oxidation of ethylene glycol at a platinum electrode in acid and base: An in situ FTIR study." Journal of Electroanalytical Chemistry and Interfacial Electrochemistry **260** (1989) 347-359.